PART - A

SEMICONDUCTIVE INVESTIGATIONS

CHAPTER - 1

GENERAL INTRODUCTION

There have been a considerable interests[1-15] in the electrical conductivity of organic semiconductors in recent years to unfold their various properties both theoretically and experimentally. Due to its wide range of applicability in a number of fields, organic semiconductor research has opened a new frontier in solid state physics[2,16-30]. The formation of charge carriers and the mode of transportation even in highly disordered solids pose continuing challenges to the very fundamental concepts of charge transport mechanism. The most important feature of the organic solid state is the persistence of molecular identity which distinguishes it from the inorganic solid state. The molecular identity derives from the weakness of the interaction between the molecules. The traditional energy band model, though applied in some cases, is only partially successful in the case of organic molecular crystals.

Gas or vapour adsorption effect on the biologically important semiconductors was used to explain the olfactory transduction by Rosenberg, Misra and Switzer[36]. Gas or vapour adsorption is known to enhance the conductivity with concomitant change in the semiconduction activation energy and the pre-exponential factor in the

conductivity equation. At present, however, there does not seem to be any convincing evidence in favour of any particular assumption as to the type of interaction of the gas with the substrate. Though, a weak charge transfer complex formation has often been suggested[36-38].

Compensation behaviour[40-50] in dark conduction processes of the organic semiconductors is among the central problems in the field. Recent interest yielded many new observations along with some theoretical developments.

The present investigation is concerned with the semiconductive properties, in particular the gas or vapour adsorption effect and the compensation effect, of some nitroaromatic semiconductors.

In the subsequent sections of this chapter we will briefly review the theoretical back-ground.

1.1 Band Theory and Molecular Crystals

The band theory, originally developed for metals, ionic and valence crystals has been applied with some success to molecular crystals as well[51-54].

In one electron approximation, the wave function for a single electron can be written as

$$\Psi_k(\bar{r}) = \Phi_k(\bar{r}) \exp(i\bar{k}\cdot\bar{r}) \qquad (1.11)$$

where the wavenumber vector $\bar{k} = \frac{2\pi}{\lambda}$, λ is the associated wave length; Φ_k is the function which has the translational periodicity of the crystal lattice. If $\Phi_k(\bar{r})$ is constant throughout the crystal, then Ψ_k is applicable to the metals. But if $\Phi_k(\bar{r})$ varies greatly within a unit cell and falls to zero between adjecent cells, then the motion of the electron is restricted and we get a "tight bonding condition".[56-59] This tight bonding is a characteristic of molecular crystals. Unier this approximation, the one electron crystal wavefunctions Ψ_k are constructed from linear combinations of one electron molecular functions χ_n:

$$\Psi_k(\bar{r}) = N^{-\frac{1}{2}} \sum_{n=1}^{N} \exp(i\bar{k}\cdot\bar{r}_n)\chi_n(\bar{r}-\bar{r}_n) \qquad (1.12)$$

Here, $\bar{r}_n$ locates the geometrical centre of n th molecule and N is the total number of molecules in the crystal. It is assumed that $\langle \chi_m | \chi_n \rangle = 0$ if $m \neq n$.

The crystal field is approximated by :

$$V(\bar{r}) = \sum_n V_n(\bar{r}-\bar{r}_n) \qquad (1.13)$$

where V_n is the Hartee Fock type of potential of an isolated

neutral molecule. [This consists of three components - V′: field acting on the electron that arises from all the nuclei, V″: the coulomb potential of the electronic charge distribution and V‴: the exchange term.]

The eigen value of ψ_k is written as :

$$\mathcal{E}(\bar{K}) = \mathcal{E}_0 + \mathcal{E}_1 + 2\sum_s{}' \mathcal{E}_s \cos(\bar{K}\cdot\bar{r}_s) \qquad (1.14)$$

where

$$\mathcal{E}_0 = \int \chi_n \left[-(\hbar^2\Delta/2m) - eV_n\right] \chi_n \, d\tau$$

$$\mathcal{E}_1 = \sum_s{}' \int |\chi_n|^2 V_{n+s} \, d\tau \qquad s \neq 0$$

$$\mathcal{E}_s = \int \chi_{n+s} V_{n+s} \chi_n \, d\tau$$

and the lattice vectors ($\bar{r}_s$) and ($-\bar{r}_s$) are counted as one in the equation (1.14). The prime on $\sum$ indicates that the term with $\bar{r}_s = 0$ is omitted from the summation.

The intermolecular resonance integrals $\mathcal{E}_s$ determine the structure of the band[60]. The resonance integrals fall off rapidly with intermolecular distance and only nearest neighbour interactions are found to be important. Functional forms of V_n and the appropriate χ_n are required to evaluate $\mathcal{E}_s$. The band structure depends on the crystal lattice structure.

1.2 Operational Definition of Semiconductor

If the interaction between different carrier species is neglected, then for semiconductor, where the charge carriers are electrons (e) and holes (h), the conduction equation is :

$$\sigma = n_e e \mu_e + n_h e \mu_h \qquad (1.21)$$

where n is the density of the charge carriers in their respective bands, e is the electronic charge and μ is the mobility of the carriers.

The densities of the electrons in the conduction band and that of holes in the valence band are given by[56,58] ,

$$n_e = 2(2\pi m_e^* kT/h^2)^{3/2} \exp[(E_f - E_c)/kT] \qquad (1.22)$$

and $$n_h = 2(2\pi m_h^* kT/h^2)^{3/2} \exp[(E_v - E_f)/kT] \qquad (1.23)$$

respectively. Here m^* represents the effective mass near the conduction band E_c for electrons and near the top of the valence band E_v for holes. E_f is the Fermi - energy. From (1.22) and (1.23) and taking $n_e = n_h$ one gets :

$$E_f = [(E_c + E_v)/2] + \frac{3}{4} kT \log(m_h^*/m_e^*) \qquad (1.24)$$

Substitution of the value of E_f from (1.24) into (1.22) or (1.23) yields :

$$n_e = n_h = 2(2\pi RT/h^2)^{3/2}(m_e^* m_h^*)^{3/4} e^{-E/2RT} \quad (1.25)$$

where E represents the energy gap between the valance and conduction bands.

Equation (1.25) is applicable to an intrinsic semiconductor in thermal equilibrium and hence the conduction equation (1.21) becomes :

$$\sigma = \sigma_0 \exp(-E/2RT) \quad (1.26)$$

where $\sigma_0 = 2e(2\pi RT/h^2)^{3/2}(m_e^* m_h^*)^{3/4}(\mu_e + \mu_h)$

1.3 Tunneling and Hopping Mechanisms in Dark Conduction

1.31 Tunneling Mechanism :

The tunneling, an out come of the quantum mechanical concepts, is a mechanism in which a particle without even acquiring enough energy can pass through a potential barrier. Riley and Willis[61] have originally proposed that the dark conduction is possible through this mechanism.

In dark conduction, the charge carriers penetrate an intermolecular potential barrier. The number of times an electron penetrates this barrier gives a measure of its drift velocity (v_{de}). If the net displacement of the electron upon going through the barrier is (a + l) then the drift velocity is given by :

$$v_{de} = \left(\frac{v_e}{2l}\right)(a+l)(P_f - P_r) \qquad (1.311)$$

where P_f and P_r are the barrier penetration ~~penetration~~ probabilities in the direction of the field and in the reverse direction respectively; l is the distance across the potential well of width a and v_e is the velocity of the electron in the $(\frac{N}{2} + 1)$th level moving between the potential wells and is equal to $\left[\left(\frac{N}{2}+1\right)\cdot\left(h/2l\,m_e^*\right)\right]$. The current density which is equal to ($n_e \cdot v_{de}$) thus becomes :

$$i = \left[2\left(2\pi m_e^* kT\right)^{3/2}/h^3\right]\left[\exp\left(-E/2kT\right)\right]\left(\frac{N}{2}+1\right)\cdot$$

$$eh(a+l)(P_f - P_r)/4l^2 m_e^* \qquad (1.312)$$

which is of the form of the conductivity equation :

$$i = \sigma_0 V \exp\left(-B/2kT\right) \qquad (1.313)$$

1.32 Hopping Mechanism :

Hopping is a process in which a charge carrier on a molecular site can move to the other by moving over the barrier between the sites via an activated state.

A simple hopping model for the dark conduction in organic solids has been applied by Pohl[62] and by Pohl and Opp[63]. In the hopping process, the motion of the carriers to the neighbouring sites is random except for the anisotropy caused by the applied field F. Hopping of the carriers depends upon the following factors :

1) The average angle of hopping with the field direction,
2) The intermolecular distance,
3) Number of the neighbouring sites,
4) Frequency of vibration in the two directions normal to the carrier motion's direction across the barrier, and
5) The barrier height.

The interaction of the carriers with vibration in the lattice may also give hopping of charge carriers without having these to cross the barrier[64]. For hopping, it is essential that the relaxation time in which the electrons hops from a site to the another must be much greater than the period of a vibration.

1.4 Polarons & Role in conduction Process in Molecular Crystals Through Tunneling and Hopping

A polaron is an entity of electron accompanied by a localised vibration which moves through the crystal under some circumstances when electron - phonon interaction leads to the electrons being trapped in a self-induced potential wells[64]. A major contribution to the polaron formation comes from the molecular vibrations. Slow intermolecular vibrations of the lattice weakly interact with the carriers and can be neglected. Siebrand[65] has considered a molecular crystal with one excess electron and calculated the binding energy of the polaron as :

$$E_b = \frac{1}{2} \sum_q M_q^2 \omega_q (\Delta x_q)^2 \qquad (1)$$

where M_q is the reduced mass of the q th oscillator; ω_q is the frequency and Δx_q is the difference between the equilibrium distances of the molecule and the ion.

By treating electron overlap as perturbation, the formation of Bloch-type bands from polarons are obtained. These bands are narrower than the corresponding electron bands by a vibrational overlap factor. Their width are approximately given by :

$$J_\upsilon(\upsilon^\circ+\upsilon) \simeq J_k (E_b/\hbar\omega)^{\upsilon^\circ+\upsilon} [\exp(-E_b/\hbar\omega)] \qquad (2)$$

where v° and v are vibrational quantum numbers of the neutral molecule and the ion respectively and J_k is the half width of one electron band in the tight-binding approximation. Thus, there exists a series of polaron bands below the electron band.

At a very low temperature, carriers will occupy the lowest - lying polaron band and will have very low mobility restricted by the lattice phonon scattering. In this case $\mu \propto T^{-3/2}$ to T^{-1}. Higher polaron bands will be populated with the rise in temperature (T) and the effective band - width will exponentially increase with T. As T approches E_b/k, the mobility is governed by the distribution between polaron bands and the electron band and the transport of carriers becomes an activated hoping process. $(d\mu / dT)$ gradually changes the sign. As T exceeds E_b/k, the distribution over the bands is approximately independent of T and the temperature dependence of μ becomes as that at low temperature.

For the strongly bound polarons, we have $E_b \quad J_k$ and $E_b >> \hbar\omega >> 2\pi J_\omega$. An electron should then remain on a lattice site for a much longer period than the period of vibration in order to get polaron formed. At temperature E_b/k the polaron will dissociate thermally. When the width of the polaron band is approximately equal to $\hbar\omega$, the electron will not remain on the lattice site longer than the period of vibration and so it

can be said to dissociate kinatically. Siebrand applied this notion to the case in which the carrier moves by activated hopping process from a polaron band to the electron band and showed that $\mu < 1\ cm^{-1}\ volt^{-1}\ sec^{-1}$.

When the carriers interact strongly with molecular vibrations, this interaction whould be included in zeroth order carrier wave functions and so the seperation into electronic and vibrational parts of the total wave function for the crystal is no longer possible. The electron vibration interaction results in a narrower band - widths. The coupling criteria has been discussed by Ho Hao and Siebrand[66] and are generatised by Siebrand[67] in three dimensions.

Now, we will discuss tunneling and hopping of polarons briefly. When an electron is surrounded by a cloud of phonons, transition from sites j to j'results in the destruction and creation of the cloud at j and j' respectively. The electron is scattered many times during the jump due to a large number of emissions and absorptions accompanying the transition. When electron on a site is trapped in a potential well, it is to pass a barrier of height equal to the polaron biming energy. The passage may be tunneling or hopping. Tunneling applies when the vibrational sites involve only a few quanta and are well seperated while hopping applies when a large number of excited vibrational states are crowded together and consists of randomly performed

jumps. If the phonon band-width exceeds that of the polaron band, the dispersion of the lattice frequencies introduces enough randomness to annihilate the polaron band structure. The crystal may, then, behave like a liquid drop in this circumstance with respect to the carrier transport (through hopping) and the mobility should not change much upon melting contrary to that generally observed[60]. Thus, the mechanism of carrier transport in molecular crystals is thought to be polaron tunneling. Tunneling is analogous to wave like motion and the translational symmetry of the lattice necessarily implies the same[68]. The thermal motion may however, destroy the translational symmetry.

1.5 Adsorption Process

When a gas is allowed to come to equilibrium with a solid or liquid surface, the concentration of the gas molecules is always found to be greater in the immediate vicinity of the surface than in the free gas phase, regardless of the nature of the gas or surface. The process by which this surface excess is found is termed "ADSORPTION"[69,70]. There are two types of adsorption ; Physical and Chemical, depending on the nature of the forces involved. Physical adsorption, also termed Vander waals adsorption (binding energy of the order of 10^{-2} ev[70-73]) is caused by molecular interaction forces whereas chemical adsorption (binding energy of the order of several ev[70-73]) involves transfer of

electrons i.e. a state of chemical binding between the solid and the gas. The shapes of the adsorption isotherms[69,70], which are the plots of free energy change as a function of the amount of vapour adsorbed, can also yield qualitative information about the adsorption process. Physisorption is of interest in its suggested role as a precursor stage of chemisorption and in the evaluation of the adsorption mechanism[71].

Various attempts have been made to understand the nature of the vander waals forces[74-95] resulting in several formulations of the interactions. The method presented by Pollard[83] uses classical dipole - dipole interaction[77] between the gas molecule and the solid substrate in the evaluation of the vander waals' interaction and Heitler-London coupling scheme in the estimation of the repulsive term. The calculation of Mavroyannis[80], on the other hand is based on the work of Lifshitz[82] and Dzyaloshinskii et al[79], where a uniform continuous model of the surface is employed and ignores the presence of the repulsive forces entirely. The neglect of repulsive contribution to the energy of physisorption, the assumption of an equilibrium position for the physisorbed atom, and the approximations introduced in the expression for the energy cause serious difficulties[85]. For atomic vapour adsorption on metal surface, the attractive and repulsive contributions to the physisorption interaction energy are derived from the assumption of weak coupling between an atom and a metal surface[86].

The effect of adsorption and desorption of oxygen on the oxides of copper, nickel, manganese and zinc of extremely high purity[130] shows that the rate of adsorption of oxygen is a function of the number of vacant sites present in the surface. They have considered the first order, second order and exponential relationships i.e. $\frac{dN_t}{dt} = KN_t$, $\frac{dN_t}{dt} = KN_t^2$ and $\frac{dN_t}{dt} = ae^{-\alpha N_t}$ respectively, where N_t is the number of atoms adsorbed at time t; K, a and α are constants. Derivation of these relationships were performed by many authors by measuring directly the amount of gases adsorbed[136,137(a),(b)]. Gray et al[130] have shown that the exponential plot is a better overall approximation for the complex order process than for one obeying the first order kinetics or a combination of the second and first order processes at the initial and final period of adsorption respectively. In working out the kinetics, the assumption made by Gray et al is that the measured conductivity is either proportional to $\sqrt{N_t}$ or to N_t. In some cases of vapour adsorption, adsorption time curves follow the Roginsky - Zeldovich equation in a slightly modified form.

Adsorption of water on some proteins followed the Brunauer - Emmett - Teller (B.E.T.) isotherm equation[133] i.e.

$$\left[X/V(1-X)\right] = \left[1/V_m c\right] + \left[(c-1)/V_m c\right] . X \quad (1.51)$$

where X is the relative pressure, V is the adsorbed vapour

expressed in gms per 100 gm of the adsorbate. By plotting the data according to this equation, V_m and C can be derived from slope and intercept. Here V_m is the quantity of adsorbed vapour corresponding to the monolayer and C is a constant related to the heat of adsorption. Heats of entropies of adsorption can be evaluated by thermodynamic methods. At low coverages, the strongly negative entropies of adsorption in many proteins indicated by localisation of water molecules on polar groups. Positive entropies of adsorption at low coverages were observed for crystalline albumin which is attributed to the configurational changes induced in the protein chains. The subject of adsorption thermodynamics has been developed by Hill[133(a),(b)].

1.6 Theory of the Compensation Effect

The compensation rule or Meyer-Neldel rule, a linear relationship between the logarithm of the pre-exponential factor (σ_0) and the activation energy (E), has been a subject of great interest[40-50, 96-99] and controversy[100-104] for many years. It was first noted by Many et al[96] that for a variety of polynuclear hydrocarbons and phthalocyanines, the value of varied over a range of 10^{23} and hence a rough correlation existed between the E's and σ_0's. Gutmann and Lyons[97] showed a linear relationship of the form:

$$\log \sigma_0 \simeq \alpha E + \beta \qquad (1.61)$$

for an entire class of substances where α and β are

constants. Cardew and Eley[98] have found a similar type of correlation to hold for a series of amino acids and proteins. Rosenberg et al[40] showed evidence that this formula is valid for a single organic substance when E is varied by hydration and complex formation.

Several mechanisms, namely, the charge carrier injection model[105], the tunneling of electrons from thermally activated energy levels through intermolecular potential barriers[43], thermally assisted tunneling (FAT) and pseudointrinsic conduction[106] were discussed by a number of authors[41-45, 105, 106] for the interpretation of the compensation effect. A simple quantum mechanical model Hamiltonian which described the physical picture of the 'Conferon' satisfying both the effects was proposed[42,44]. Kemeny and Mahanti[45] attempted to derive the compensation rule in the theory of rate processes within the quadratic polaron and Spin polaron models.

1.61 Charge-carrier Injection Model

A model for the generation of the charge carriers in organic substances was proposed by Green[107] which assumes injection of charge carriers at the surface of the crystal in a modification of a form of surface barrier proposed by Bardeen[108]. According to this model, the pre-exponential factor :

$$\sigma_0 \simeq n_0 (RT/h) K \qquad (1.612)$$

where n_o is the carrier density of the electrode, k is Boltzmann's constant, T is the absolute temperature, h is Planck's constant and K is the transmission co-efficient for tunneling through the barrier given by[107] :

$$\ln K \simeq -4\pi \left(\frac{2m}{h^2}\right)^{1/2} \left(\frac{2}{3Z}\right) \cdot \left[(x_1 - E_{act} + Za)^{3/2} - (x_1 - E_{act})^{3/2}\right] \qquad (1.613)$$

Here 'm' represents the electron mass, X_1 and X_2 are the work functions of the electrode and semiconductor respectively, E_{act} is the energy obtained from the slope of a $\ln\sigma$ vs. $1/T$ plot, 'a' is the barrier width and $Z = (X_2 - X_1)/a$. Assuming $E_{act} < X_1, X_2$, the right hand side of equation (1.613) can be approximated to

$$\ln K \simeq A + B E_{act} + C E_{act}^2 \qquad (1.614)$$

where,

$$A = -8\pi(3Z)^{-1}(2m/h^2)^{1/2}\left[(x_1+Za)^{3/2} - x_1^{3/2}\right] \qquad (1.615')$$

$$B = 4\pi(Z)^{-1}(2m/h^2)^{1/2}\left[(x_1+Za)^{1/2} - x_1^{1/2}\right] \qquad (1.615'')$$

$$C = -4\pi(3Z)^{-1}(2m/h^2)^{1/2}\left[(x_1+Za)^{-1/2} - x_1^{-1/2}\right] \qquad (1.616''')$$

For reasonable values of the parameters involved, the term in E_{act}^2 contributes approximately 10% - 20% of the linear term. If this quadratic term is neglected, equation (1.614) reduces to equation (1.61). For the validity of this model, X_2 must be greater than X_1 which is generally fulfilled in practice.

1.62 Electron Tunneling Model

The organic molecular solids consist of molecules with potential barriers surrounding them. For electrical conduction the electrons have to pass over or through these barriers. The first possibility requires high activation energies where as the latter requires a long time. If the effective wall height E_w is smaller than the total height E_p, the electrons can tunnel from activated levels of energy E through the potential barrier without requiring $E \simeq E_p$. Then the conductivity $\sigma(T)$ consists of three parts : (1) the temperature dependent exponential part (2) the exponential part of the barrier transmissivity and (3) a factor σ_x consisting of the non-exponential part of the barrier transmissivity and of the propagation characteristics of the electrons within the molecules. Employing the barrier transmissivity calculations of Mott and Gneddon[109]

$$\sigma(T) = \sigma_x \exp\left[-\left(\frac{2a}{\hbar}\right)(2m^* E_w)^{1/2}\right] e^{-E/2RT} \quad (1.621a)$$

for the square barrier and

$$\sigma(T) = \sigma_x \exp\left[-(4a/3\hbar)(2m^*)^{1/2}(E_W^{3/2}/E_T)\right] \cdot \exp(-E/2RT) \qquad (1.621\ b)$$

for the triangular barrier.

Here 'a' is the barrier width and m^* is the effective mass of the electron in the activated level involved in the tunneling. The barrier height E_T is equal to or less than the ionisation potential of the molecule for the square and the triangular barrier respectively. The tunneling electron will experience a potential which is the sum of the approximate coulomb potential attracting the electron to a positive ion and the potential of electron affinity of the originally neutral molecule, both varying smoothly being approximated better by the triangular than by the square barrier. For tunneling model to be satisfied, $E < E_T$ must be satisfied, otherwise there would be no tunneling and electrons would pass over the barrier. Therefore, substituting

$$E_W = E_T - E \qquad (1.622)$$

in equation (1.621) and expanding the fractional powers of E_W in a series stopping at the term linear in E gives

$$\sigma(T) = \sigma_x \exp\left[(-2a/\hbar)(2m^* E_T)^{1/2}\right] \cdot \exp\left[(a/\hbar)(2m^*/E_T)^{1/2} E\right] \exp(-E/2RT) \qquad (1.623\ a)$$

and

$$\sigma(T) = \sigma_x \exp\left[\left(-\frac{4a}{3\hbar}\right)(2m^* E_T)^{1/2}\right] \exp\left[\left(\frac{2a}{\hbar}\right)(2m^*/E_T)^{1/2} E\right] \exp\left(-\frac{E}{2RT}\right)$$

(1.623 b)

for the square and triangular barrier respectively. If $E < E_T$ but close to it, a better approximation is required.

For the materials obeying compensation rule leads to $E_T \simeq$ 2ev and 6 ev for the square and triangular barriers respectively. Only the last value i.e. 6 ev is reasonable so that the activation energies[40,99] are well below the top of the barrier in which case only the tunneling model is acceptable and is explained satisfactorily by the triangular barrier. If $m^* = 100\ m_0$, the intermolecular seperation $a \simeq 3 \times 10^{-8}$ cm which is quite justified. So the effective mass of the electron in the activated level is of the order of 100 electron masses.

1.63 Polaron Tunneling Model

An effective mass of 100 m_0, considered in the electron tunneling model, is much larger than those predicted[110,111]. In the narrow energy bands of organic semiconductors, tunneling of small polarons in thermally activated energy levels is possible. Holstein[112] deduced the mobility :

$$\mu = (e l^2 \tau / kT)(J_\omega / 2\hbar)^2 \qquad (1.631)$$

where l is the periodicity length, τ is the life-time of the polaron in a band state and $J_\sim$ is the small polaron band-width. Equation (1.631) is valid for $T < \theta/4$, where θ is the Debye temperature[112], and also satisfies the condition

$$J_\sim \ll kT \qquad (1.632)$$

so that all states in the polaron band are equally populated.

Two cases of small polaron theory may arise. The perturbation case for which $J < \hbar\omega_0$,

$$J_\sim = 2J \exp(-\gamma) \qquad (1.633\ a)$$

and the adiabatic case for which $J > \hbar\omega_0$

$$J_\sim = 2\hbar\omega_0 \exp(-\gamma) \qquad (1.633\ b)$$

and

$$\gamma = E_b/\hbar\omega_0 \qquad (1.633\ c)$$

E_b is the polaron binding energy, ω_0 is the optical vibration frequency and J is the hopping integral. The polarons which exist in a molecular lattice may have strong ionic properties upon complex formation. In an ionic system the coupling can be expressed using the effective dielectric constant as :

$$1/K_p = 1/K_\infty - 1/K \qquad (1.634)$$

where K and K_∞ are the static and high frequency dielectric constants

respectively. The coupling in a molecular lattice can also be expressed[113] in terms of K_p. Assimilating both effects into the effective dielectric constant, the binding energy of small polaron becomes :

$$E_b = \tfrac{1}{2} \left(e^2 / K_p r_p \right) \qquad (1.635)$$

where 'r_p' is the radious of the small polaron and may be less than half the periodicity length 'l'. The change in the polaron binding energy due to complex formation is then given by :

$$E_b - E_b^{(o)} = \tfrac{1}{2} \left(e^2 / r_p \right) \left[\left(1/K_p \right) - \left(1/K_p^{(o)} \right) \right] \qquad (1.636)$$

where the superscript (o) signifies the original semiconductor. K_∞ and $K_\infty^{(o)}$ are related to the refractive index, which is probably invarient, so that

$$E_b - E_b^{(o)} = \tfrac{1}{2} \left(e^2/r_p \right) \left(1/K^{(o)} \right) - \left(1/K \right) \qquad (1.637)$$

similarly

$$E - E^{(o)} = \left(- e^2/r_p \right) \left[\left(1/K^{(o)} \right) - \left(1/K \right) \right] \qquad (1.638)$$

where $E^{(o)}$ and E are the activation energy before and after complex formation. Substituting equation (1.638) in

equation (1.637), one gets :

$$E_b = E_b^{(o)} + \frac{1}{2}\left(E^{(o)} - E \right) \qquad (1.639)$$

or, $E + 2E_b = E^{(o)} + 2E_b^{(o)} \Rightarrow$ invariant (1.6310)

Now, the conductivity can be written as

$$\sigma = n e \mu = N \exp(-E/2kT)\, e\mu \qquad (1.6311)$$

where N is the number of electrons per unit volume available for activation. Making use of the equations (1.631) and (1.633) and (1.630), equation (1.6311) can be written as :

$$\sigma = \left(\frac{N e^2 l^2 \tau}{kT}\right)\left(\frac{J}{\hbar}\right)^2 \exp\left[\frac{2E_b^{(o)} + E^{(o)}}{\hbar\omega_o}\right] \exp\left\{E\left[(\hbar\omega_o)^{-1} - (2kT)^{-1}\right]\right\} \qquad (1.6312\,a)$$

for the perturbation case and

$$\sigma = \left(\frac{N e^2 l^2 \tau}{kT}\right)\omega_o^2 \exp\left[-\frac{(2E_b^{(o)} + E^{(o)}}{\hbar\omega_o}\right] \exp\left[E\left\{(\hbar\omega_o)^{-1} - (2kT)^{-1}\right\}\right] \qquad (1.6312\,b)$$

for the adiabatic case.

For the perturbation case, J and thus the rigid lattice

band-width depends[43] on the depth of the activated energy level below the top of the tunneling barrier and on the shape and width of the barrier. From equation (1.623), the formula for J is given by[43]

$$J^2 = J_o^2 \exp\left[(2a/\hbar)(2m^*/E_T)^{1/2} E\right] \qquad (1.6313)$$

where

$$J_o^2 = J_o'^2 \exp\left[(-4a/3\hbar)(3m^* E_T)^{1/2}\right] \qquad (1.6314)$$

J_o being the hopping integral for E = 0.

Substituting equation (1.6313) in equation (1.6312 a) we get :

$$\sigma = \frac{Ne^2 l^2 C}{RT} \left(\frac{J_o}{\hbar}\right)^2 \exp\left(-\frac{(2E_b^{(o)} + E^{(o)})}{\hbar\omega_o}\right) \cdot \exp\left[E\left\{(\hbar\omega_o)^{-1} + \left(\frac{2a}{\hbar}\right)\left(\frac{2m^*}{E_T}\right)^{1/2} - (2RT)^{-1}\right\}\right] \qquad (1.6315)$$

Therefore equations (1.6312 b) and (1.6315) are in the form of the compensation law.

1.64 Electronic states - Vibrational States Coupling Model

Kemeny and Goklany[42] noted that at experimental temperatures, small polaron tunneling is not possible, so that within

the assumption that conductivity is due to small polaron motion, hopping rather than tunneling must be the dominant conduction mechanism. But polaron hopping can not lead to the compensation effect via the mobility alone. Thus both the electron occupancy number 'n' and mobility ' μ ' are thought to be the sources for the compensation law. The mechanism postulated by Kemeny and Goldani is an interaction between the electrons and the vibrational motion which is able to explain both the enormous enhancement in the conductivity and the compensation effect. A change in electronic state gives rise to an activation entropy Δs because of a change in vibrational frequencies probably associated with the conformational changes[116] and this would contribute to the prefactor, giving its required enhancement.

Kaplan and Mohanti[44] considered only the contribution of 'n' to explain the conductivity enhancement and the compensation effect. Consider a solid made-up of N_M larger organic molecules. Each molecule has only two electronic states with energies $\varepsilon_1 < \varepsilon_2$ plus vibrational levels, and the total number of electrons is 1 per molecule. The vibrational frequencies are supposed to be different depending on the occupancy of these electronic states. Also, electron spin is neglected for simplicity. Then the physical picture of 'conformon' is clearly embodied in the Hamiltonian :

$$H = \sum_{i\nu} \varepsilon_\nu n_{i\nu} + \sum_{iK} \omega_K (n_{i1}, n_{i2}) (N_{iK} + \tfrac{1}{2}) \quad (1.641)$$

where $i = 1, 2, \cdots \cdots N$ labels the molecules; $\nu = 1, 2$ labels the one-electron states with energies $\varepsilon_1, \varepsilon_2$; $\omega_K(n_{i1}, n_{i2})$ is the vibrational frequency for mode K (with $\hbar = 1$); and, as the notation indicates, ω_K depends on the electron occupancy numbers $n_{i\nu}$ which have the possible values $n_{i\nu} = 0, 1$. N_{ik} labels the states of excitation of the k th vibrational mode on the i th molecule and takes on the values $0, 1, 2, \cdots \infty$. $E = (\varepsilon_2 - \varepsilon_1)$ is the electronic energy gap. If $E \simeq 1$ ev and the temperature is around room temperature and below, the number of electrons per molecule to the upper or conduction band is

$$\bar{n}_2 \simeq \exp\left[-\beta/2 (E + \Delta f_u)\right] \quad (1.642)$$

where Δf_u is the change in vibrational free energy in creating unbound electron-hole pair. In the low and high temperature region

$$n = n_0 \exp\left(-E_{eff}/2kT\right) \quad (1.643)$$

where E_{eff} is the modified activation energy. ω_K which contributes mainly to the free energy changes is ω_c. For $kT > \omega_c$,

$$\left.\begin{aligned} E_{eff} &\simeq E, \\ n_0 &\simeq \exp\left(\frac{S_a}{k}\right) \end{aligned}\right\} \quad (1.644)_c$$

and for $kT < \omega_c$,

$$E_{eff} \cong E + \tfrac{1}{2}\sum \left[\omega_k(1,1) + \omega_k(0,0) - 2\omega_k(1,0) \right]$$

$$n_0 \cong 1 \qquad (1.645)$$

Here, $$\frac{S_a}{k} = -\frac{1}{2}\sum_k \ln \frac{\omega_k(1,1)\,\omega_k(0,0)}{[\omega_k(1,0)]^2} \qquad (1.646)$$

Thus, an activated behaviour with an enhanced n_0 is obtained for high temperature range. Again $S_a > 0$, i.e. there is entropy enhancement if $\{\omega_k(1,1)\,\omega_k(0,0)/[\omega_k(1,0)]^2\} < 1$ which means that if there is an average softening of the vibrational modes upon the creation of the carriers. In the low temperature range, the entropic enhancement disappears, and the activation energy is modified by the zero-point energy.

In order to obtain compensation behaviour from this model, the vibrations in both the electronic energy gap E and the activation entropy S_a in going from one member to another within a given class is considered.

1.65 Quadratic Polaron Model

A theory for electronic charge transport as involved in kinetic processes has been derived by Kemeny and Mahanti[45] for quadratic generalisation of Holstein's one dimensional linear polaron theory[112]. To deduce the equation for the transition

rate per unit time they considered a system consisting of one electron and two possible sites (i = 1,2) in which the electron can reside. There are N oscillators corresponding to each site and J is the electronic transfer matrix element between two sites. Thus, in absence of the electron the potential energy of the system of N oscillators associated with the ith site, V_i, is given by

$$V_i = K \sum_{\mu=1}^{N} X_{i\mu}^2 \qquad (1.661)$$

where $X_{i\mu}$ is the displacement of the μ th oscillator from its equilibrium position and K is the force constant.

When the electron is present at the i th site it couples with the N oscillators associated with that site and there is an extra energy Φ_i which is given by :

$$\Phi_i = B \sum_{\mu=1}^{N} X_{i\mu}^2 - A \sum_{\mu=1}^{N} X_{i\mu} \qquad (1.662)$$

which is a generalisation of Holstein's linear polaron model in which B = 0 and N = 1. The probability that the electron initially at the site 1 goes to the site 2 is given by :

$$\left.\begin{aligned} i \frac{\partial a_1(t)}{\partial t} &= J a_2(t) + \Phi_1(t) a_1(t) \\ i \frac{\partial a_2(t)}{\partial t} &= J a_1(t) + \Phi_2(t) a_2(t) \end{aligned}\right\} \qquad (1.663)$$

where a_i (t) is the electronic amplitude associated with the i th site at time t and Φ_i (t) is a function of time through $X_{i\mu}$ (t). Equation (1.653) is valid only in the perturbation limit, i.e., for small J. In this limit, the electronic transition rate is obtained after carrying out the thermal average over all possible oscillator co-ordinates and velocities. At time $t = t_c$, where t_c is the coincidence point,

$$\Phi_1(t) = \Phi_2(t) \qquad (1.654)$$

and can be written as

$$\Phi(t_c) \equiv \Phi_1(\cdots x_{1\mu}(t_c)\cdots) - \Phi_2(\cdots x_{2\mu}(t_c)\cdots) = 0 \qquad (1.655)$$

which represents a (2N - 1) dimensional surface of stationary phase (SSP) in the space of oscillator coordinates ($\cdots x_{1\mu}\cdots$, $\cdots x_{2\mu}\cdots$). The linear term in equation (1.652) can be replaced by a simple transformation :

$$y_{i\mu} = x_{i\mu} - \frac{A}{2B} \quad , \quad i = 1, 2 \cdots \qquad (1.656)$$

Making use of equation (1.656), the equation for SSP may be denoted by

$$\Phi(t_c) = B\left[r^2(t_c) - s^2(t_c)\right] = 0 \qquad (1.657)$$

where

$$r^2 = \sum_{\mu=1}^{N} Y_{1\mu}^2 \quad \text{and} \quad S^2 = \sum_{\mu=1}^{N} Y_{2\mu}^2 \qquad (1.658)$$

The variations in r (t) and s (t) are linear in 't' in the neighbourhood of t_c and

$$\phi(t) = \phi(t_c) + \dot{\phi}(t_c)(t - t_c) \qquad (1.659)$$

The probability of a site jump per coincidence[112] W_c is given by

$$W_c = 2\pi J^2 / \dot{\phi}(t_c) \qquad (1.6510)$$

For large J, the perturbation approximation for W_c breaks down and the adiabatic approximation[112] is used.

W_c depends upon the positions and velocities of the 2N oscillators associated with the two sites. The transition rate per unit time is obtained from the probability that a coincidence occors in the interval t and t + dt for a specific position and velocity configuration of the 2N oscillators and then carry out a thermal averaging over all possible configurations which is valid in the perturbation limit.

For a particular configuration $X_{1\mu}(t)$, $X_{2\mu}(t)$, $v_{1\mu}(t)$, $v_{2\mu}(t)$, $\mu = 1, N$; the probability P_c that a

coincidence will occur during the time interval t and (t + dt) is given by the proportionality :

$$P_c \propto \delta(\Phi_1 - \Phi_2)(\dot{\Phi}_1 - \dot{\Phi}_2) \qquad (1.6511)$$

The transition rate per unit time, R, is given by

$$R = F/Z \qquad (1.6512)$$

and

$$F = \frac{2\pi J^2}{\hbar B}(\pi/2)^t \left[\frac{\pi}{\beta(K + B/2)}\right]^{N-1} \cdot \exp\frac{\beta N A^2}{2B}\left[\frac{K}{\beta}\left(\frac{K}{K + B/2}\right) - \left(\frac{K}{B} - \frac{1}{2}\right)\right] \qquad (1.6513)$$

where t = 1 if N is even and t = 0 if N is odd. Then

$$Z = \left(\frac{\pi}{K\beta}\right)^{N/2}\left(\frac{\pi}{\beta(K+B)}\right)^{N/2}\exp\left[\frac{\beta N A^2}{4(K+B)}\right] \qquad (1.6514)$$

In the theory of rate processes[116,116], the transition rate per unit time, R is given by

$$R = K\nu \exp\left[-\beta \Delta E^P + \frac{\Delta S^P}{R}\right] \qquad (1.6515)$$

where K is a transmission coefficient; ΔE^P and ΔS^P are the activation energy and entropy respectively, and the frequency ν is

given by $h\nu = RT$. Considering equations (1.6512), (1.6513) and (1.6514) and comparing with equation (1.6515) one gets :

$$\left.\begin{aligned} \frac{\Delta S^P}{R} &= N \log\left[\sqrt{K(K+B)}/(K+B/2)\right] \\ \Delta E^P &= \tfrac{1}{4} NA^2\left[\frac{1}{K+B} - \frac{1}{2K+B}\right] \end{aligned}\right\}$$

and

$$K\nu = 2\left(\frac{\pi}{2}\right)^{\frac{1}{2}} \frac{\beta J^2}{\hbar}\left(\frac{K}{B} + \frac{1}{2}\right) \qquad \left.\vphantom{\begin{aligned} a \\ b \end{aligned}}\right\} \text{(1.6516)}$$

From equation (1.6516) it is evident that if $B \neq 0$, it is important to have a nonzero value of A (linear coupling) to get an activation energy which is always positive whether B is positive or negative. For $B << K$, the activation energy is

$$E_a = \frac{NA^2}{8K}\left[1 - \frac{6B}{K}\right] \qquad \text{(1.6517)}$$

For positive B (hardening), E_a decreases, whereas for negative B (softening), E_a increases. The activation entropy is negative both for $B > 0$ and $B < 0$. The linear term does not contribute to the activation entropy. Thus, the quadratic polaron model hints out a transition rate which is always decreased by the entropy effect. Both ΔS^P and ΔE^P are proportional to N which provides the compensation rule and yields a negative compensation temperature $T_c = \frac{\Delta E^P}{\Delta S^P}$

1.66 Spin Polaron Model

Spin polaron or magnetic polaron model involves the coupling of electrons with a set of spins.

Let us consider two electronic sites each coupled to N spins μ_{ip} ($i = 1,2$ and $P = 1, \cdots N$) each of which can take two possible orientations, i.e., $\mu_{ip} = \pm 1$. In the absence of the electron the energy of the spins associated with the i th site, V_i, is given by

$$V_i = -B \sum_{p=1}^{N} \mu_{ip} \qquad (1.661)$$

where B is some sort of magnetic field which tends to order all the spins in one specific direction. If an electron is present at the i th site, then it couples to the N spins associated with that site and the additional interaction energy between the electron and the spins, Φ_i, is given by

$$\Phi_i = 2B \sum_{p=1}^{N} \mu_{ip} \qquad (1.662)$$

Therefore, the absence or presence of an electron leads to equally strong but oppositely oriented magnetic fields on the spins.

So the transition rate per unit time, R, is proportional to $\Gamma / _{B}$ and is given by

$$R = \frac{J^2}{2B\hbar} \left\{ \lfloor 2N / (\lfloor N)^2 \right\} \left(e^{-\beta B} + e^{\beta B} \right)^{-2N}$$

(1.663)

Equation (1.663) shows that, in spin polaron model, the transition rate R is activated only for temperatures $KT << B$, whereas for $KT \gg B$, there is no activation energy. It is due to the fact that at high temperature, both sites are essencially disordered and appear identical from an electron's point of view. At low T and large N,

$$R = K\nu \; e^{\Delta S^P / K} \; e^{-\Delta E^P / KT}$$

(1.664)

comparing equations (1.663) and (1.664) we have,

$$\left.\begin{aligned} K\nu &= \pi J^2 / hB, \\ \frac{\Delta S^P}{K} &= 2N \ln 2 \\ \text{and} \quad \Delta E^P &= 2NB \end{aligned}\right\} \qquad (1.665)$$

Here, both ΔS^P and ΔE^P are positive and proportional to 2N following a positive compensation temperature $T_c = \frac{B}{\ln 2}$. The activation energy 2 NB corresponds to flipping of half the total number of spins at both sites.

CHAPTER - 3

EXPERIMENTAL -- SET-UP -- PROCEDURE

In this chapter, we describe the general experimental techniques used in the present investigation on the electrical properties of organic semiconductors. Details of any particular experimental procedure will be described in conjunction with the discussions of the results thereby obtained in chapters 3 and 4.

1. Chemicals

The Eastman Organic Chemicals, nitro-aromatic semiconductors used in this investigation are 9-nitroanthracene, 2-nitrofluorene 1,4 dinitronaphthalene, 1,3,5-trinitrobenzene, o-, m- and p-nitrobenzoic acids which have been recrystallised several times from purified solvents before use. The organic liquids used were of spectrograde quality of B.D.H. and E. Merck. The teflon spacers and the conducting glass electrodes were obtained from Dielectric Corporation (U. S. A.) and Fisher Scientific Co. (U. S. A.) respectively.

2. Preparation of the Conductivity Cell

Applying the usual procedures[33,34,117,118], the conductivity sandwich cells were prepared in air by putting about 5 mgs of the

semiconducting materials on a clean stainless steel flat electrode surface in safe light illumination. Two teflon spacers, 2 mils (0.005 cm) thick, were positioned near the edges of the electrode, and the powdered crystals were flattened by gently rotating the conducting glass electrode with the conducting side in contact with the specimen. The teflon spacers maintained the seperation between the electrodes. Two spring clips were fixed at a moderate pressure to the ends of the electrodes in order to maintain the sandwich cell.

3. The Experimental Arrangement

The experimental set-up (Fig. 2.1) for the studies of semiconductivity is similar to that of Rosenberg et al[36,113]. The sandwich cells were placed in a conductivity chamber made of brass and fashioned entirely with teflon. (all the electrical surface leakage parts were also of teflon). The stainless steel electrode was placed on a thermal copper bar platform in good thermal contact through thermal paste and thus the temperature of the cell could be controlled from out side. A d.c. voltage of 22.5 volts from dry batteries was applied across the cells. There was a gas inlet and an out-let in the chamber for gas adsorption study and an arrangement for connecting the out-let with a suction pump. The chamber atmosphere could circulate freely through the opposite open sides of the sandwich cell.

FIGURE - 2.1

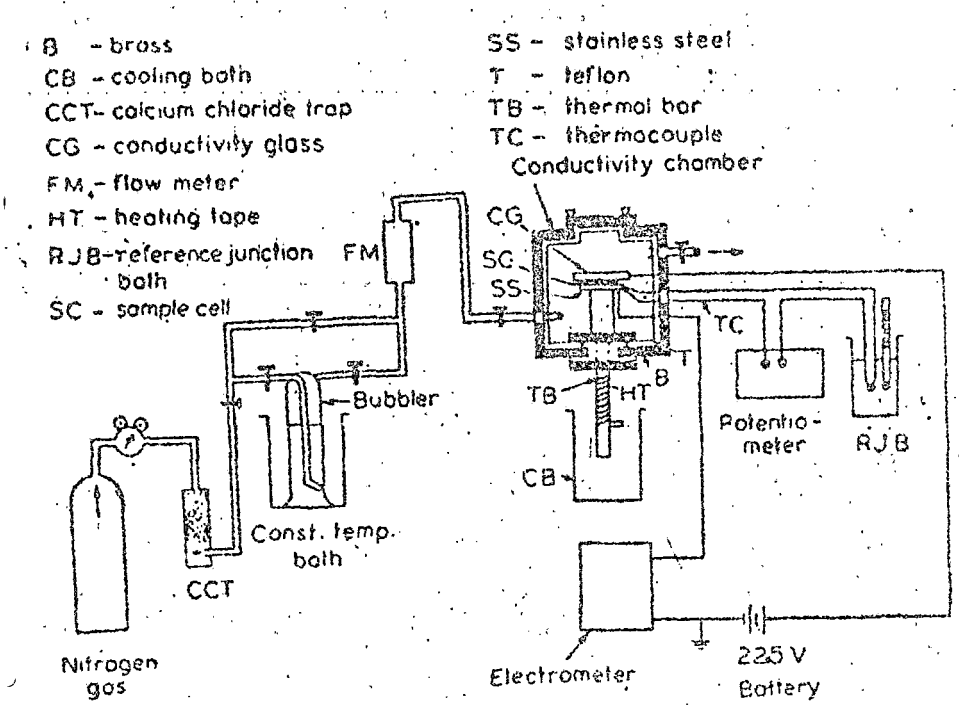

A schematic diagram of the apparatus used to study the effects of the adsorbed vapours on the conductivity of the nitroaromatic semiconductors.

Temperature measurements were made using a copper-constantan thermocouple attached at the top of the metal electrode and a millivolt potentiometer of Toshniwal Brothers Pvt. Ltd., India. The semiconduction currents were measured with an electrometer amplifier EA 813 of the Electronic Corporation of India Ltd. In order to eliminate the effects of oxygen, water vapour or any other vapours or gases adsorbed by the sample before experiment, the chamber was thoroughly flushed with dry nitrogen gas and the sample was then given repeated heating and cooling treatments in nitrogen atmosphere over the temperature range to be studied.

To pass various vapours inside the chamber, dry nitrogen gas was used as a carrier which was passed through a bubbler containing the organic liquid kept at a required temperature to maintain a fixed partial vapour pressure less than the saturation vapour pressure at sample cell temperatures. For desorption studies, dry nitrogen gas was allowed to pass directly through the chamber. The measurement of dark currents at a constant or different cell temperatures was carried out maintaining the cells in nitrogen, vacuum or different ambient atmospheres according to the experimental requirements.

CHAPTER - 3

ADSORPTION AND DESORPTION PROCESSES IN SOME NITROAROMATIC SEMICONDUCTOR-VAPOUR SYSTEMS : VAPOUR PRESSURE DEPENDENCE AND KINETIC ANALYSIS

1. Introduction

Adsorption of chemical vapours or gases produces a pronounced increase in the semiconduction currents of both organic[36,117,119-126] and inorganic[127-131] solids. It has been observed[36,117,119, 132] that the conductivity change is generally reversible i.e. the original vacuum or nitrogen atmosphere values are obtained by gently pumping the conductivity chamber or simply by flushing the chamber by dry nitrogen. This implies that the gas or vapour molecules are bound to the surface of semiconductor molecules by weak coupling forces[144]. In some cases, when the process is not efficiently reversible or the original value is not even regained, strong bound complexes are formed[133]. In polyenes,[134,135] adsorption and desorption kinetic analysis shows that the weakly bound complexes are formed and the adsorption and desorption is a 'two-stage process'.

Roginsky - Zeldovich (R - Z) equation[136,137] in a modified

form was applied to interprete the kinetic data in cases of hydration of proteins[133], adsorption of gases on β - carotene[117] and some linear long chain polyenes,[134,135] which may be written as :

$$dm/dt = A \exp\left[-\beta m / RT\right] \qquad (1.1)$$

where A and β are constants at a particular pressure. The derivation of E - S equation assumes that the rate of adsorption possesses an activation energy which increases linearly with the amount of the adsorbed gas or vapour. It has also been shown with a good degree of certainty that at a constant temperature and for lower percentage of gas adsorption, conductivity increases exponentially with the amount adsorbed.

It appears that the kinetic studies can throw much light on the nature of interaction and also on the process involved during adsorption and desorption of vapours on the semiconductor. We have examined the adsorption and desorption kinetics in a number of nitroaromatic semiconductor-vapour systems and found that along with a general two stage process in some cases of vapour adsorption a different three stage process is also operative.

In this chapter, we present our results followed by discussions on how the conductivity depends on the pressure of the

adsorbed vapour, the validity of R = Z equation and finally on the possible models for adsorption processes.

2. Experimental and Results

2.1 The effect of adsorption of vapours on the semiconduction current of the nitroaromatics :

The effects of adsorption of a series of vapours were studied in the usual manner as described in the previous chapter. The sandwich cell was temperature-cycled and dry nitrogen gas was allowed to pass through the chamber to desorb any vapour or gas adsorbed by the sample prior to the experiment. The cell was then kept at a constant temperature and the flow of the carrier gas, dry nitrogen, was maintained through the bubbler containing the reagent liquid at a constant temperature to attain a required vapour pressure. After a short pulse, when the powdered sample started adsorbing the vapour from the chamber atmosphere, the current increases and finally attains a saturation value after some time in most of the vapour - semiconductor systems. In some cases, the current enhancement was by several orders of magnitude. The result of such a measurement for vapour adsorption in 9-nitroanthracene, 1,4-dinitronaphthalene, 1,3,5-trinitrobenzene; 2-nitrofluorene; O-, m- and p- nitrobenzoic acids is shown in Fig. 3.1 - 3.7. When the chamber was flushed with dry nitrogen gas,

FIGURE - 3.1

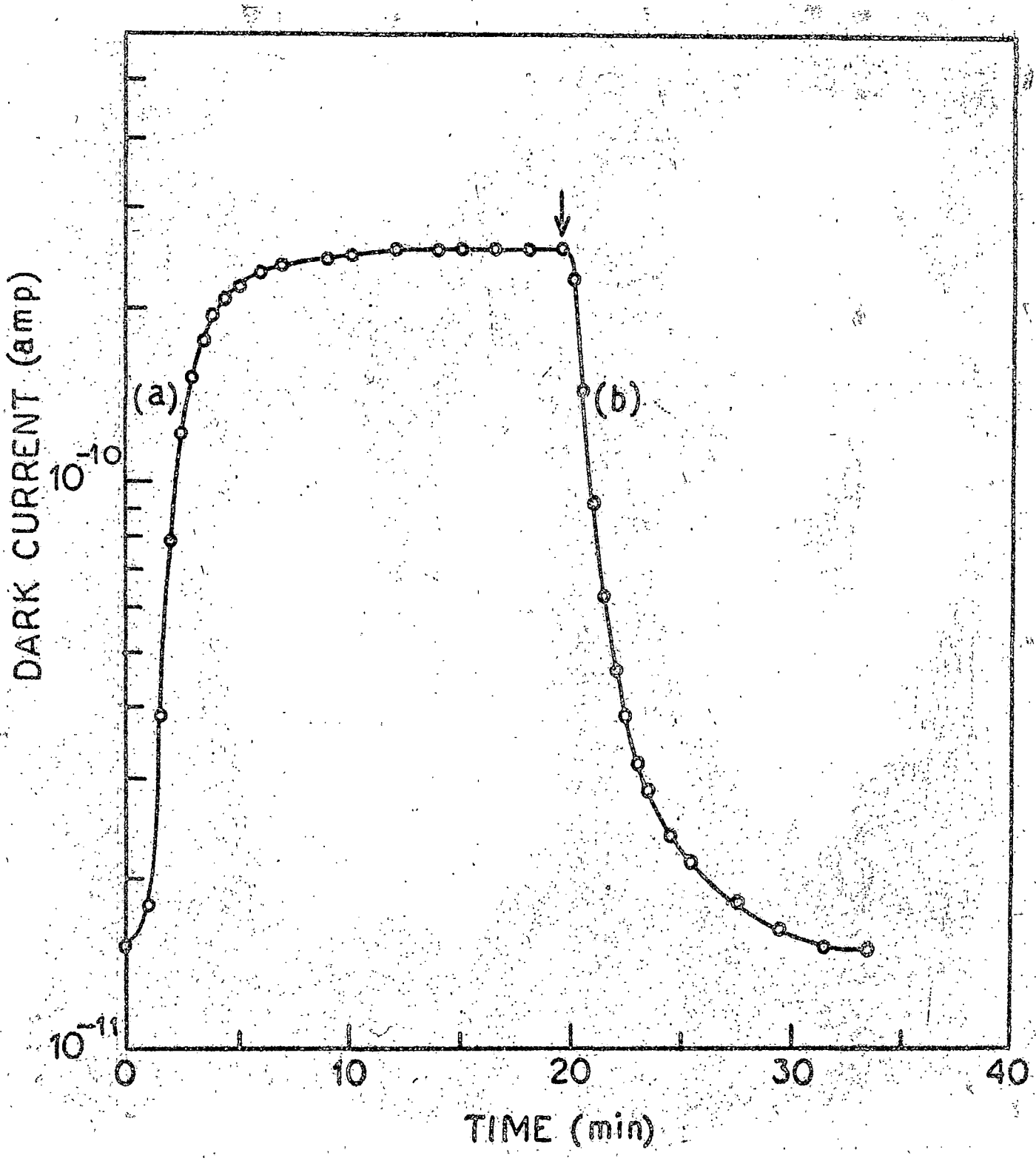

The change in dark current in a 9-nitroanthracene powder cell kept at 22°C with (a) adsorption and (b) desorption of carbontetrachloride vapour at 72.5 mm pressure.

FIGURE - 3.2

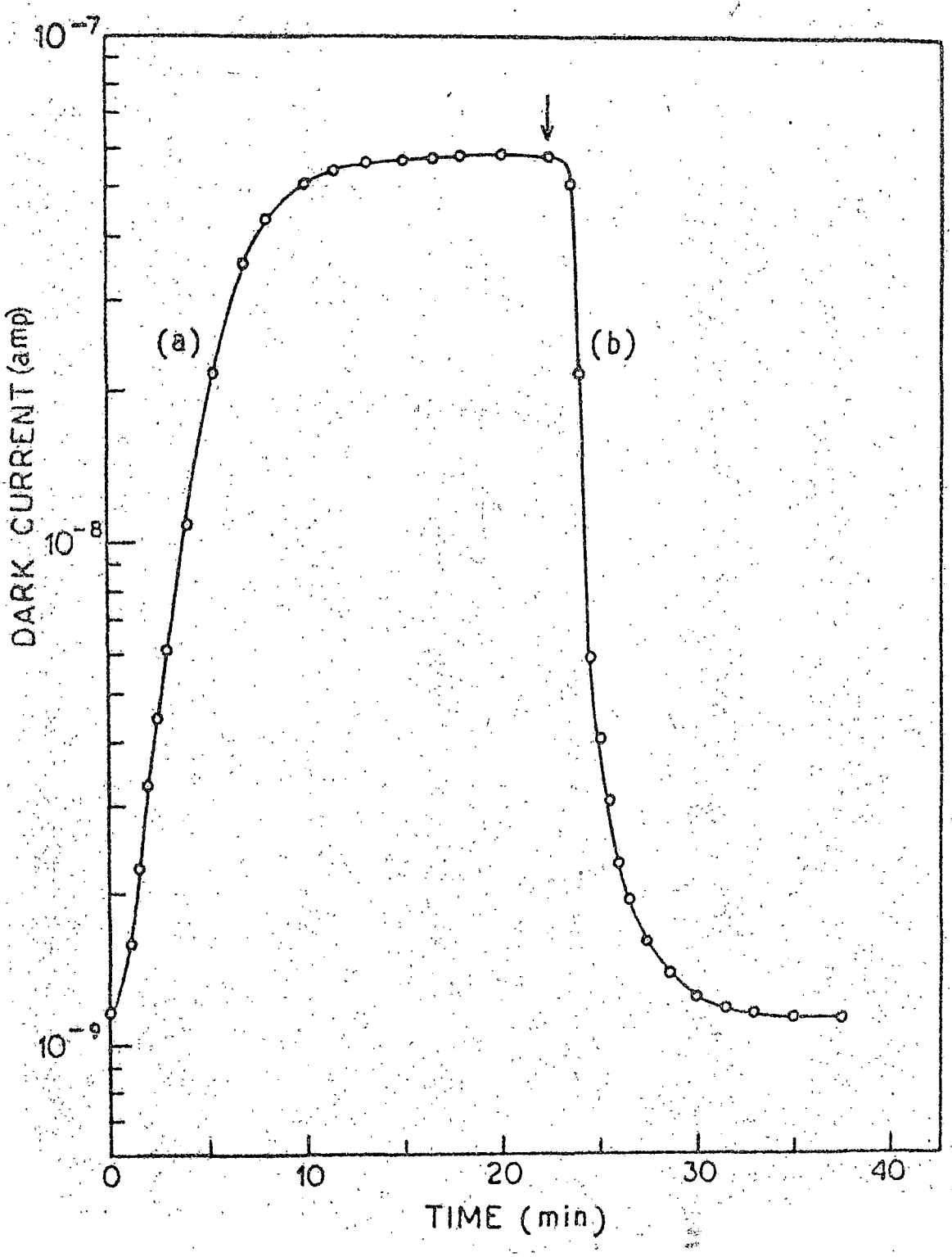

The change in dark current in a 1,4-dinitronaphthalene powder cell kept at 22°C with (a) adsorption and (b) desorption of methanol vapour at 71.3 mm pressure.

FIGURE - 3.3

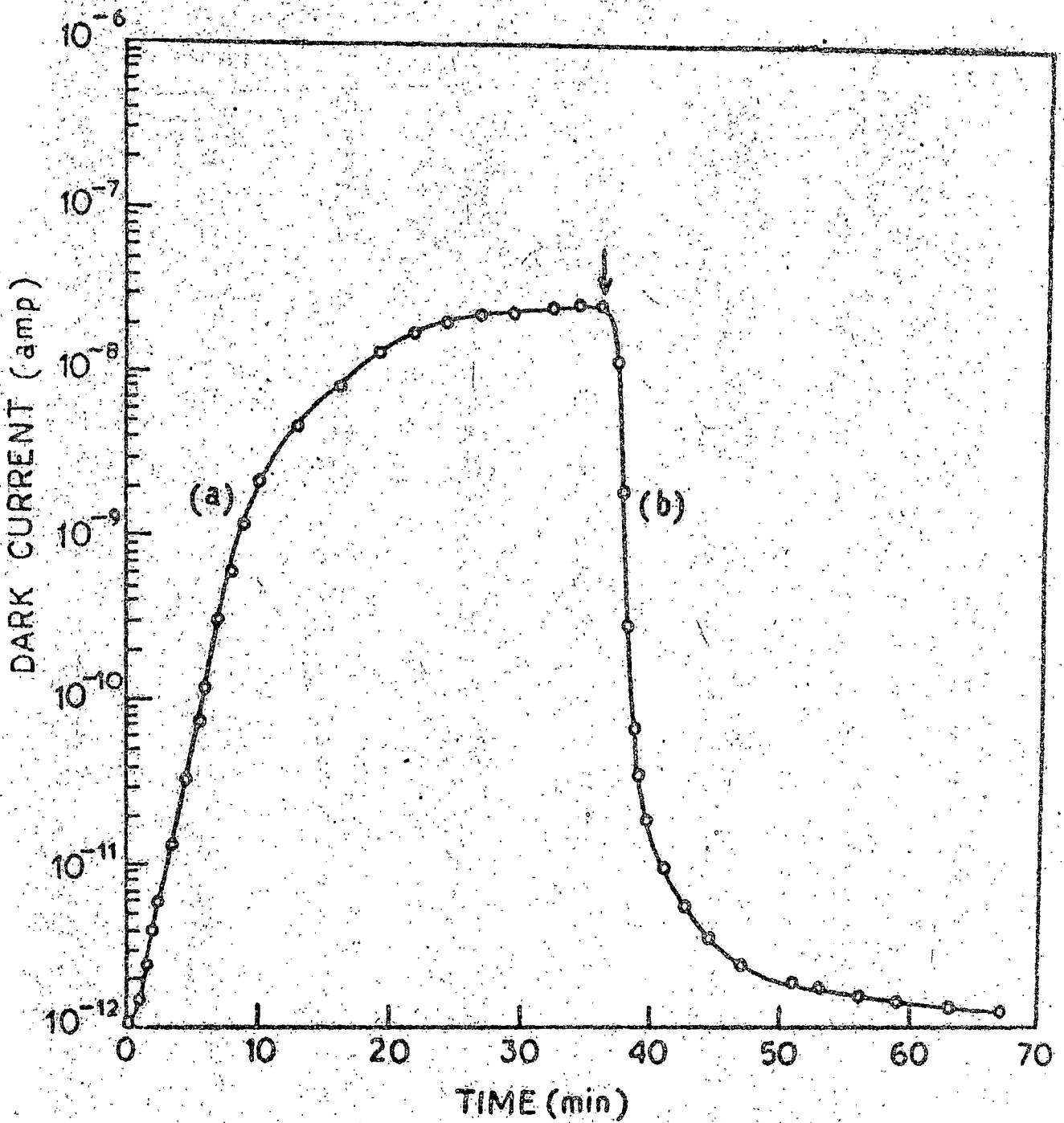

The change in dark current in a 1,3,5-trinitrobenzene powder cell kept at 22°C with (a) adsorption and (b) desorption of ethanol vapour at 38.8 mm pressure.

FIGURE - 3.4

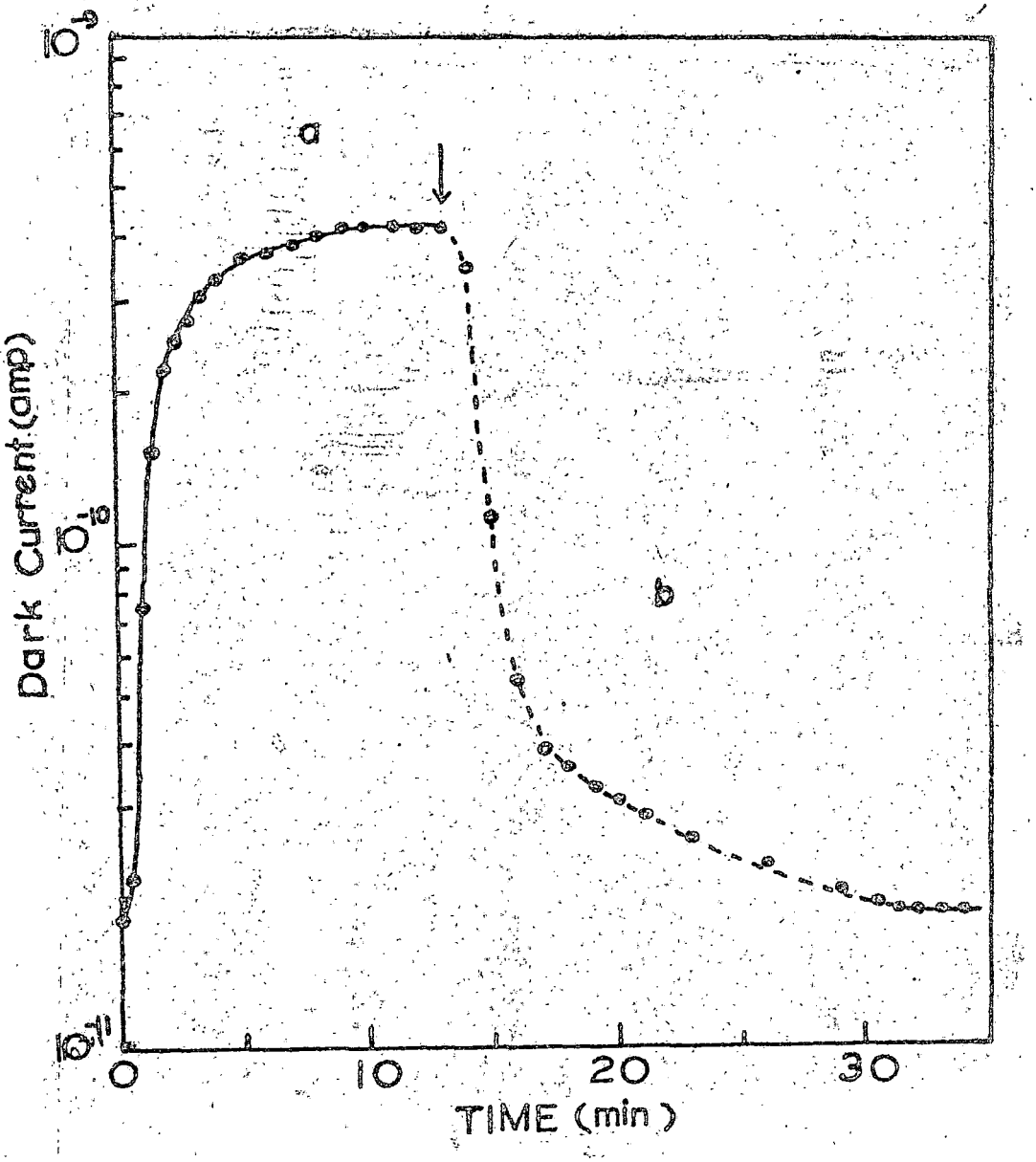

The change in dark current in a 2-nitrofluorene powder cell kept at 25°C with (a) adsorption and (b) desorption of ethylacetate vapour at 55 mm pressure.

FIGURE - 3.5

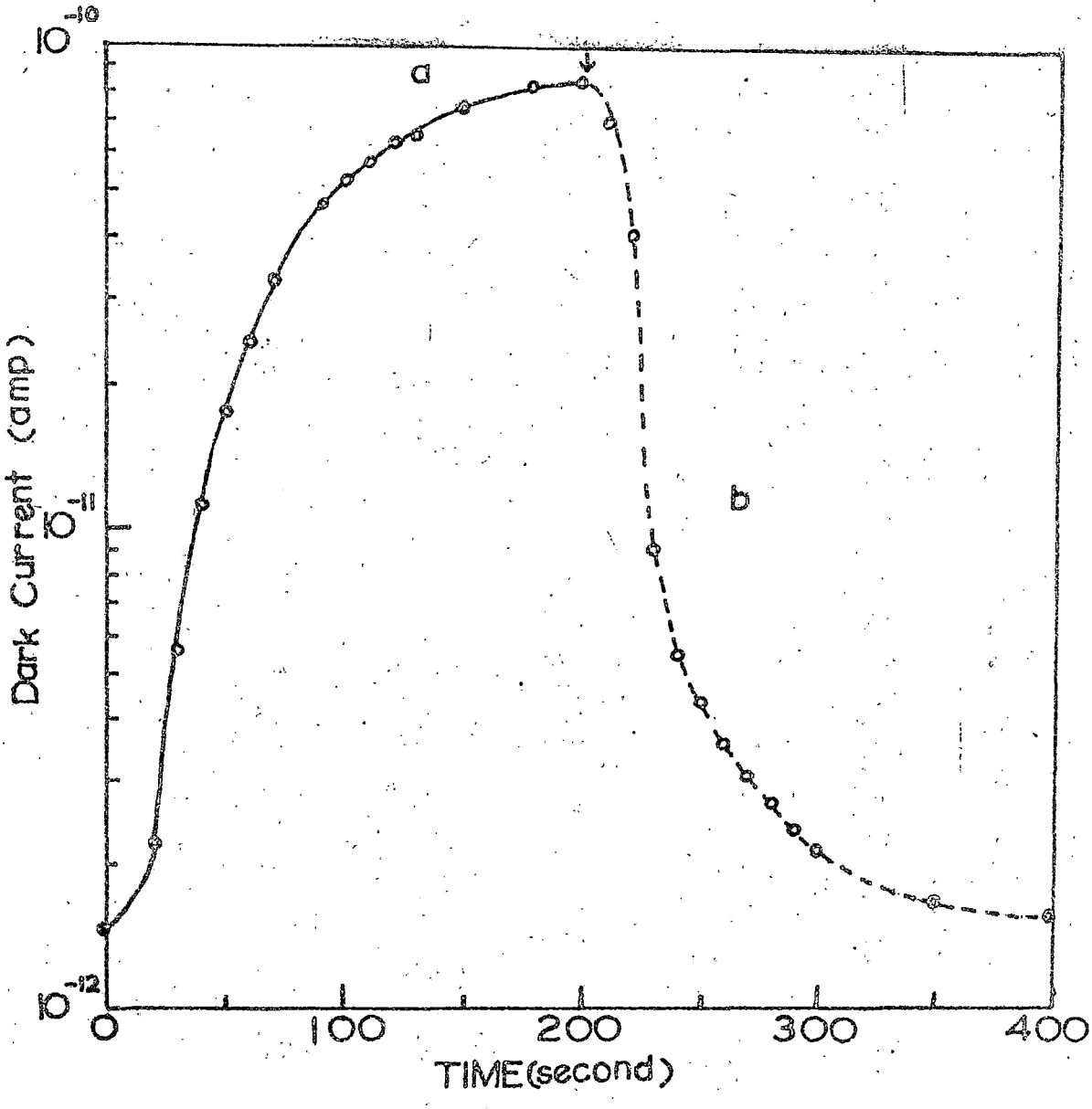

The change in dark current in a O-nitrobenzoic acid powder cell kept at 28°C with (a) adsorption and (b) desorption of ethyl-acetate vapour at 18.2 mm pressure.

FIGURE - 3.6

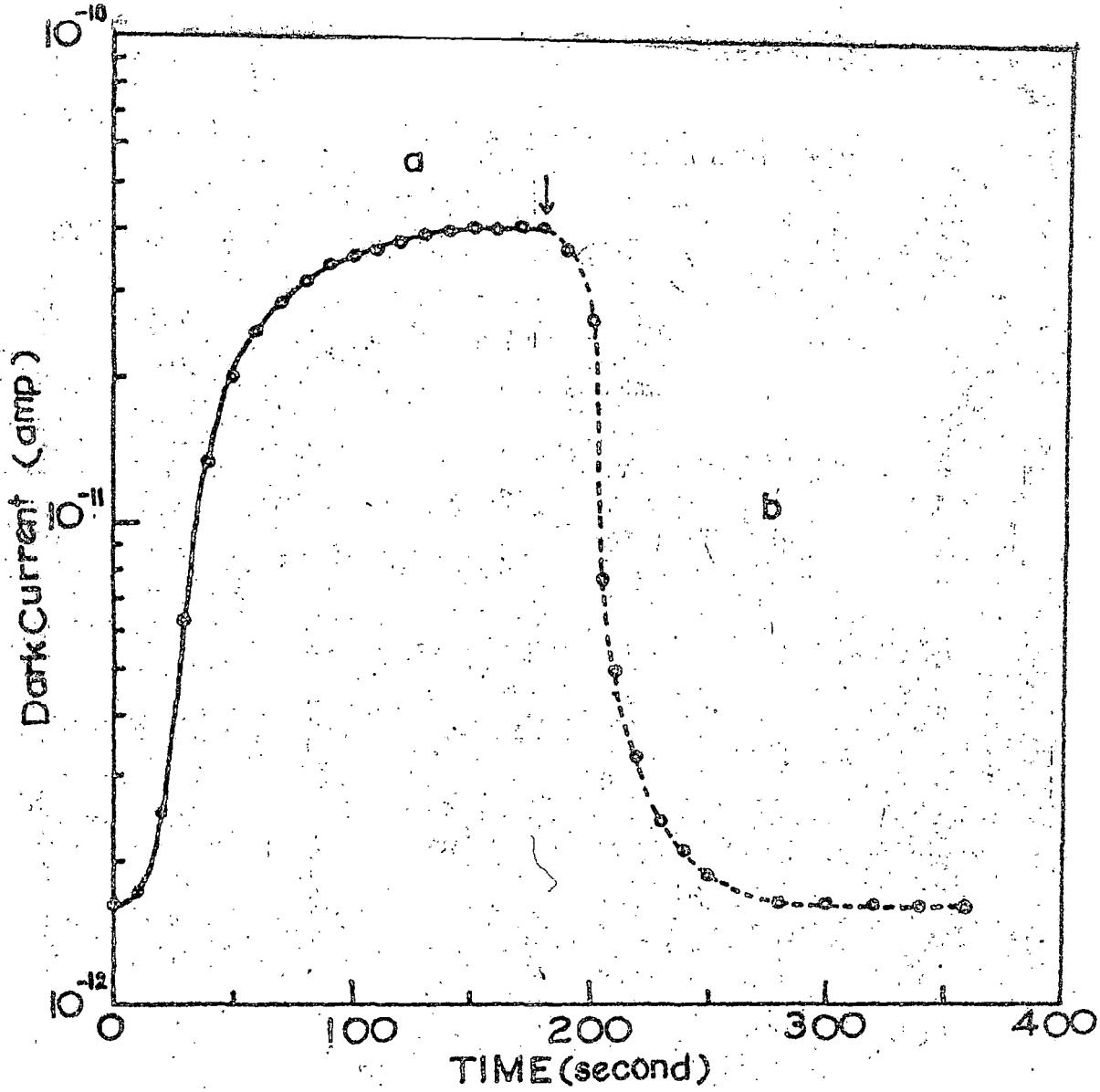

The change in dark current in a m-nitrobenzoic acid powder cell kept at 25°C with (a) adsorption and (b) desorption of ethylacetate vapour at 25.3 mm pressure.

FIGURE - 3.7

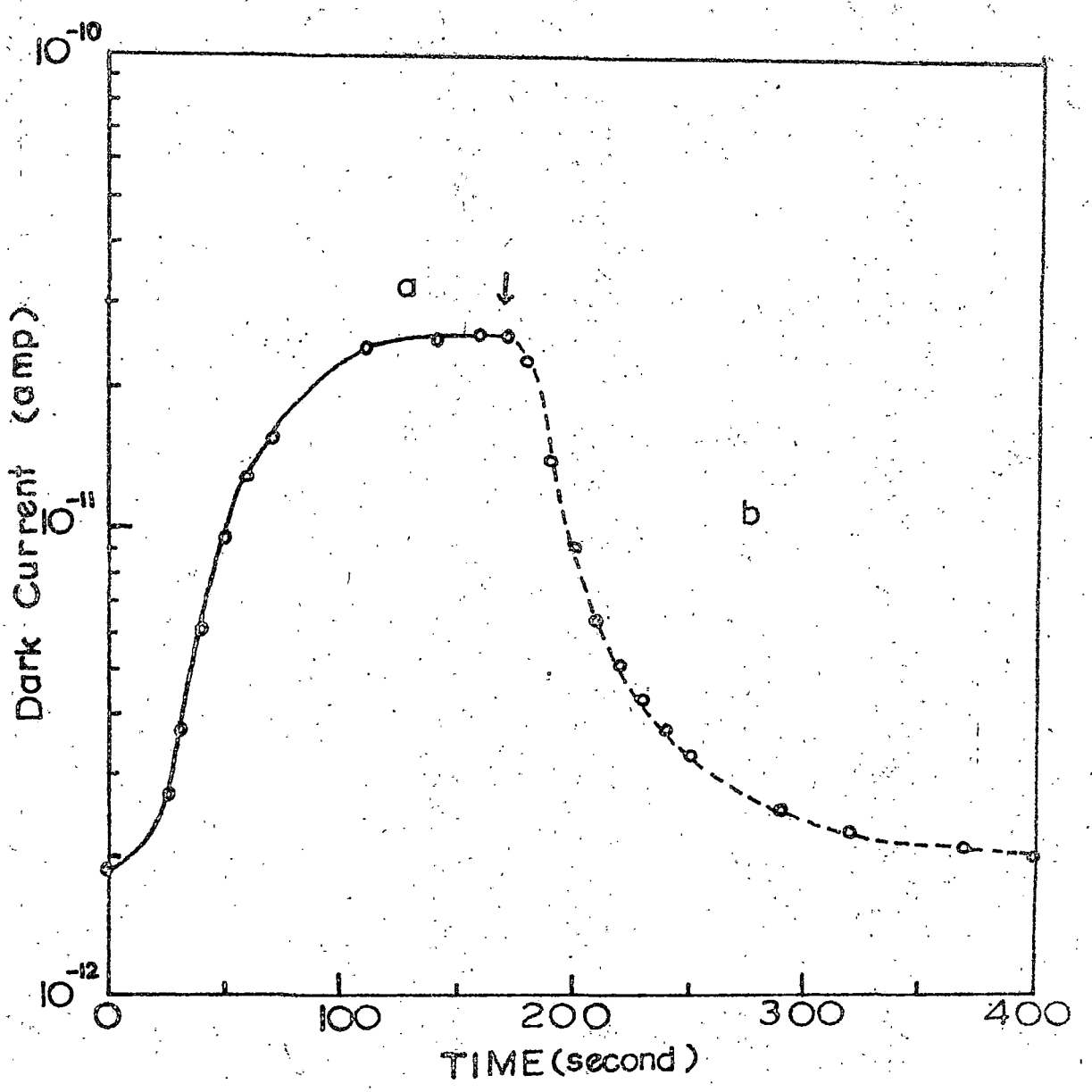

The change in dark current in a p-nitrobenzoic acid powder cell kept at 25°C with (a) adsorption and (b) desorption of ethylacetate vapour at 25.8 m pressure.

the vapour desorbs from the crystallite surfaces and the current comes back to the initial value. These are shown by the portion (b) of the curves. The arrow indicates the time when desorption starts. Such adsorption and desorption curves were obtained with other vapours also. Adsorption and desorption of vapours n-hexane, cyclohexane; carbontotrachlorides, methanol, benzene, ethyl acetate and ethanol on and from 9-nitroanthracene; 2-nitrofluorene; O-, m - and p - nitrobenzoic acids, vapours of ethanol, methanol and cyclohexane on and from 1,4 dinitronaphthalene and of ethanol, methanol, n - hexane and cyclohexane on and from 1,3,5-trinitrobenzene show similar behaviour as shown in Fig. 3.1 - 3.7.

But with certain vapour on 1,4 dinitronaphthalene and 1,3,5-trinitrobenzene such a saturation value was not reached and only a trend to reach a saturation value was observed in a long-time region as shown in Fig. 3.8 and 3.9. When the chamber was flushed with dry nitrogen the initial value was not attained even after 60 minutes. Adsorption and desorption curves similar to that shown in figure 3.8 and 3.9 are obtained for ethylacetate, benzene, carbontetrachloride and n-hexane adsorption on 1, 4 - dinitronaphthalene and for ethylacetate, benzene, carbontetrachloride, toluene, n-heptane and methyl-cyclohexane adsorption on 1,3,5-trinitrobenzene.

FIGURE - 3.8

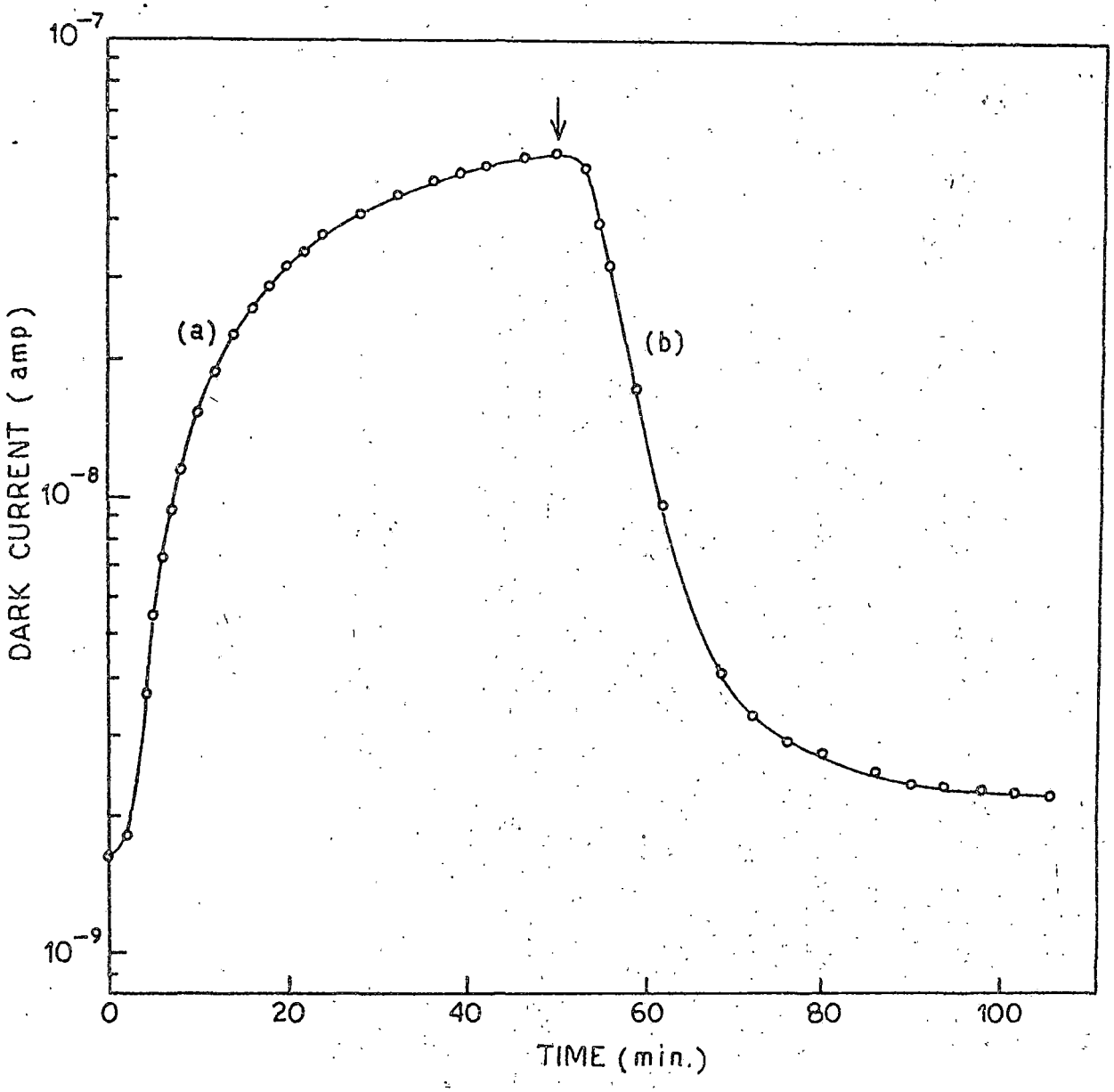

The change in dark current in a 1,4-dinitronaphthalene powder cell kept at 22°C with (a) adsorption and (b) desorption of ethylacetate vapour at 49.5 mm pressure (a trend to reach a saturation dark current value is seen at long time region).

FIGURE - 3.9

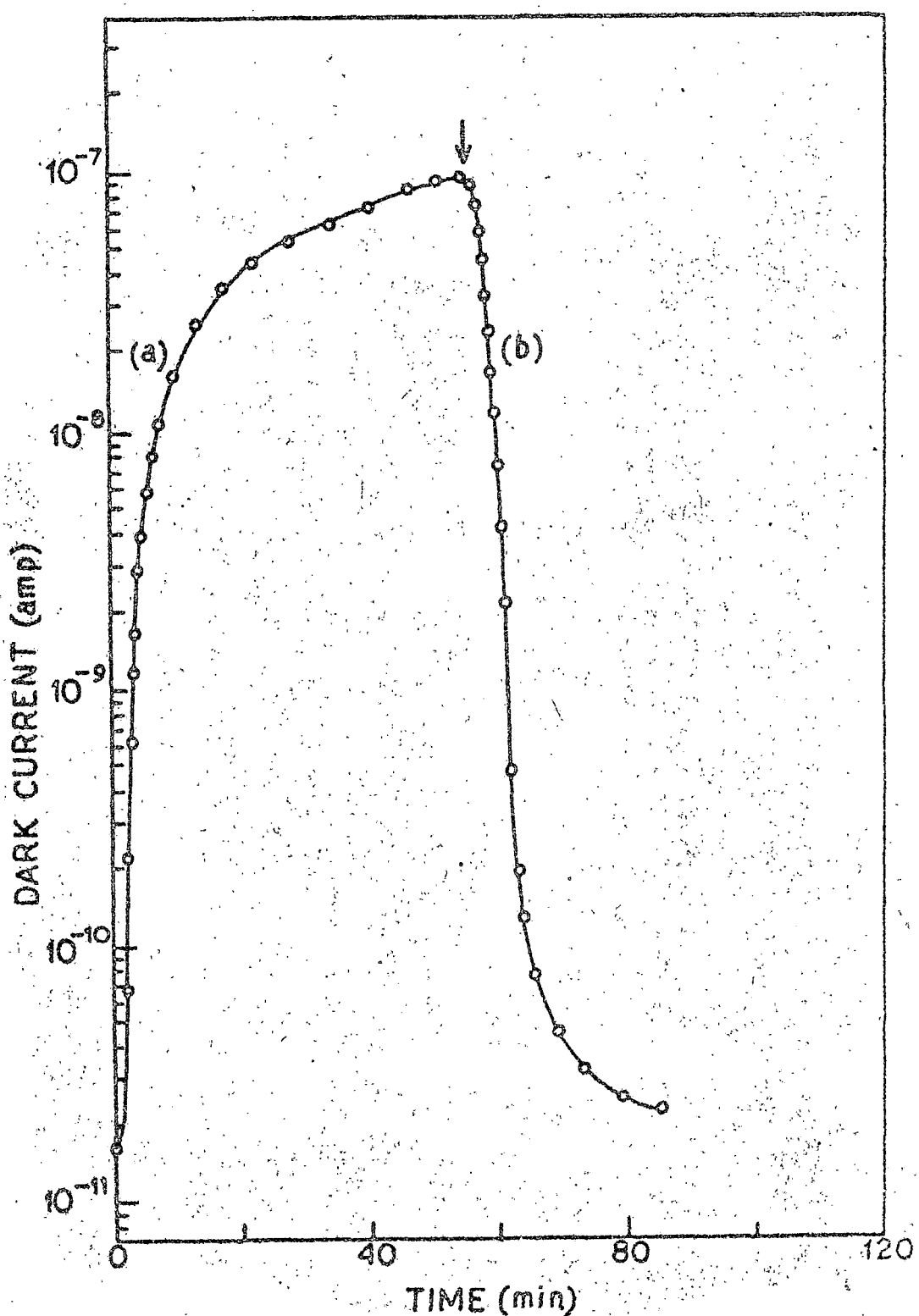

The change in dark current in a 1,3,5-trinitrobenzene powder cell kept at 32°C with (a) adsorption and (b) desorption of ethylacetate vapour at 61.4 mm pressure (a trend to reach a saturation dark current value is seen at long time region).

The saturation value of current in a vapour-semiconductor system under particular experimental condition depends on the vapour pressure of the reagent liquid and at the cell temperature, the time to attain this steady state value being dependent on the flow rate.

The sensitivity as measured by (σ_A/σ_V) values for adsorption of various vapours on the surfaces of different nitroaromatic semiconductors are summarised in tables 3.1 (a) and (b), where σ_A is the specific conductivity at saturation after vapour adsorption and σ_V is that before adsorption. The sensitivity depends on the chemical nature of the adsorbed molecules.

2.2 Vapour pressure dependence of conductivity

The magnitude of the current enhancement at a constant cell temperature was studied as a function of partial pressure of the vapours in the chamber. The partial pressure of the vapour in the chamber was varied by changing the temperature of the reagent chemical in the bubbler through which the dry nitrogen gas was passed and fed into the conductivity chamber. At a constant flow rate, the partial pressure of the reagent liquid vapour in the chamber atmosphere was proportional to the vapour pressure of the liquid at the temperature it was kept. The steady state

Table 3.1 (a)

Rise in the dark current in the powder cells of some nitroaromatic semiconductors at 22°C on adsorption of various vapours at the same pressure (p) for semiconductor-vapour pair where quick saturation is reached.

Vapour used	σ_A/σ_V		
	9-nitro-anthracene (p = 60 mm)	1,4-dinitro-naphthalene (p = 50 mm)	1,3,5-trinitro-benzene (p = 60 mm)
n-Hexane	-	-	8.5
Cyclo-hexane	-	3	10
Carbontetra-chloride	3	-	-
Methanol	6	8	2×10^1
Benzene	3×10^1	-	-
Ethyl-acetate	3×10^1	-	-
Ethanol	1.2×10^3	3×10^2	5×10^6

Table 3.1 (b)

Rise in the dark current in the powder cells of some nitroaromatic semiconductors at 25°C on adsorption of various vapours at the same pressure (50 mm) for semiconductor-vapour pair where quick saturation is reached.

Vapour used	σ_A/σ_V			
	nitro-fluorene	O-nitro-benzoic-acid	m-nitro-benzoic-acid	p-nitro-benzoic acid
n-Hexane	0.25 x 10	0.15 x 10	0.2 x 10	0.2 x 10
Cyclohexane	0.3 x 10	0.2 x 10	0.25x 10	0.27x 10
CCl_4	0.40 x 10	4.0	3.0	2.0
C_6H_6	0.1 x 10^2	4.30 x 10	6.0	2.5
Ethyl-acetate	0.14 x 10^2	1.00 x 10^4	1.3 x 10^3	9.0
Methanol	0.49 x 10^2	2.5 x 10^2	2.4 x 10^2	9.0
Ethanol	1.2 x 10^3	1.0 x 10^4	3.7 x 10^3	6.8 x 10^2

current (i.e. the saturation current) was noted for different vapour pressures. The kinetic data for the dark current enhancement for ethyl-acetate vapour adsorption at different vapour pressures were also recorded.

3. Discussions

3.1 Dependence of the conductivity on vapour pressure :

The rise in conductivity of the nitroaromatic semiconductors was studied as a function of the partial pressure of a vapour at a constant sample temperature.

At constant flow and constant vapour pressure, the conductivity after adsorption $\sigma_A(m)$ follows a relation

$$\sigma_A(m) = \sigma_V \exp (\alpha m) \qquad (3.11)$$

where ' α ' is a constant and 'm' is the amount of vapour adsorbed.

It is assumed that 'm' depends on the partial pressure (P) of the reagent chemical and in the initial period, also on the time of exposure. After some time, however, an equilibrium is established. Thus, we assume[119,133-135, 147] that in the initial

region

$$m(t) = Q(t) \cdot p \qquad (3.12)$$

where Q (t) is a function of time.

At equilibrium,

$$m_0 = Q_0 \cdot p \qquad (3.13)$$

where Q_0 now becomes independent of time. This is expected from Langmuir's adsorption isotherms[139], when a small fraction of the surface is covered by the gas or vapour molecules. Substituting equation (3.12) in equation (3.11), we get :

$$\sigma_A [m(t)] = \sigma_v \exp[\alpha \cdot Q(t) \cdot p] \qquad (3.14)$$

and at equilibrium,

$$\sigma_A (m_0) = \sigma_v \exp(\alpha \cdot Q_0 \cdot p) \qquad (3.15)$$

A plot of log σ_A (m_0) or logarithm of the saturation current vs. p at equilibrium is expected to be linear from equation (3.15).

In Figs. 3.10 and 3.11, we show such plots of the logarithm of the saturation dark current against the vapour pressure (p) at equilibrium if the adsorption kinetics are of the type shown

FIGURE - 3.10

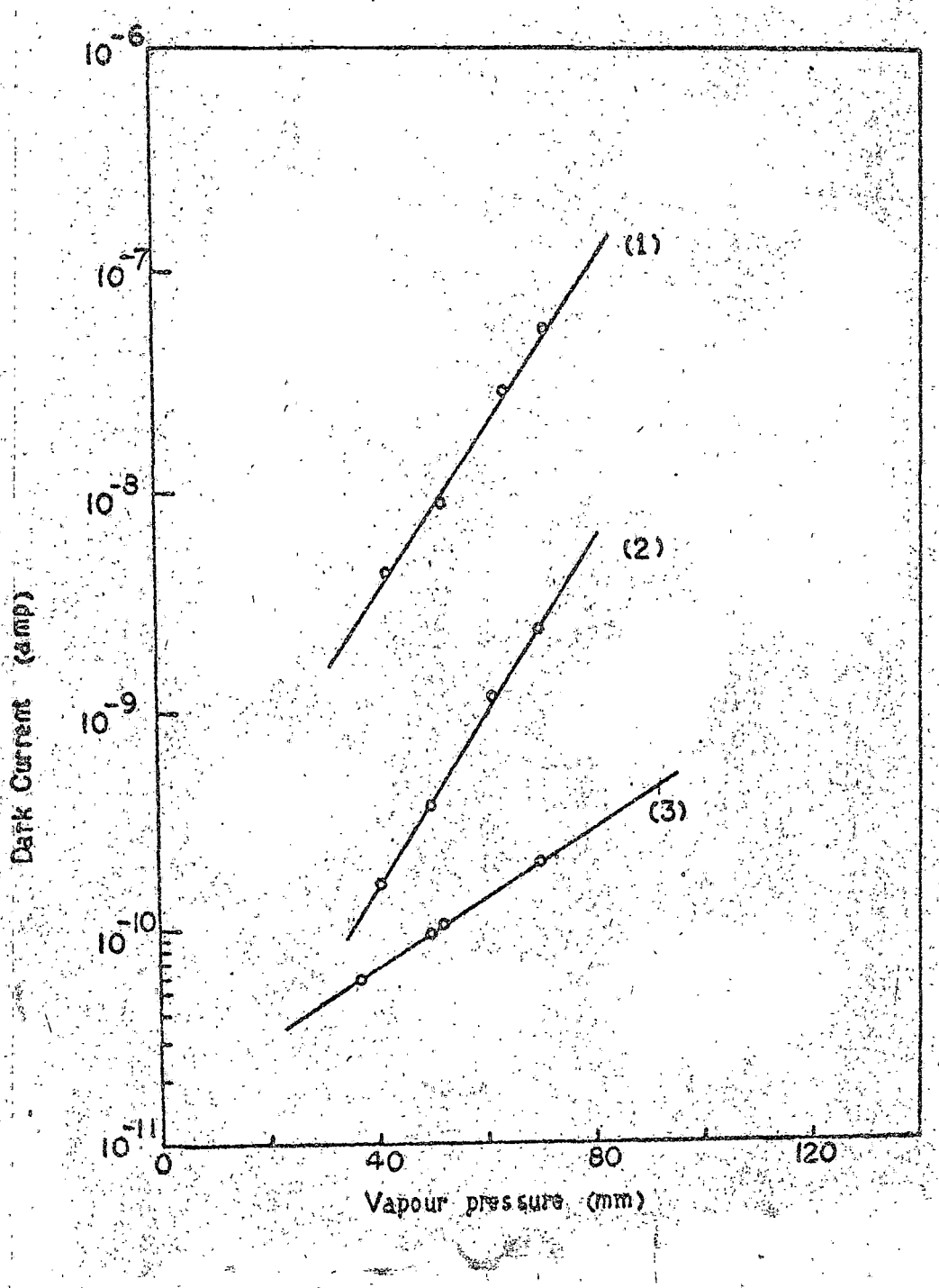

The change in dark current of (1) 1,4-dinitronaphthalene, (2) 1,3,6-trinitrobenzene and (3) 9-nitroanthracene powder cells at a constant cell temperature at 22°C as a function of the vapour pressure of methanol.

FIGURE - 2.11

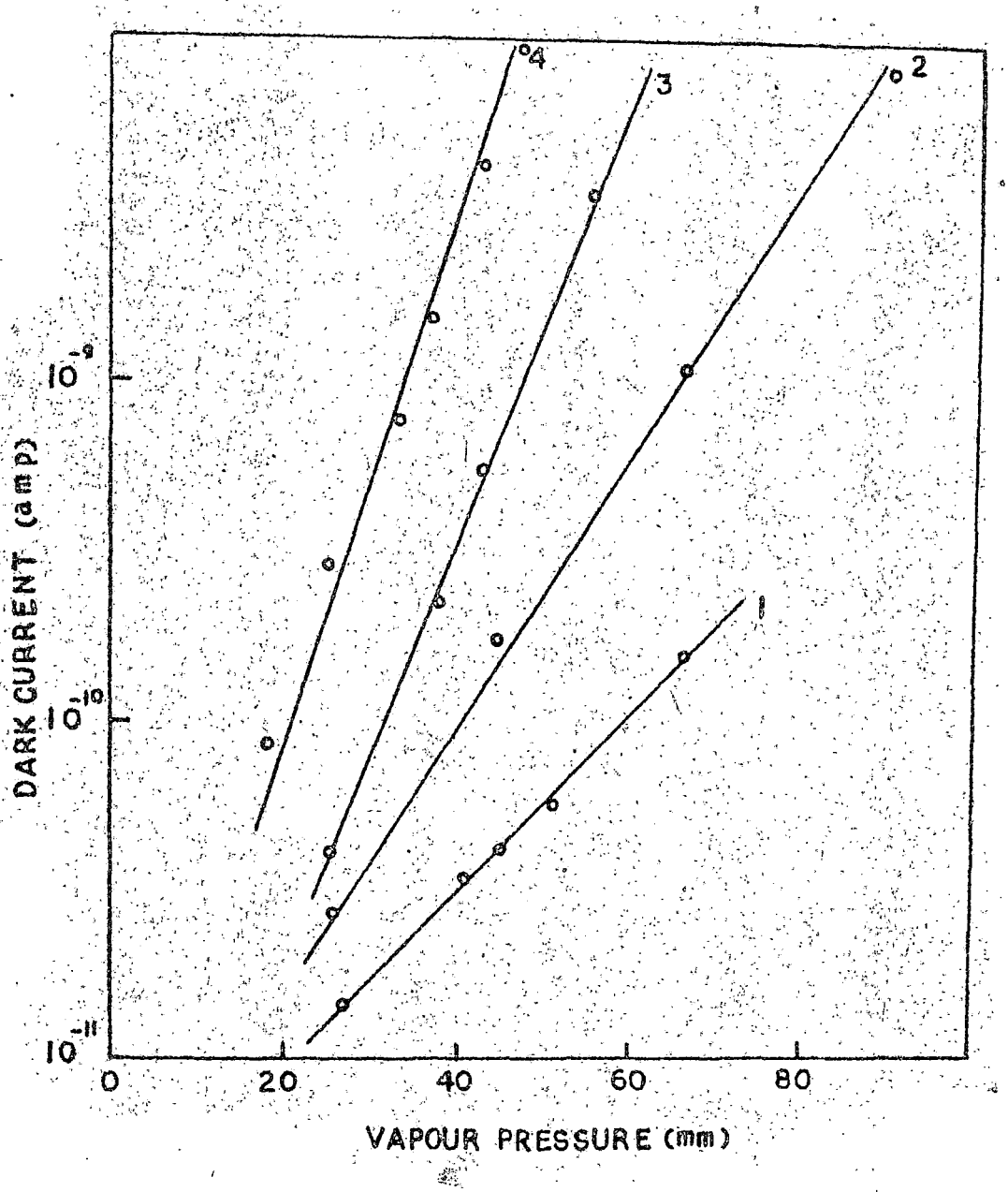

The change in saturation dark current of (1) 2-nitrofluorene, (2) p-nitrobenzoic acid, (3) m-nitrobenzoic acid and (4) o-nitrobenzoic acid powder cells at a constant cell temperature (25°C) as a function of the vapour pressure of ethyl acetate.

in Figs. 3.1 - 3.7. Fairly good straight lines are obtained. The slopes of these lines (αq_0) is the measure of the strength of interaction between the vapour molecules and the semiconductors. The values of αq_0 for different vapour - semiconductor pairs are presented in table 3.2 to gauge the relative strength of interaction. The linear plots (Figs. 3.10 and 3.11) suggest the applicability of the Langmuir's adsorption isotherm for small fraction of surface coverage in these cases of vapour adsorption.

3.2 Adsorption and desorption kinetics

In order to test whether the adsorption and desorption kinetics follow the Roginsky Zeldovich equation, let us integrate equation (1.1) giving :

$$n(t) = \frac{RT}{\beta} \log (t + t_0) + \text{const.} \quad (3.21)$$

From equations (3.11) and (3.21), we get :

$$\log \sigma_A = \frac{\alpha RT}{\beta} \log (t + t_0) + \text{const.} \quad (3.22)$$

Similarly, a suitable equation for desorption kinetics may be given by :

$$\log \sigma_A' = - \frac{\alpha RT}{\beta^*} \log (t + t'_0) + \text{const.} \quad (3.23)$$

Table 3.2

Values of ($\alpha \cdot Q_0$) for different vapour-semiconductor pairs

Semiconductor	Vapour	$\alpha \cdot Q_0$ (mm^{-1})
9-nitroanthracene	CCl_4	0.022
	Methanol	0.037
	Benzene	0.041
	Ethanol	0.125
1,4-dinitronaphthalene	Methanol	0.087
	Ethanol	0.176
1,3,5-trinitrobenzene	Methanol	0.094
	Ethanol	0.247
2-nitrofluorene	Ethyl acetate	0.0503
O-nitrobenzoic acid	Ethyl acetate	0.0179
m-nitrobenzoic acid	Ethyl acetate	0.0147
p-nitrobenzoic acid	Ethyl acetate	0.0943

Thus, for any empirically chosen t_o or t'_o, linear plots of log σ_A vs. log ($t + t_o$) for adsorption and log σ_A vs. log ($t + t'_o$) for desorption are suggested in the initial region of adsorption and desorption respectively.

Figures 3.12 - 3.20 show such R - z plots for adsorption whereas Figs 3.21 - 3.29 represent the same plots for desorption kinetic data. The time indicated in the abscissa is the time measured from the initiation of adsorption or desorption.

R - z plots of the kinetic data show that in the initial region of adsorption and desorption the slopes of the curves at different vapour pressures are different. This shows the pressure dependence of β and β^*. The higher the partial vapour pressure, the higher is the slope. The values of β/α ($= \beta'$) and β^*/α ($= \beta^{*\prime}$) have been estimated from the slopes. The variation of β' and $\beta^{*\prime}$ with vapour pressure are shown in table 3.3. Like β', $\beta^{*\prime}$ also decreases with increasing vapour pressure. For any particular pressure of ambient vapour, $\beta^{*\prime}$ is larger than β'.

Examination of Figs. 3.19, 3.20, 3.28 and 3.29 indicates that in the long time region the experimental points in R - z plots show excellent linearity with a different slope than the one in the short time region. This is different from that observed in Figs. 3.12 - 3.18 and 3.21 - 3.27 where in the long time region,

FIGURE - 3.12

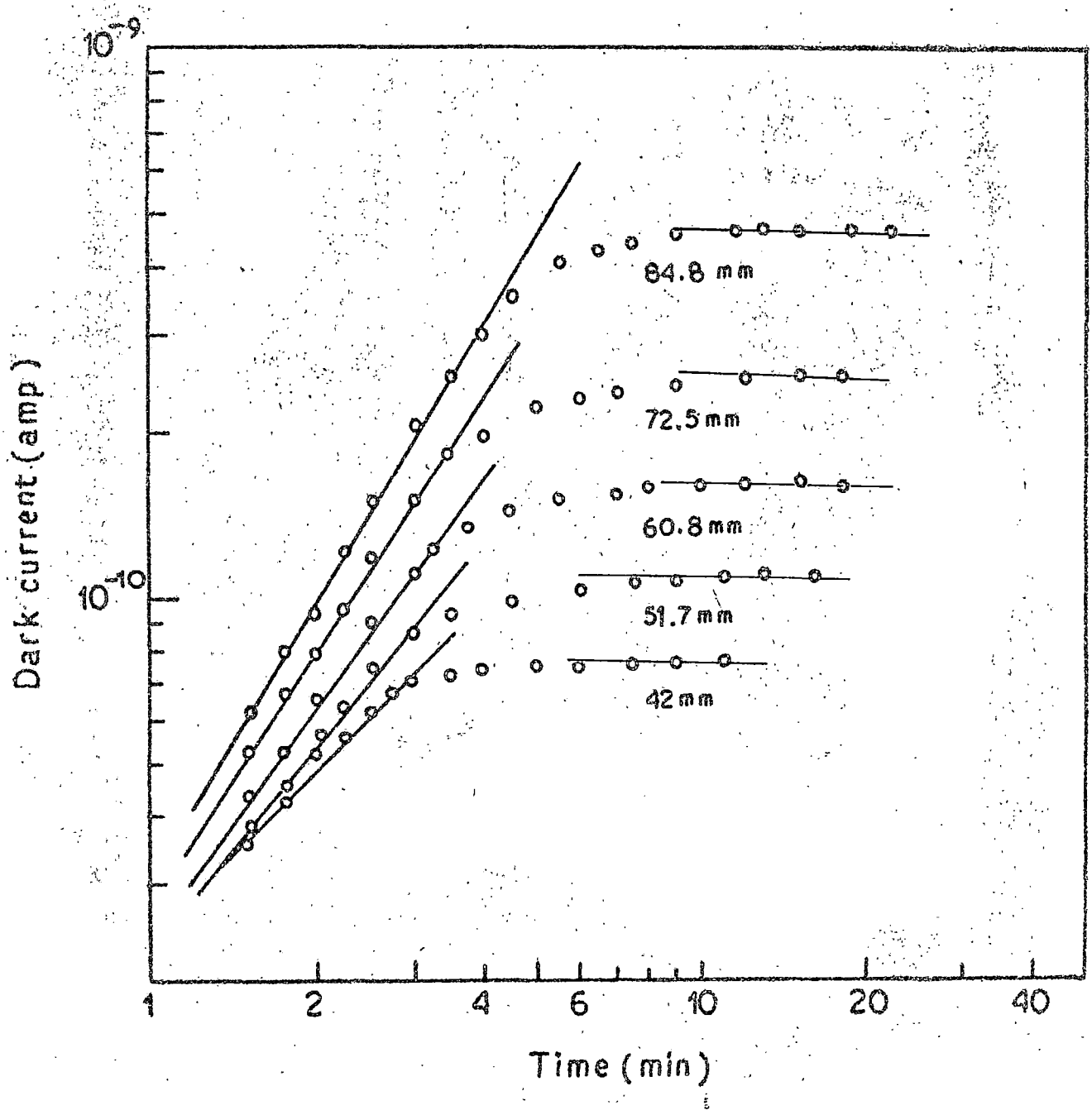

The R - S plot of the kinetic data at different vapour pressures for carbontetrachloride vapour adsorption on 9-nitro-anthracene.

FIGURE - 3.13

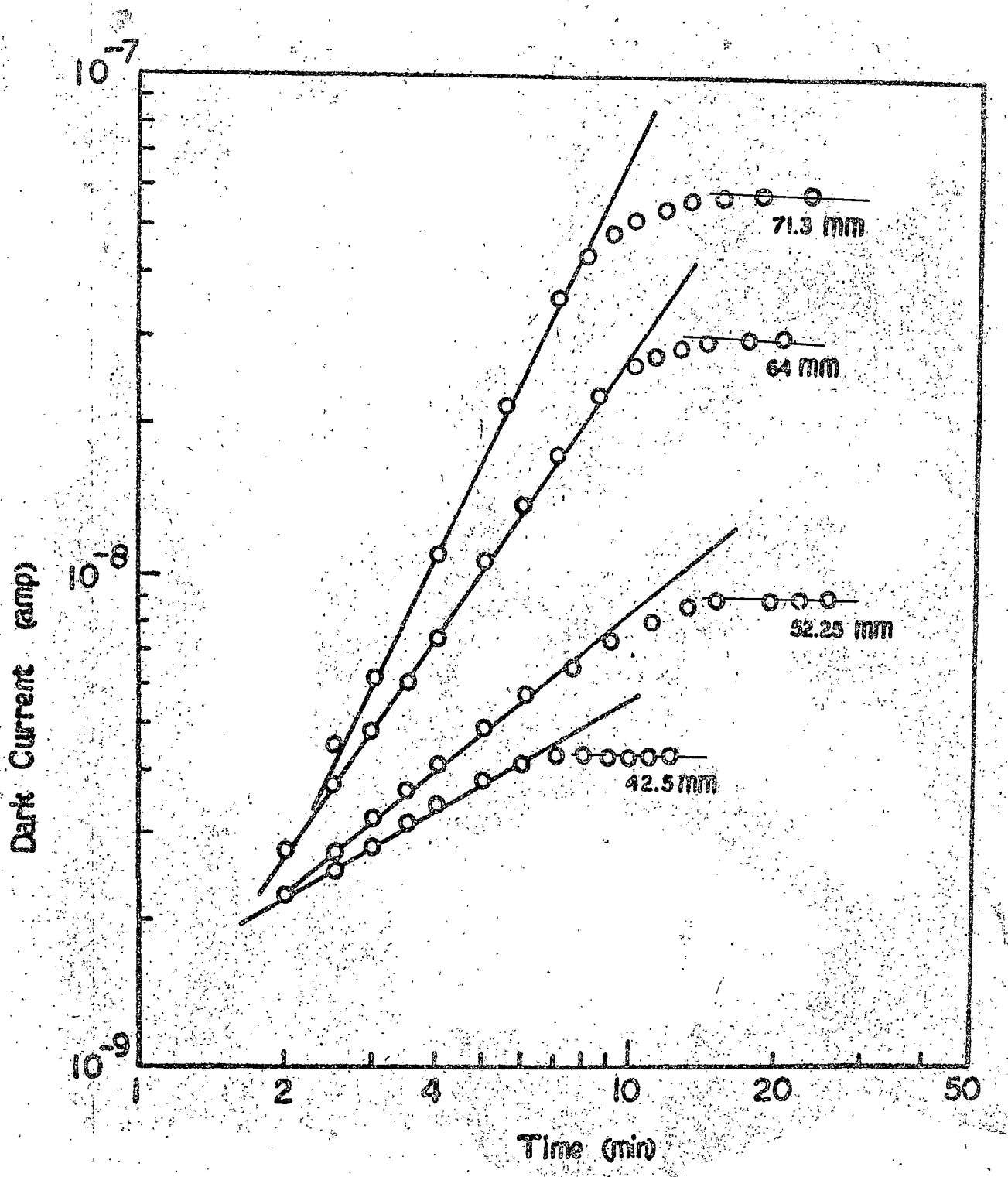

The H - Z plot of the kinetic data at different vapour pressures for methanol vapour adsorption on 1,4-dinitronaphthalene.

FIGURE - 3.14

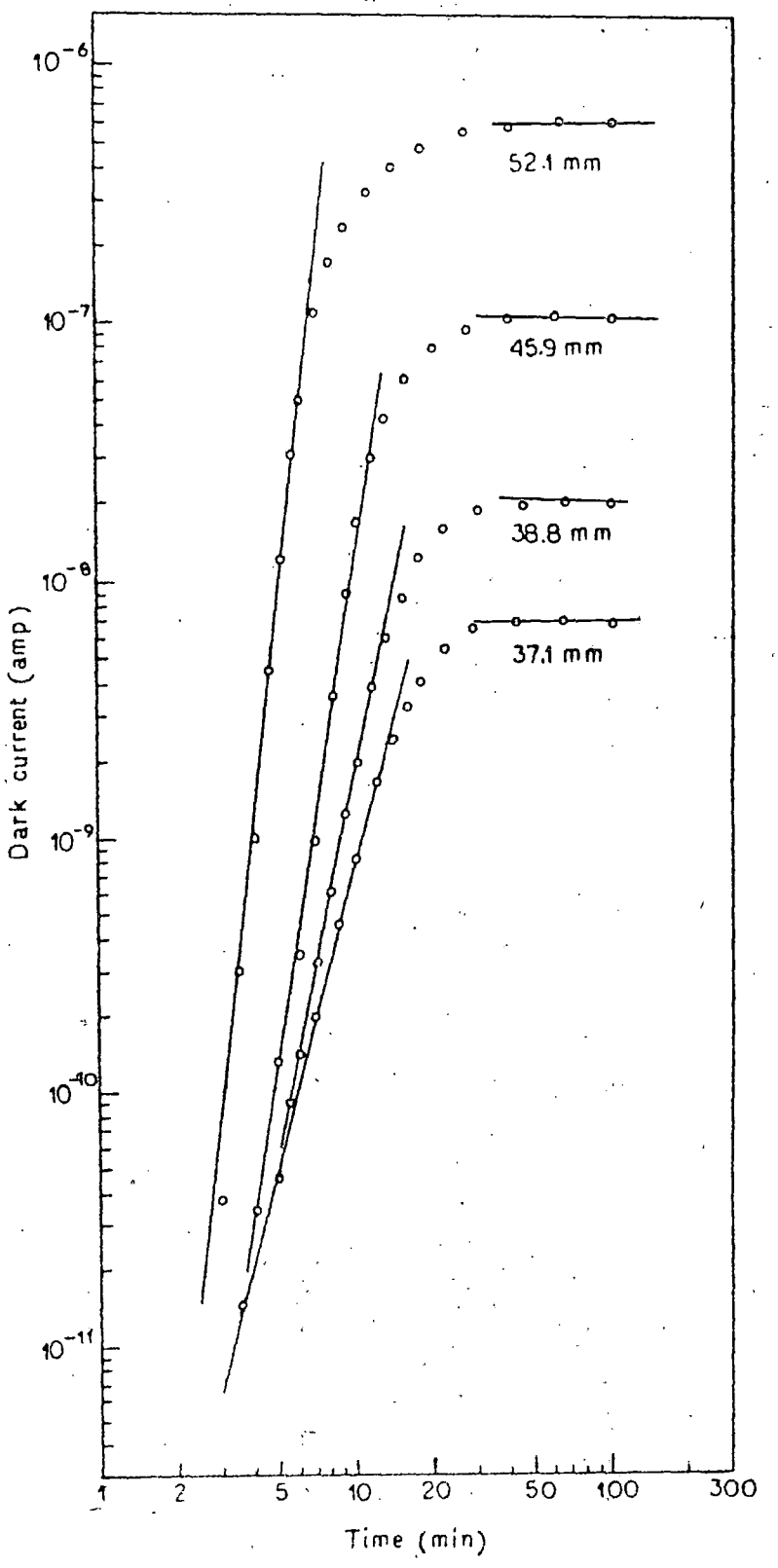

The n - t plot of the kinetic data at different vapour pressures for ethanol vapour adsorption on 1,3,5-trinitrobenzene.

FIGURE - 3.15

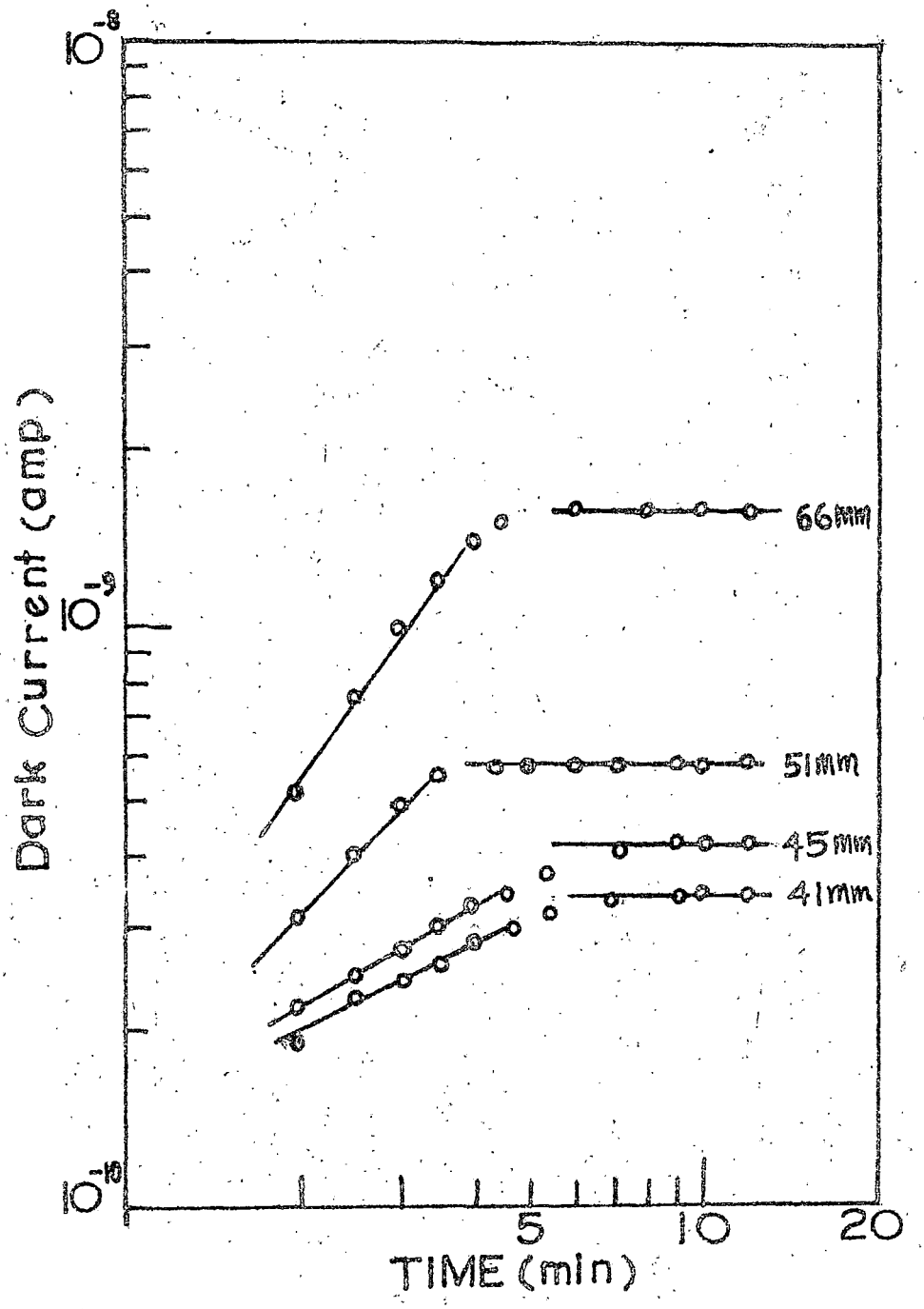

The R - t plot of adsorption kinetic data at different vapour pressures for ethyl acetate vapour adsorption on 2-nitrofluorene.

FIGURE - 3.16

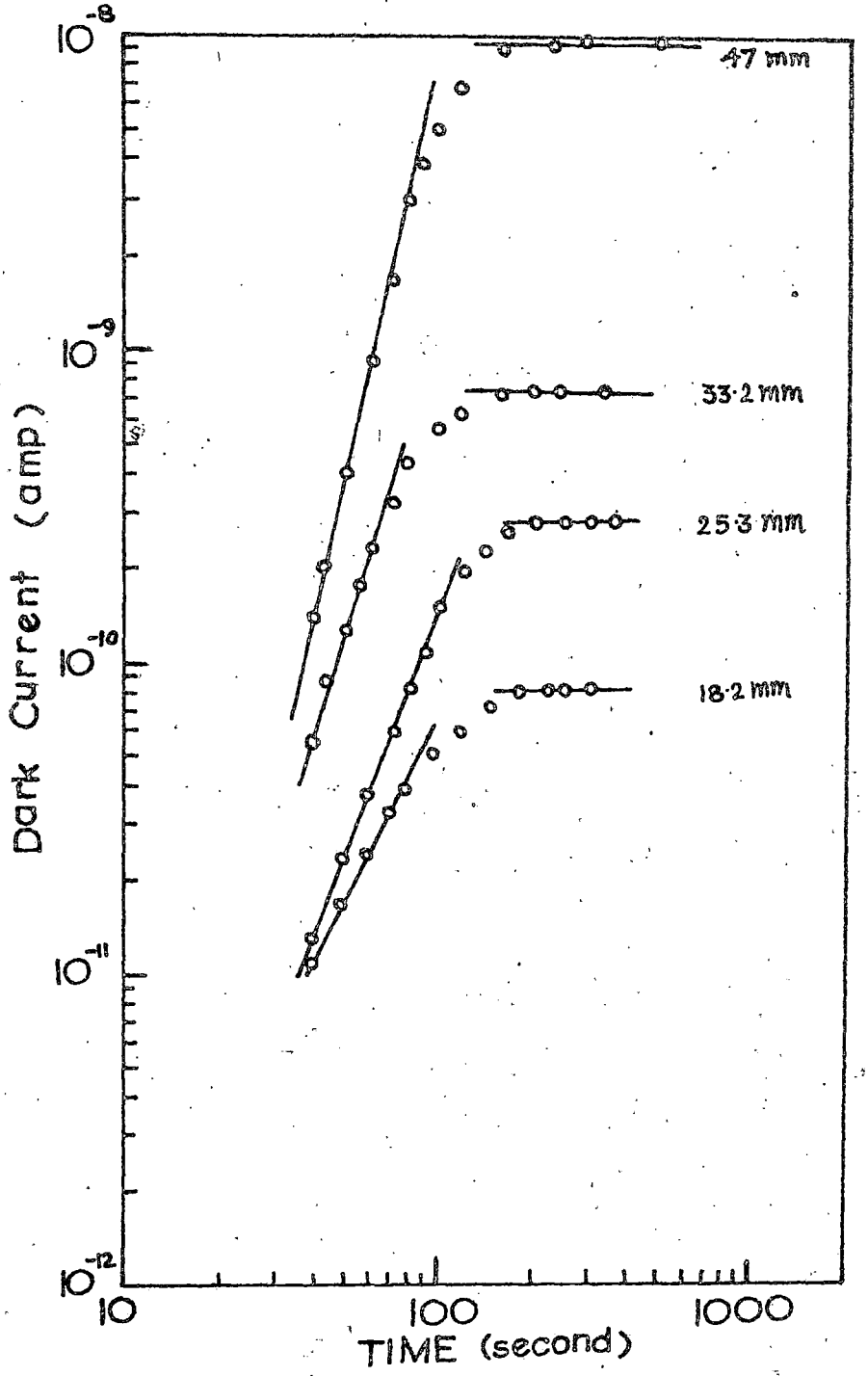

The R - 2 plot of adsorption kinetic data at different vapour pressures for ethyl acetate vapour adsorption on O-nitrobenzoic acid.

FIGURE - 3.17

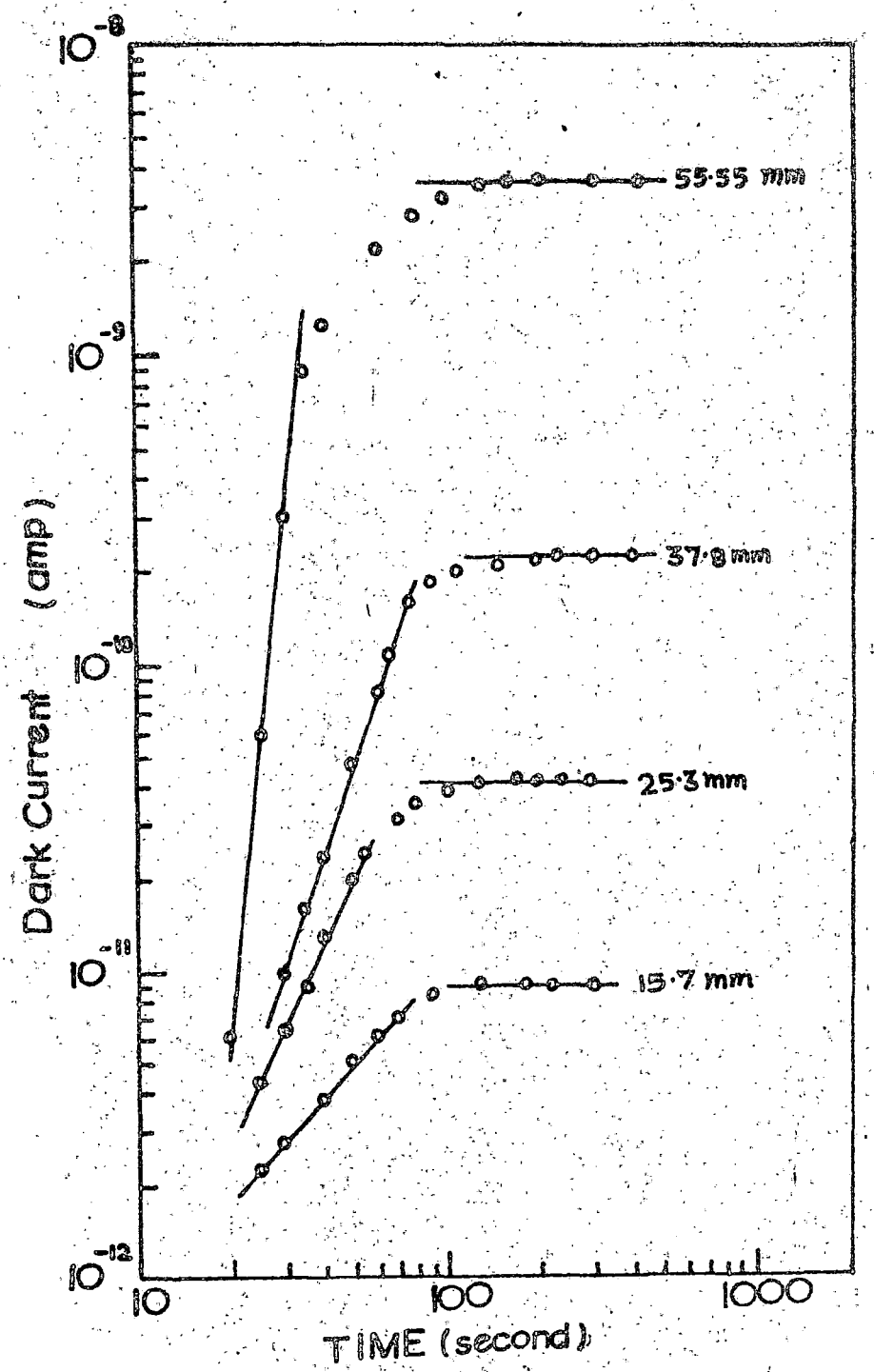

The B - t plot of adsorption kinetic data at different vapour pressures for ethyl acetate vapour adsorption on m-nitrobenzoic acid.

FIGURE - 3.18

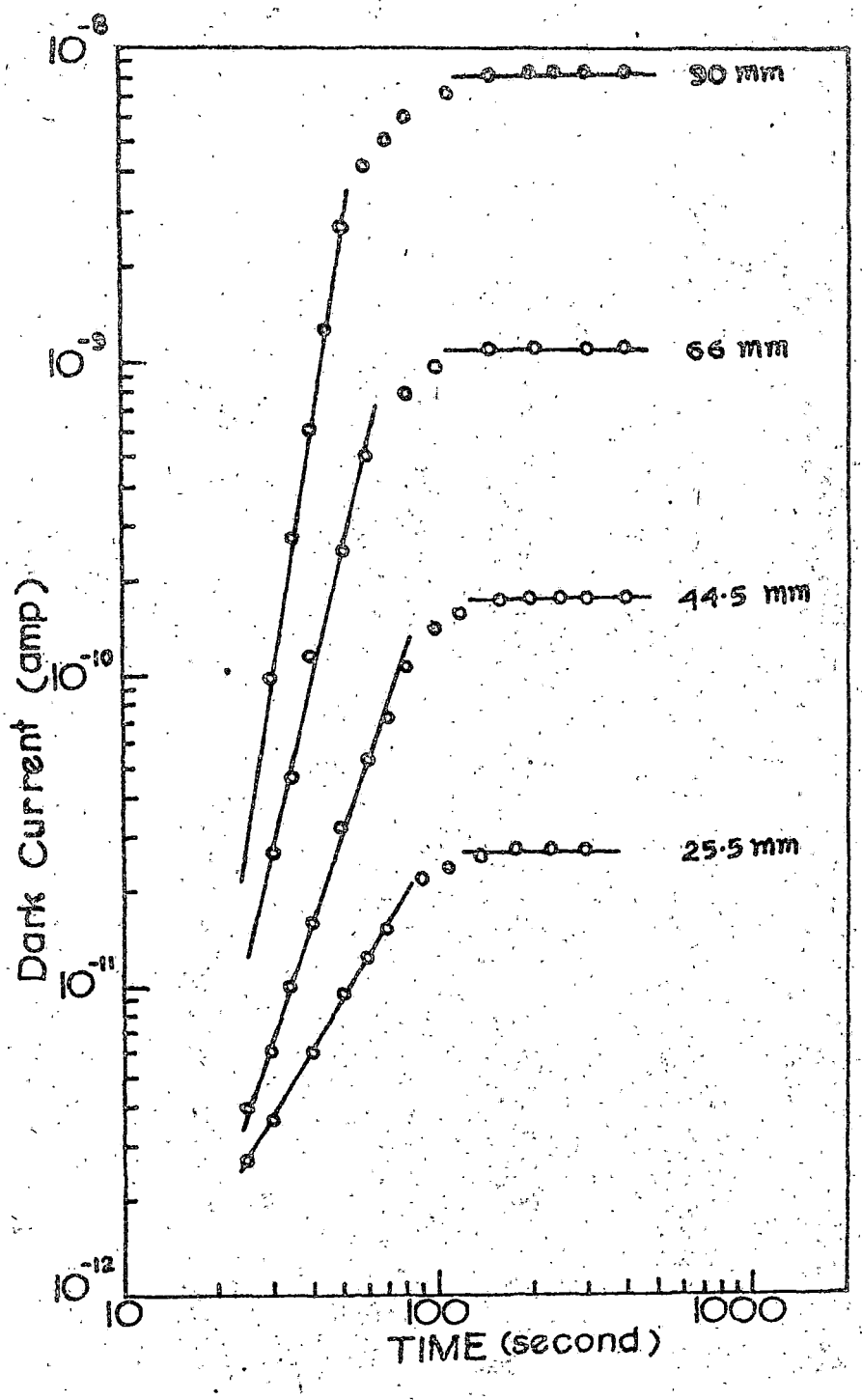

The R - S plot of adsorption kinetic data at different vapour pressures for ethyl acetate vapour adsorption on p-nitrobenzoic acid.

FIGURE - 3.10

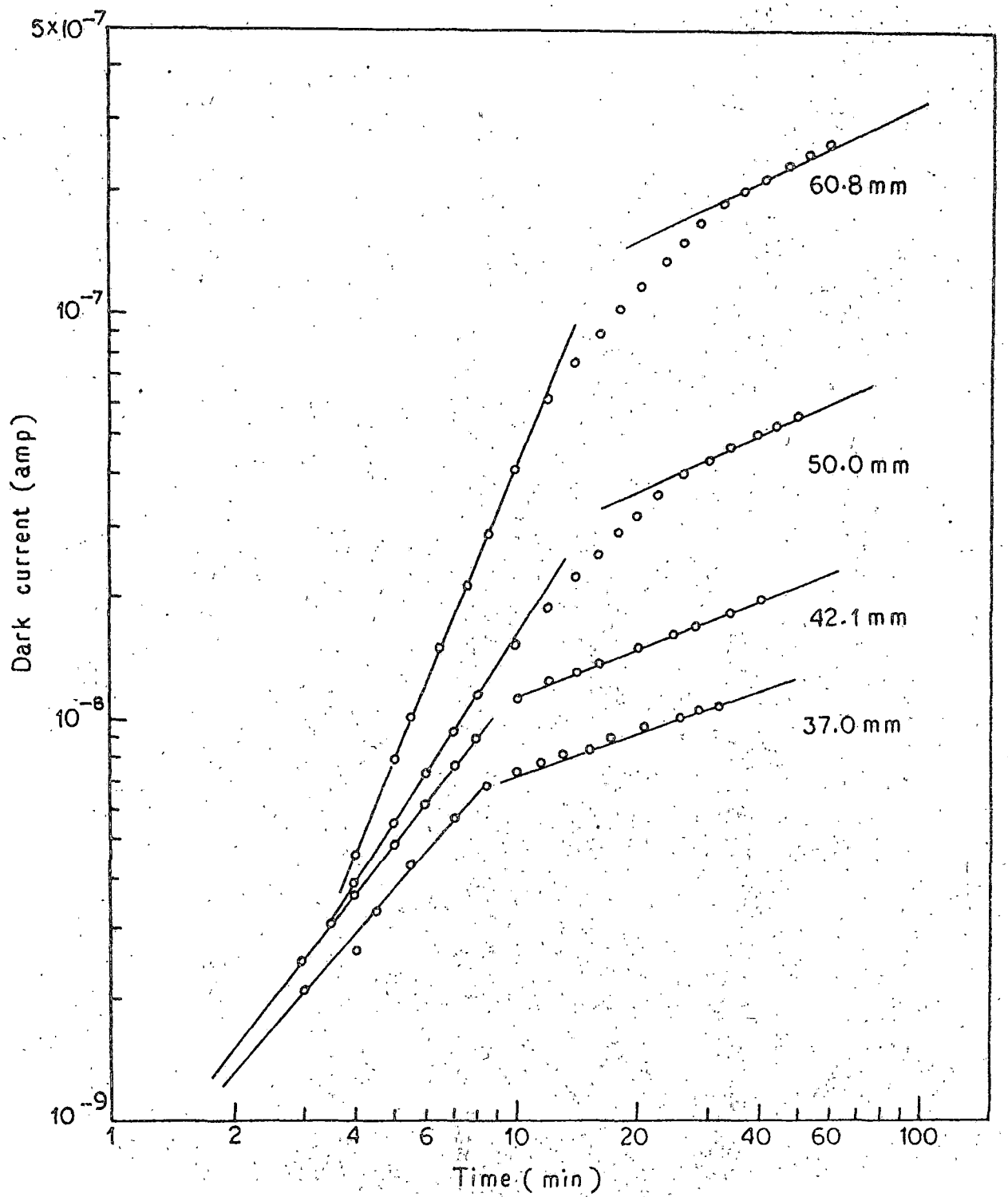

The n - t plot of adsorption kinetic data at different vapour pressures for ethyl acetate vapour adsorption on 1,4-dinitronaphthalene . (Showing two region linearity before reaching saturation)

FIGURE - 3.20

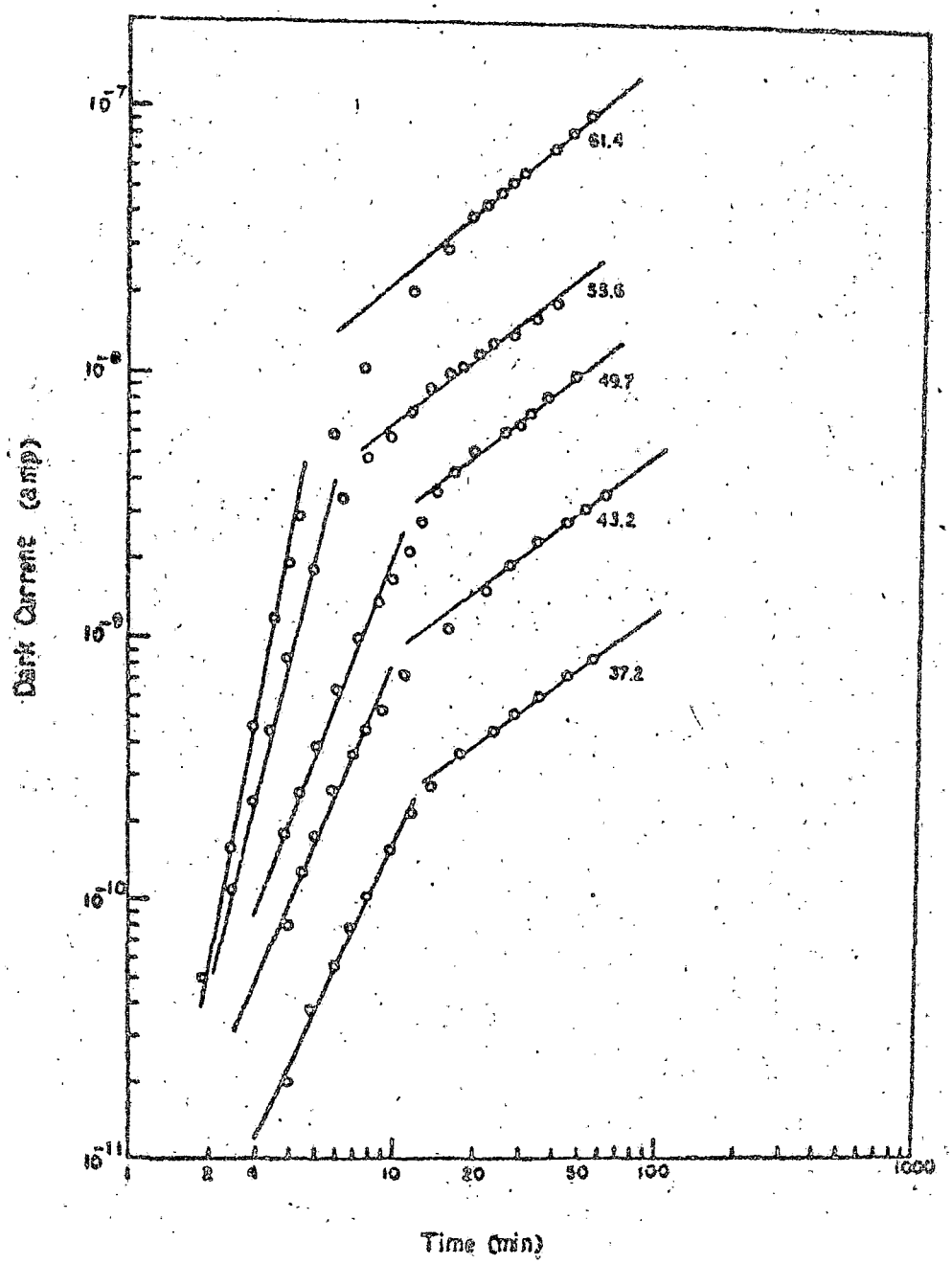

The R - t plot of adsorption kinetic data at different vapour pressures for ethyl acetate vapour adsorption on 1,3,5-trinitrobenzene. (Showing two region linearity before reaching saturation)

FIGURE - 3.21

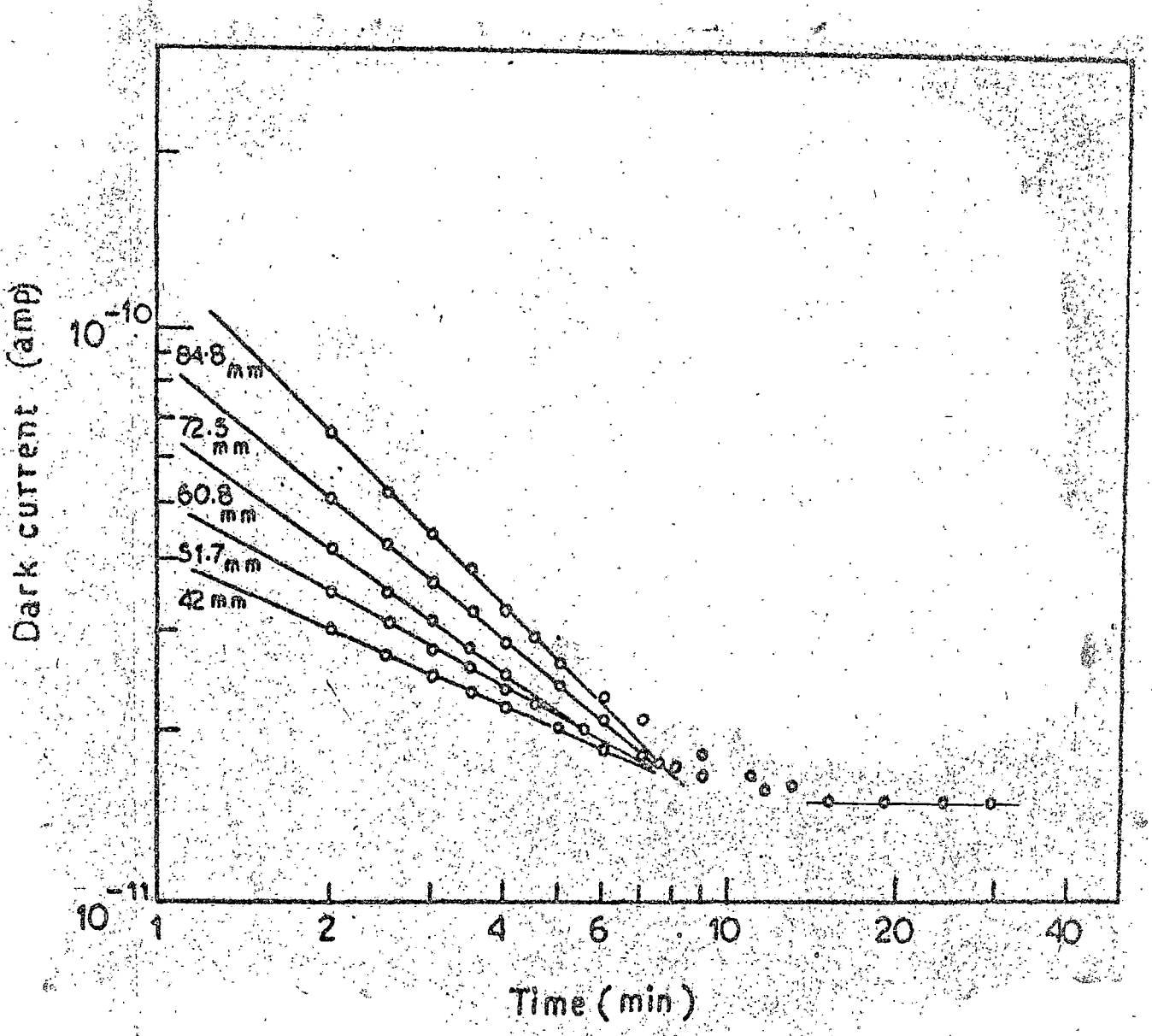

The R - t plot of desorption kinetic data at different vapour pressure for carbontotrachloride vapour desorption from 9-nitroanthracene.

FIGURE - 3.22

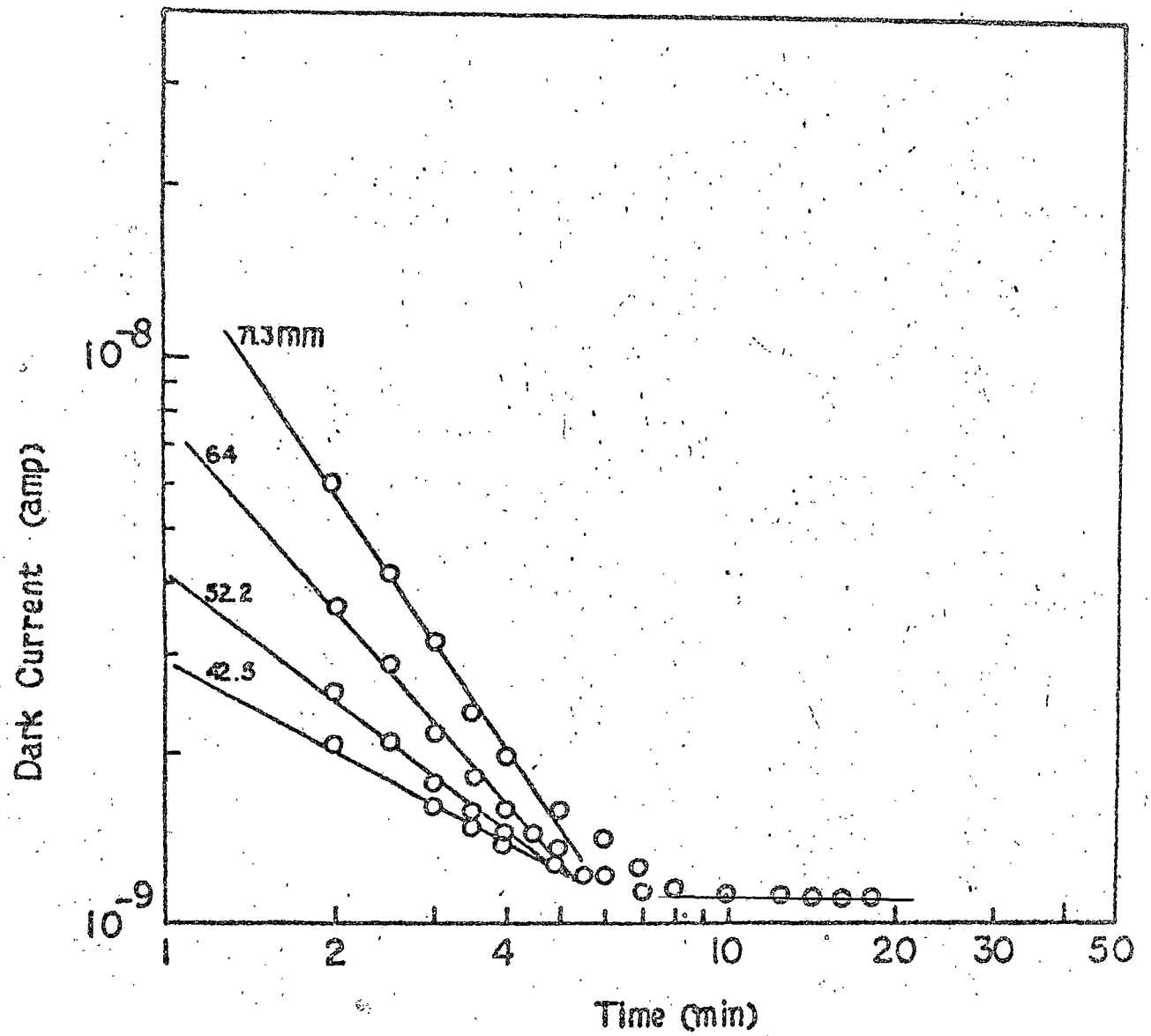

The R - S plot of desorption kinetic data at different vapour pressures for methanol vapour desorption from 1,4-dinitronaphthalene.

FIGURE - 3.23

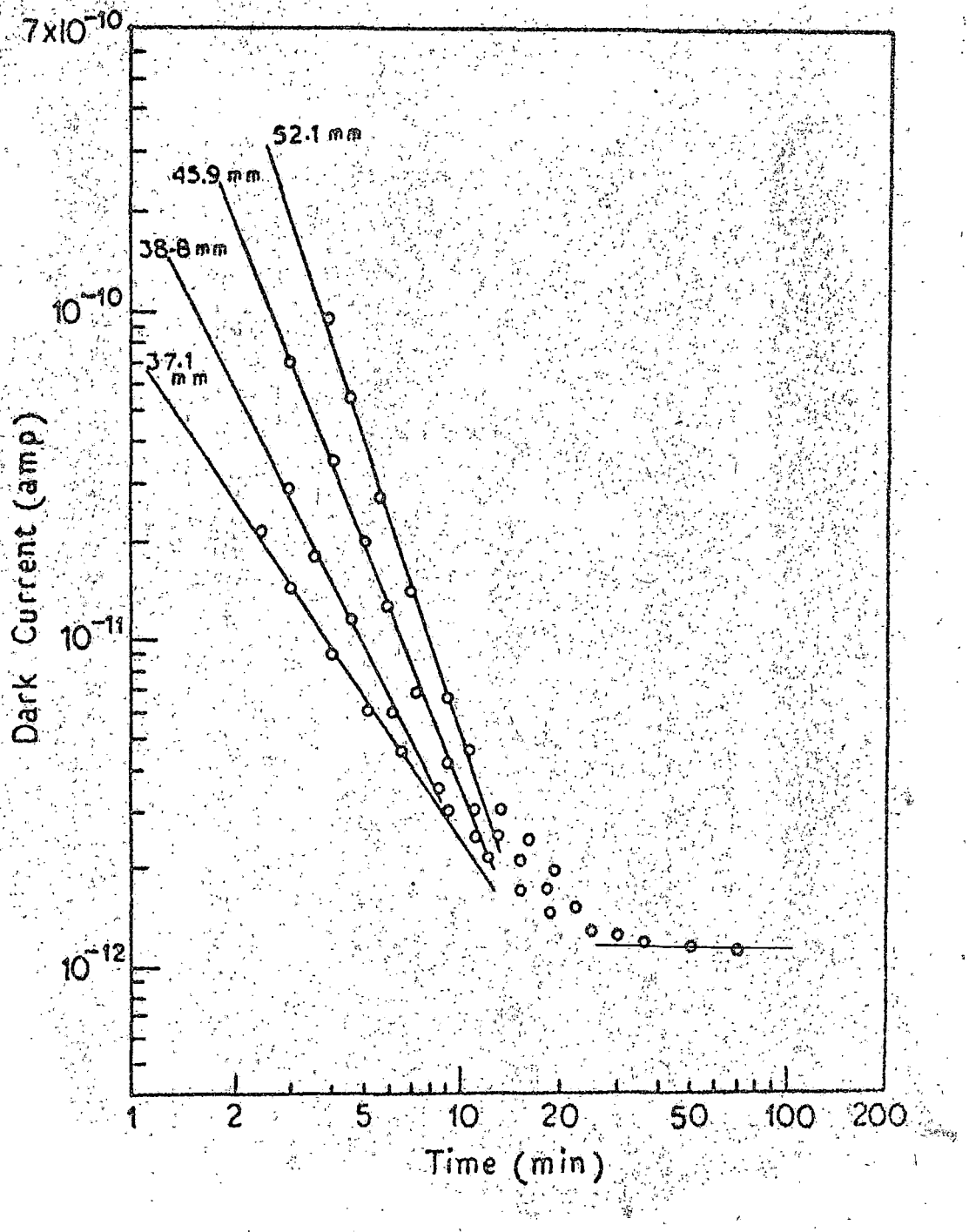

The n - t plot of desorption kinetic data at different vapour pressures for ethanol vapour desorption from 1, 3, 5-trinitrobenzene.

FIGURE - 3.24

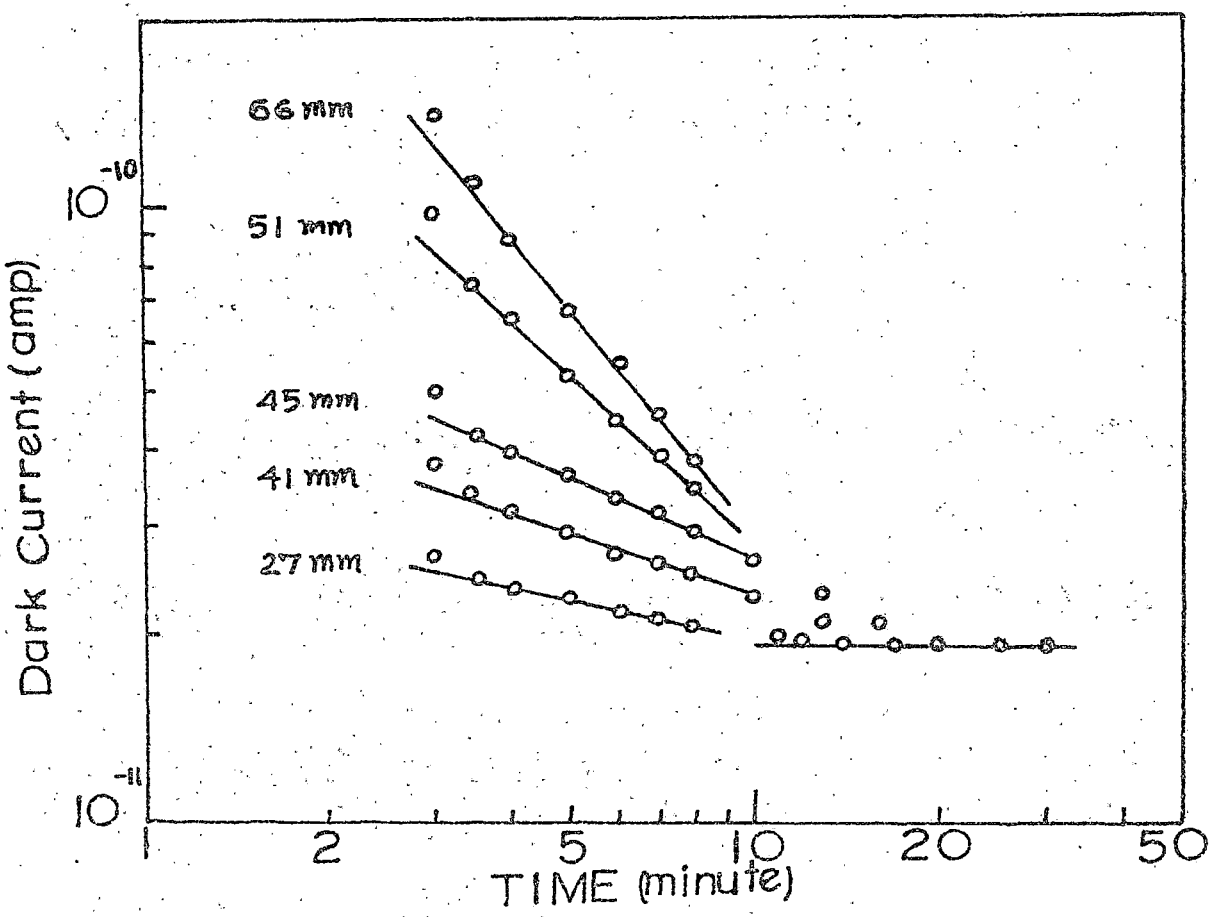

The R - t plot of desorption kinetic data at different vapour pressures for ethyl acetate vapour desorption from 2-nitrofluorene.

FIGURE - 3.25

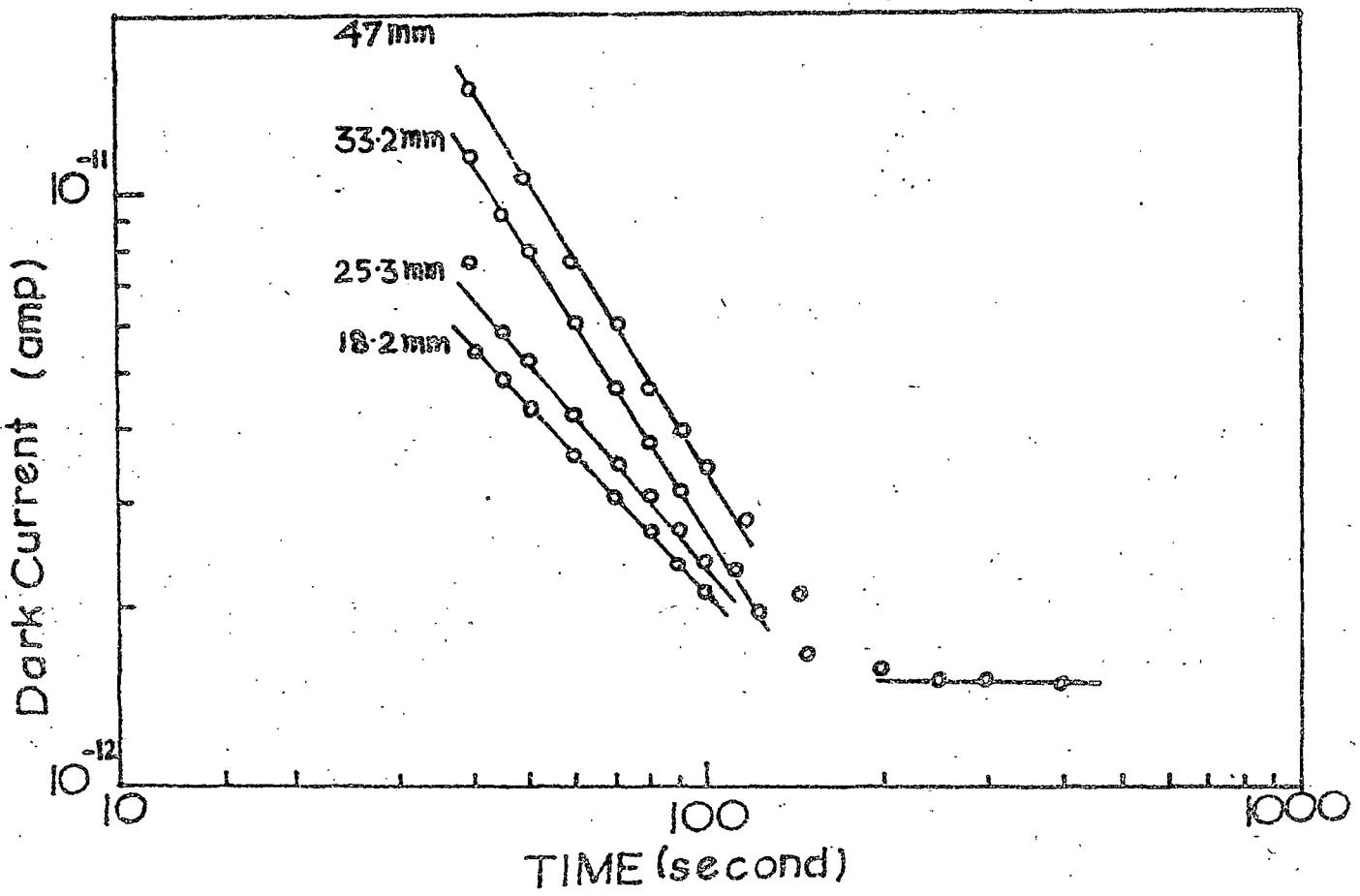

The R - t plot of desorption kinetic data at different vapour pressures for ethyl acetate vapour desorption from O-nitrobenzoic acid.

FIGURE - 3.26

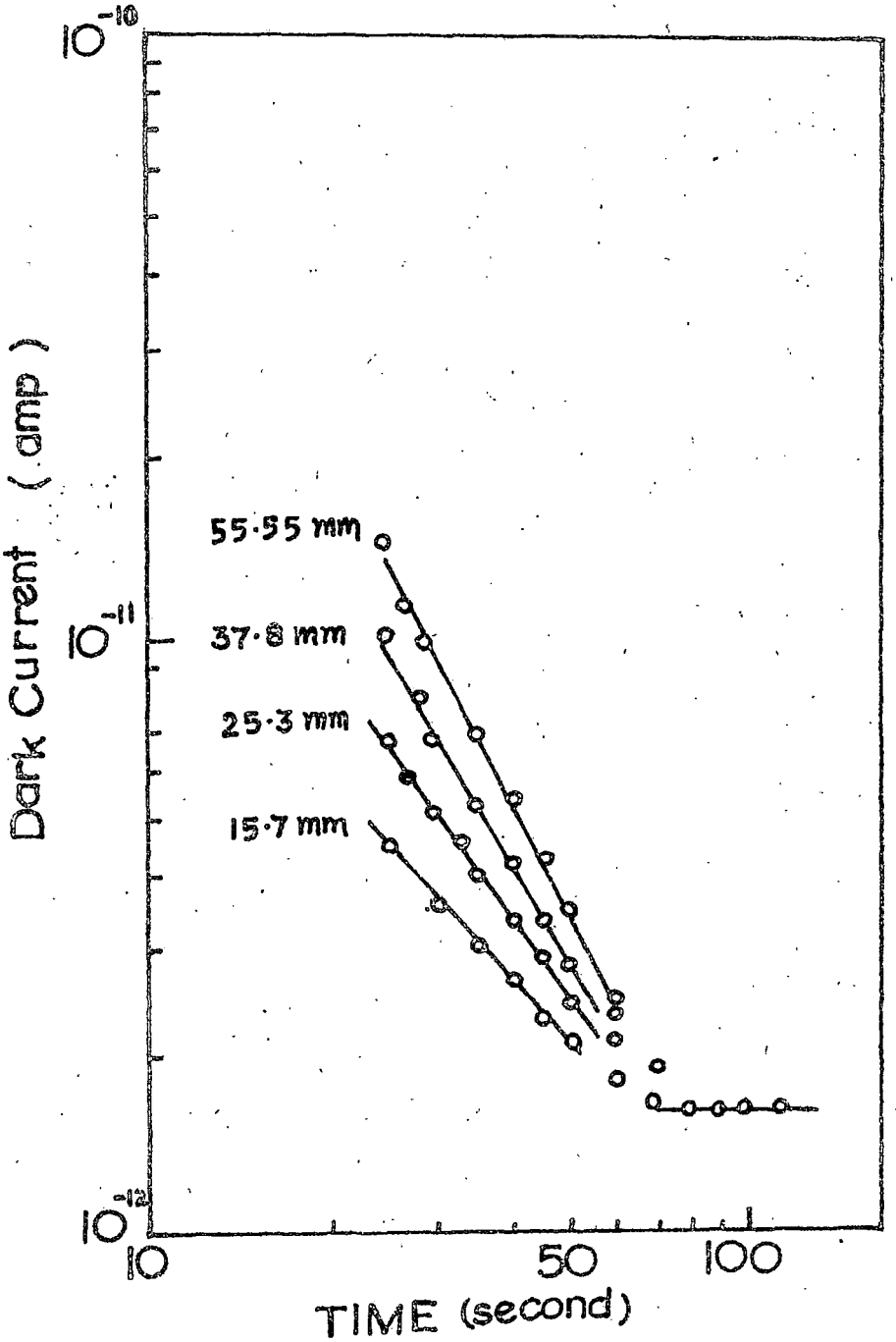

The R - t plot of desorption kinetic data at different vapour pressures for ethyl acetate vapour desorption from m-nitrobenzoic acid.

FIGURE - 3.27

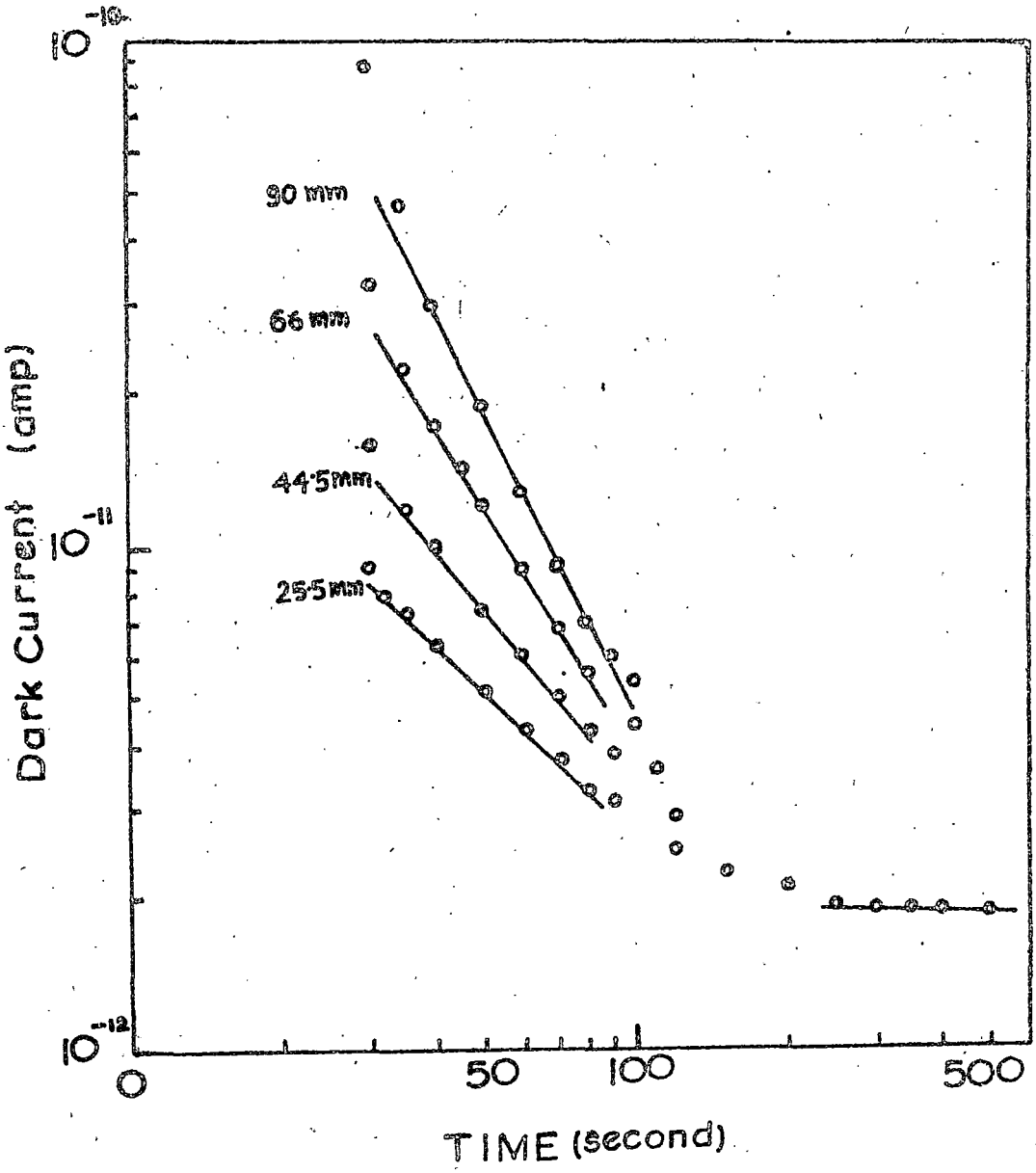

The R - t plot of desorption kinetic data at different vapour pressures for ethyl acetate vapour desorption from p-nitrobenzoic acid.

FIGURE - 3.23

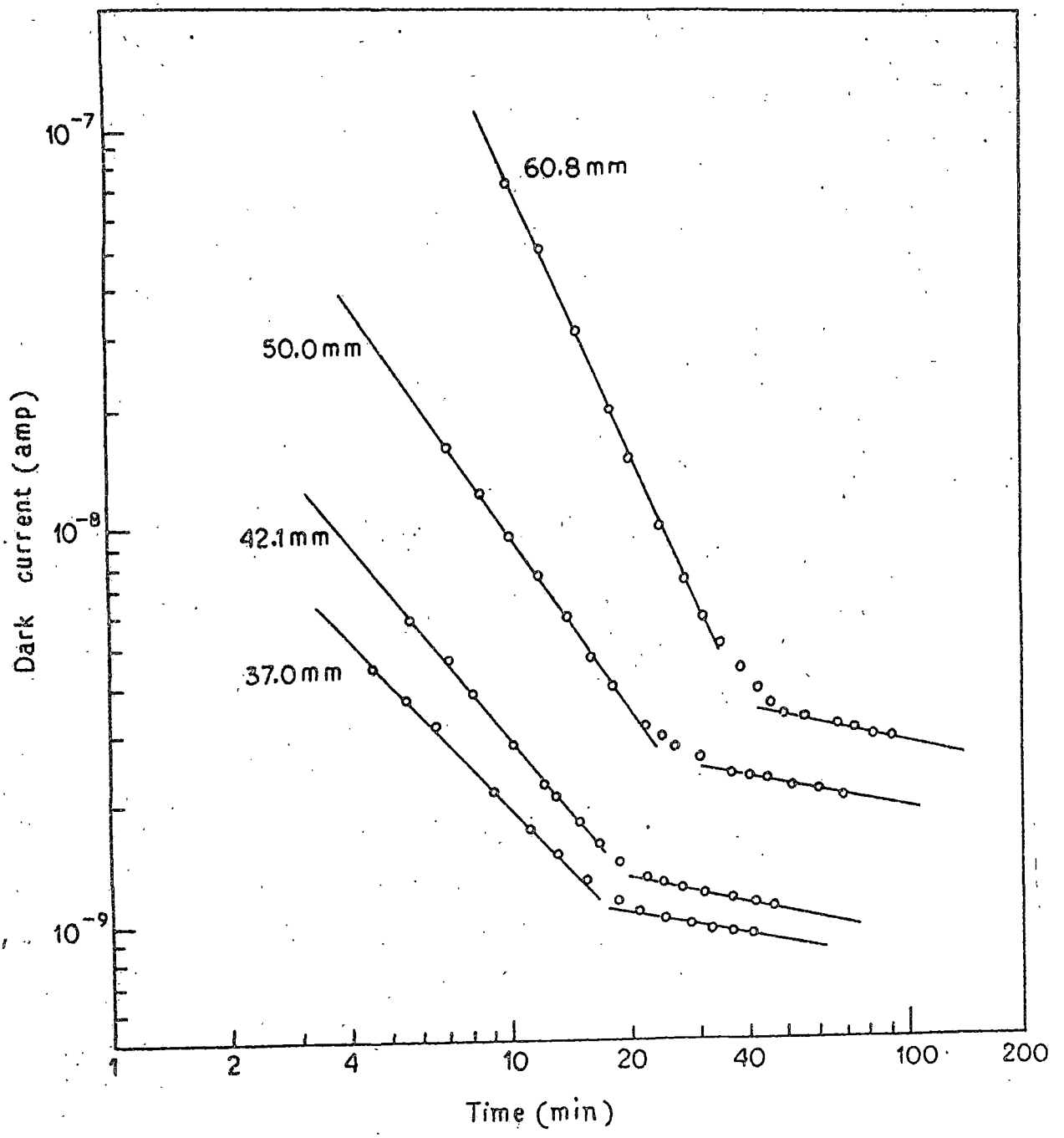

The R - T plot of desorption kinetic data at different vapour pressures for ethyl acetate vapour desorption from 1,4-dinitronaphthalene. (Showing two region linearity before reaching initial conductivity value)

FIGURE - 3.29

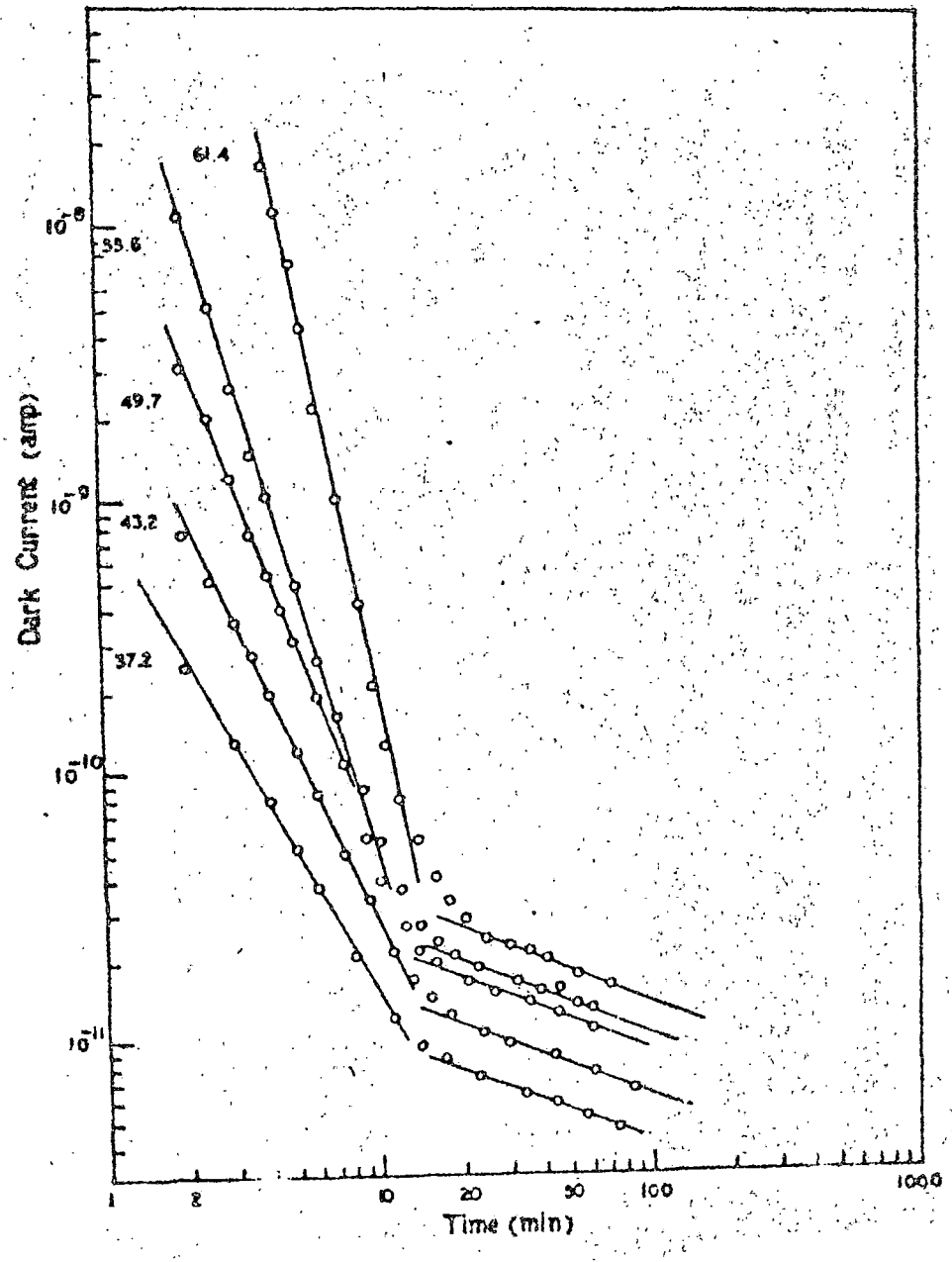

The R ~ t plot of desorption kinetic data at different vapour pressures for ethyl acetate vapour desorption from 1,3,5-trinitrobenzene. (Showing two region linearity before reaching initial conductivity value)

Table 3.3

Vapour pressure dependence of the factors β' and $\beta^{*\prime}$ for different nitroaromatic semiconductors on adsorption and desorption of respective vapours.

Semiconductor	Vapour used	Vapour pressure (mm)	$\beta' \times 10^2$ (ev)	$\beta^{*\prime} \times 10^2$ (ev)
9-nitro-anthracene*	Carbon-tetra-chloride	42.0	2.545	5.385
		51.7	2.037	4.655
		60.8	1.828	3.548
		72.5	1.639	3.244
		84.2	1.504	2.542
1,4-dinitro-naphthalene*	Methanol	42.5	4.342	4.774
		52.3	3.093	3.349
		64.0	1.721	2.249
		71.3	1.220	1.697
1,3,5-trinitro-benzene*	Ethanol	37.1	0.649	1.684
		38.8	0.502	1.247
		45.9	0.384	1.006
		52.1	0.286	0.826
2-nitro-fluorene**	Ethyl-acetate	27	9.19	11.82
		41	5.26	7.72
		45	4.36	5.81
		51	2.43	2.74
		66	1.76	2.08

Contd.

Table 3.3 (Contd.)

Semiconductor	Vapour used	Vapour pressure (mm)	β' x 10^2 (ev)	$\beta^{x'}$ x 10^2 (ev)
O-nitro-benzoic-acid**	Ethyl acetate	18.2	1.26	2.47
		25.3	0.93	2.25
		33.2	0.79	1.65
		47.0	0.56	1.55
m-nitro-benzoic acid**	Ethyl acetate	16.7	2.22	2.32
		25.3	1.18	1.76
		37.3	0.67	1.46
		55.5	0.26	1.30
p-nitro-benzoic-acid**	Ethyl acetate	25.5	1.51	2.59
		44.5	0.86	2.04
		66.0	0.59	1.62
		90.0	0.38	1.24

* Sample cell at 22°C

** Sample cell at 25°C

saturation is reached soon after the short time region linearity is completed. This suggest that R - Z equations :

$$dm/dt = \bar{A} \exp (- \bar{\beta} m / R T) \text{ and}$$

$$dm/dt = -\bar{A}^{*} \exp (- \bar{\beta}^{*} m / k T)$$

with a different activation energy and pre-exponential constant are also applicable in the long time region. Such linearity in the R - Z plots in the long time region have been obtained for adsorption and desorption of ethylacetate, benzene and carbontetrachloride vapour on and from 1,3,5-trinitrobenzene and 1,4 dinitronaphthalene. The activation energies of adsorption (β'') and desorption ($\beta^{*''}$) have been evaluated from the slopes of such lines in the long time region. In table 3.4, the values of β' and $\beta^{*'}$, β'' and $\beta^{*''}$ are presented for ethylacetate vapour adsorption at different vapour pressure. It is noted that for any particular pressure of ambient vapour $\beta^{*'} > \beta'$ and $\beta^{*''} > \beta''$.

3.3 Potential Energy Curves for Vapour Adsorption Process :

There are number of different treatments[140] for the R - Z equation. A simple two stage process after Wiley and Leslie[138] as shown in Fig. 3.30 seems quite satisfactory for vapour-semiconductor pair where the vapour adsorption saturation is quickly

Table 3.4

Vapour pressure dependence of the factors β', β'' and $\beta^{*'}$, $\beta^{*''}$ for adsorption and desorption kinetics respectively in case of ethyl acetate vapour adsorption

Semiconductor	Vapour pressure (mm)	$\beta' \times 10^2$ (ev)	$\beta'' \times 10^2$ (ev)	$\beta^{*'} \times 10^2$ (ev)	$\beta^{*''} \times 10^2$ (ev)
1,4-dinitro-naphthalene	37.0	2.20	6.412	2.385	13.84
	42.1	1.978	6.118	2.089	13.52
	50.0	1.663	5.734	1.736	13.87
	60.8	1.052	5.206	1.111	13.76
1,3,5-trinitro-benzene	37.2	1.777	3.410	1.413	6.451
	43.2	1.071	3.277	1.169	6.508
	49.7	0.965	3.238	0.932	6.469
	58.6	0.612	3.191	0.758	6.468
	61.4	0.465	2.958	0.509	6.312

FIGURE - 3.30

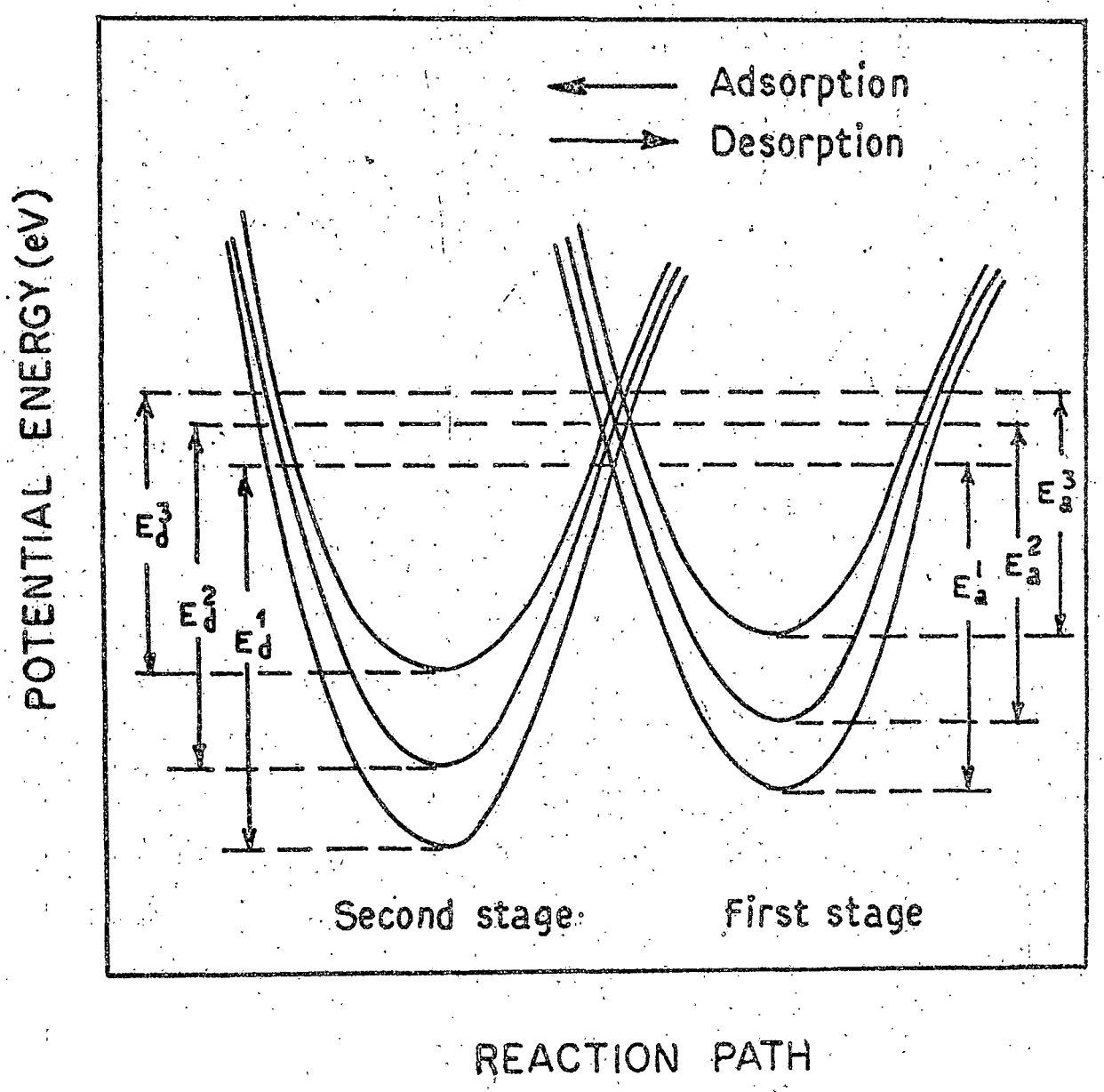

The potential energy curves for "two stage" vapour adsorption explaining the R - t plots (Figs. 3.12 - 3.18 and 3.21 - 3.27). E_d^1, E_d^2 and E_d^3 are activation energies of desorption in order of increasing pressure. Similarly E's are activation energies for adsorption.

reached and the desorption is quick and complete (Figs. 3.1-3.7). R - t plots in such cases do not show any measurable slope in the long time region. In the first stage, a mobile vander Waals' adsorption on the crystal surface gives a Lennard-Jones potential energy curve which is assumed to depend on the fraction of surface coverage. This stage is followed by a Rate determining transition over a potential energy barrier to the final stage of adsorption forming weakly bound complexes between the vapour molecules and the nitroaromatic crystallites. The barrier is formed by the intersection of the two potential energy curves. As more molecules get physically adsorbed (Vander Waals'), a repulsive interaction between the dipoles will raise the potential energy curve for the first stage thereby lowering the barrier height giving decreasing activation energy of adsorption with increasing vapour pressure. As the surface coverage of the second stage rises, this potential energy curve also rises resulting in lowering of desorption activation energy with increasing pressure. The rise of the second stage curve is such that the minimum of this curve is always at lower energy than the minimum of the first stage, the energy difference between these two minima decreases with increase in vapour pressure.

In other cases of vapour adsorption (like Figs. 3.8 and 3.9) an additional stage of adsorption is suggested by the second

linear R = 3 plot in the long time region (Figs. 3.19, 3.20, 3.22 and 3.23). A transition over this second potential barrier occurs and the vapour molecules get strongly bound to the surface molecules of the nitroaromatic crystallites. The measured values of β'' and $\beta^{*\prime\prime}$ are slightly larger than β' and $\beta^{*\prime}$. It is not possible to suggest if this means a higher potential energy barrier in the third stage adsorption than the second stage adsorption as there are no informations about the values of α and α' (α' being the value of α in second stage interaction between vapour and the surface molecules of the semiconductor). The third stage of adsorption potential is possibly smaller as α' is expected to have a smaller value. Even if $\alpha \simeq \alpha'$, Boltzmann factor for crossing the barrier on the left of the second stage potential well will be approximately equal to that on the right as the difference in the barrier heights is insignificant. However, considering the fact that the strongly bound complexes are not easily desorbed as are the weakly bound complexes in the two stage process, it seems that the potential well in the third stage is deep. A model diagram for three stage adsorption process is shown in Fig. 3.31. The desorption activation energy from the third stage, as shown in table 3.4, seems to be independent of vapour pressure. Strongly bound complexes behave more like a chemical species (though the binding energy is very much less) and a certain amount of energy is required to break the bond. $\beta^{*\prime\prime}$ m, the activation energy for

FIGURE - 3.31

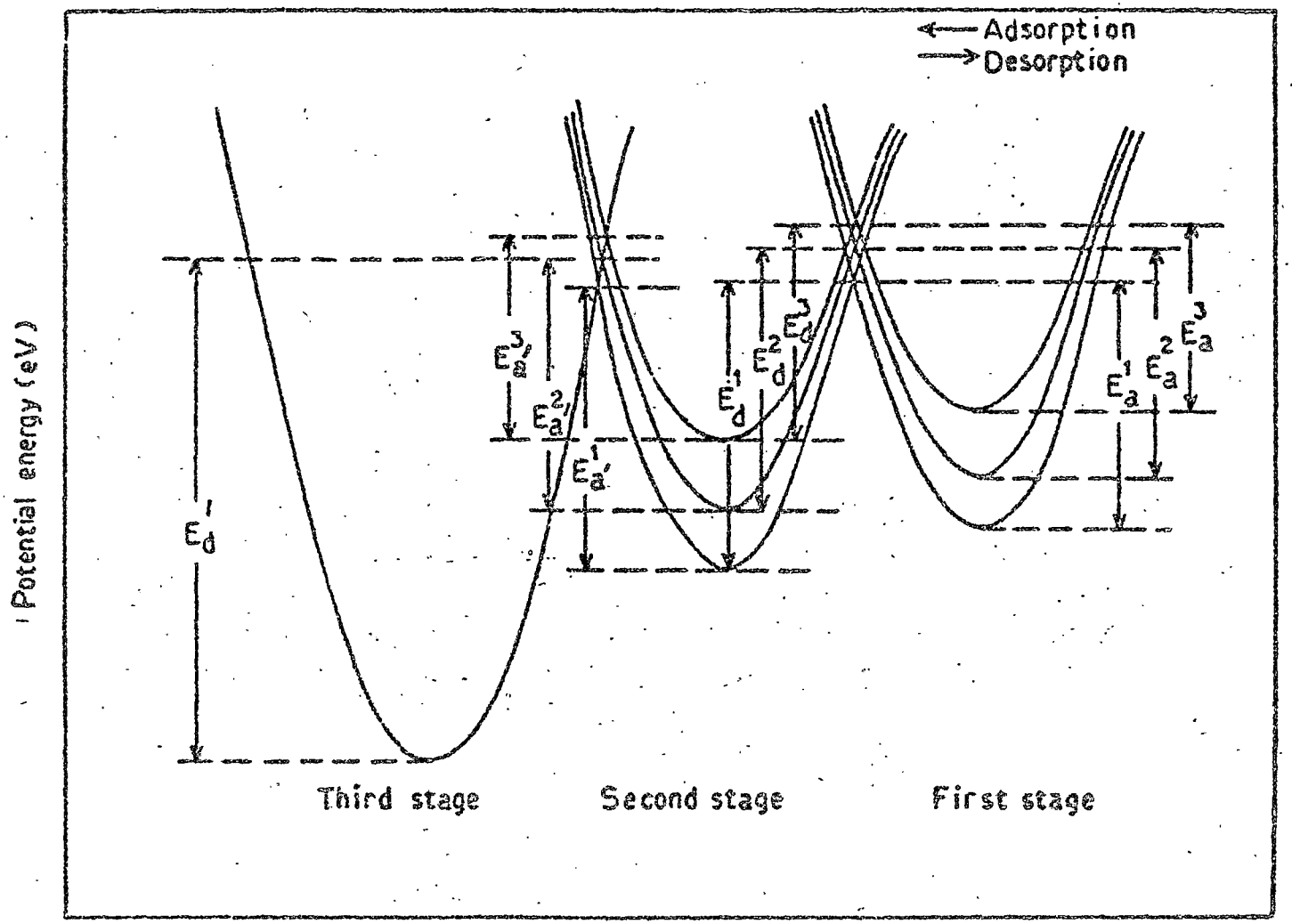

The potential energy curves for "three stage" vapour adsorption explaining the two region linearity in the E-Z plots (Figs. 3.19, 3.20 and 3.28, 3.29). E_a^1, E_a^2, E_a^3 and E_a^1, , E_a^2, , E_a^3, are the activation energies of adsorption in order of increasing pressure in the 2nd and 3rd stage respectively. E_d's are the activation energies of desorption.

desorption from third stage should, apart from a small entropy factor be equal to the binding energy of the vapour surface molecular complex. It has not been possible to estimate the binding energy because the experiments do not provide any numerical value of α and α'.

4. Conclusion

The adsorption of vapours increases the semiconduction current of the nitroaromatic semiconductors. The adsorption and desorption kinetics follow the modified Roginsky - Zeldovich equation. A two stage adsorption process is applicable for such vapour-semiconductor systems where the vapour adsorption saturation is quickly reached and the desorption is quick and complete. In some cases, however, an additional stage of adsorption is suggested by the second linear R - t plot in the long time region. A transition over this second potential barrier occurs and the vapour molecules get strongly bound to the surface molecules of the nitroaromatic crystallites.

CHAPTER - 4

COMPENSATION EFFECT IN SOME NITROAROMATIC SEMICONDUCTORS

1. Introduction

The pre-exponential factor (σ_o) in the operational definition of semiconductors has been a subject of much discussions[40,46,47,50,99,100]. Rosenberg et al[40] have proposed σ_o as an exponential function in their three constant conductivity equation :

$$\sigma_T = \sigma_o' \exp (E/2 K T_o) \exp (-E/2 K T) \quad (1.1)$$

'T_o' is the characteristic temperature often known as 'compensation temperature'. σ_o' and T_o remain invariant for the same compound. The compensation effect is defined by the linear relationship of log σ_o and the activation energy (E). The values of σ_T and E change in such a manner that their effects on σ_o are mutually compensated. Johnston and Lyons[100,101] believe that compensation effect may originate solely from the calculations and it requires no physical interpretation. However, they have suggested that if σ_o and E are physically related, one should get a linear relationship between log σ_T and E yielding the semiconductive parameters in agreement with the values obtained

from other sources. In 'apparent' compensation effect, for each particular E - value, unique values of σ_0 and σ_p does not exist and the system can not be precisely defined. In 'true' compensation effect excellent correlation between log σ_0 and E and also between log σ_p and E are obtained. Thus, both 'true' and 'apparent' compensation effects follow the linear log σ_0 vs. E relationship.

It has been established that when E is changed by chemical vapour or gas adsorption, 'true' compensation effect is indeed observed in some polyene semiconductors and the effect has a physical basis.

In the previous chapter, we have shown that two distinct adsorption processes - one forming weakly bound and the other forming strongly bound complexes characterised by two and three stage adsorption processes respectively are operative in nitro-aromatic semiconductors. In this chapter, we present our results and discussions on the validity of true compensation effect, its physical basis and its relationship with the adsorption and desorption processes in nitroaromatic semiconductor-vapour systems.

2. Experimental and Results

2.1 Effect of vapour adsorption on activation energy :

The semiconduction activation energies of the crystalline powders of the nitroaromatic compounds in a sandwich cell were measured several times in the dry nitrogen atmosphere and also in vacuum. All the measurements gave consistent values. The observed values are 2.00, 1.18, 1.73, 2.25 and 2.51 ev (approx.) for 9-nitroanthracene, 1,4-dinitronaphthalene, 1,3,5-trinitrobenzene, 2-nitrofluorene and O-nitrobenzoic acid respectively. On adsorption of various vapours on the crystallite surfaces, the semiconducting current is enhanced and the activation energy is appreciably increased.

The powdered semiconductors were used in form of a sandwich cell to determine the effect of adsorbed vapours on the semiconduction activation energy. The sample was first allowed to adsorb the vapour at a fixed pressure and come to a steady state at a constant sample cell temperature in the chamber atmosphere containing the vapour in nitrogen. The pressure of the total gas mixture in the chamber was atmospheric and the partial pressure of the vapour was the saturation vapour pressure of the reagent liquid at the temprature at which it was kept. Both inlet and outlet of the chamber were then sealed and the value of the saturation current was noted with time. The saturation current was

found to be almost constant for a long time indicating that the conduction in the system was mainly electronic[141,142]. The cell was then rapidly cooled to about - 30°C. The chamber was then flushed gently with dry nitrogen gas. The out-let of the chamber was kept open and the atmospheric pressure was maintained inside the chamber. The temperature was then slowly increased and the semiconduction current was measured with the increasing temperature of the sample cell. The results of adsorption of a vapour on different nitroaromatic semiconductors are shown in Figs. 4.1-4.5. The straight line portion in the low temperature region shows the semiconductive properties of the nitroaromatics with adsorbed vapour and the slopes of these lines give the activation energies of the respective systems. At considerable higher temperatures, the adsorbed vapour starts desorbing and the rate of desorption increases with increasing temperature and the current begins to diminish. The straight line portions of the curves at the higher temperature region above the point C, give the activation energies of the semiconductors approximately the same as that in dry nitrogen atmosphere. The observed values (1.98, 1.11, 1.75, 2.2 and 2.5 ev) are slightly lower possibly due to incomplete desorption of adsorbed vapours. Similar curves were also obtained with certain other vapours forming very weak revesible complexes with these nitroaromatic semiconductors. For the remaining vapours

FIGURE - 4.1

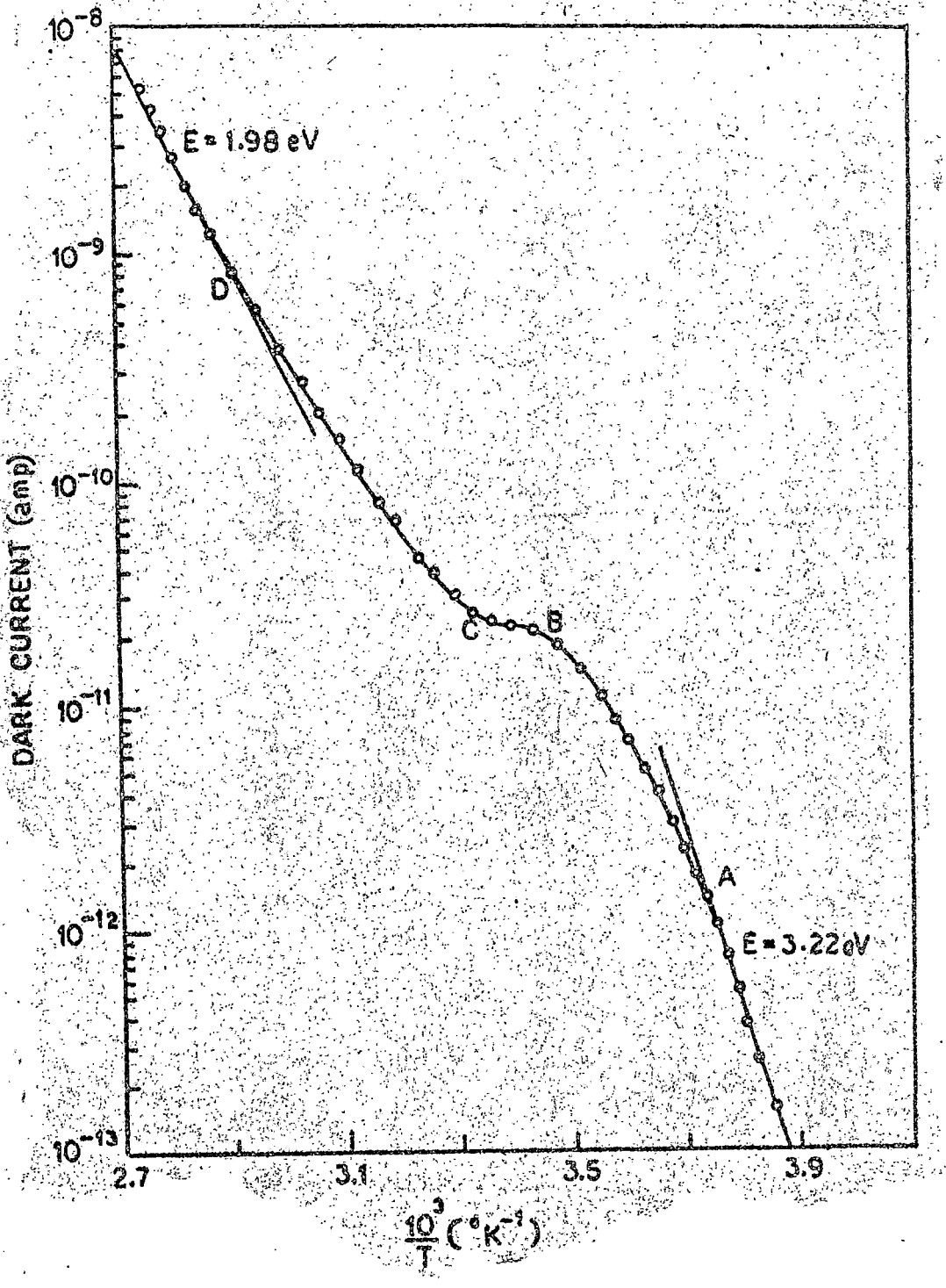

Semiconductivity in a methanol adsorbed 9-nitroanthracene powder cell as a function of temperature. (Ambient vapour pressure 50 mm; adsorbed at sample cell temperature 22°C)

FIGURE - 4.2

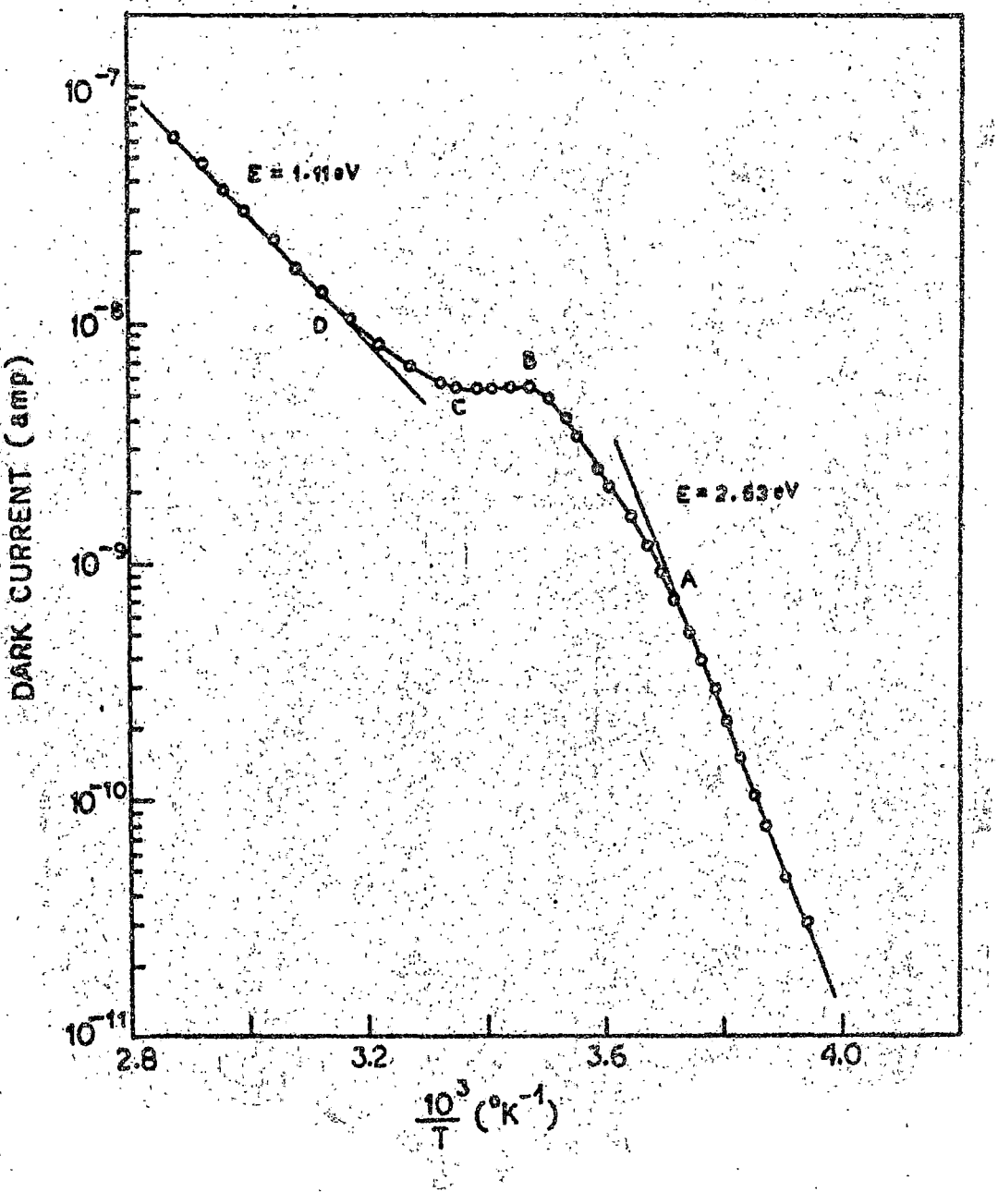

Semiconductivity in a methanol adsorbed 1,4-dinitronaphthalene powder cell as a function of temperature. (Ambient vapour pressure 50 mm, adsorbed at sample cell temperature 22°C)

FIGURE - 4.3

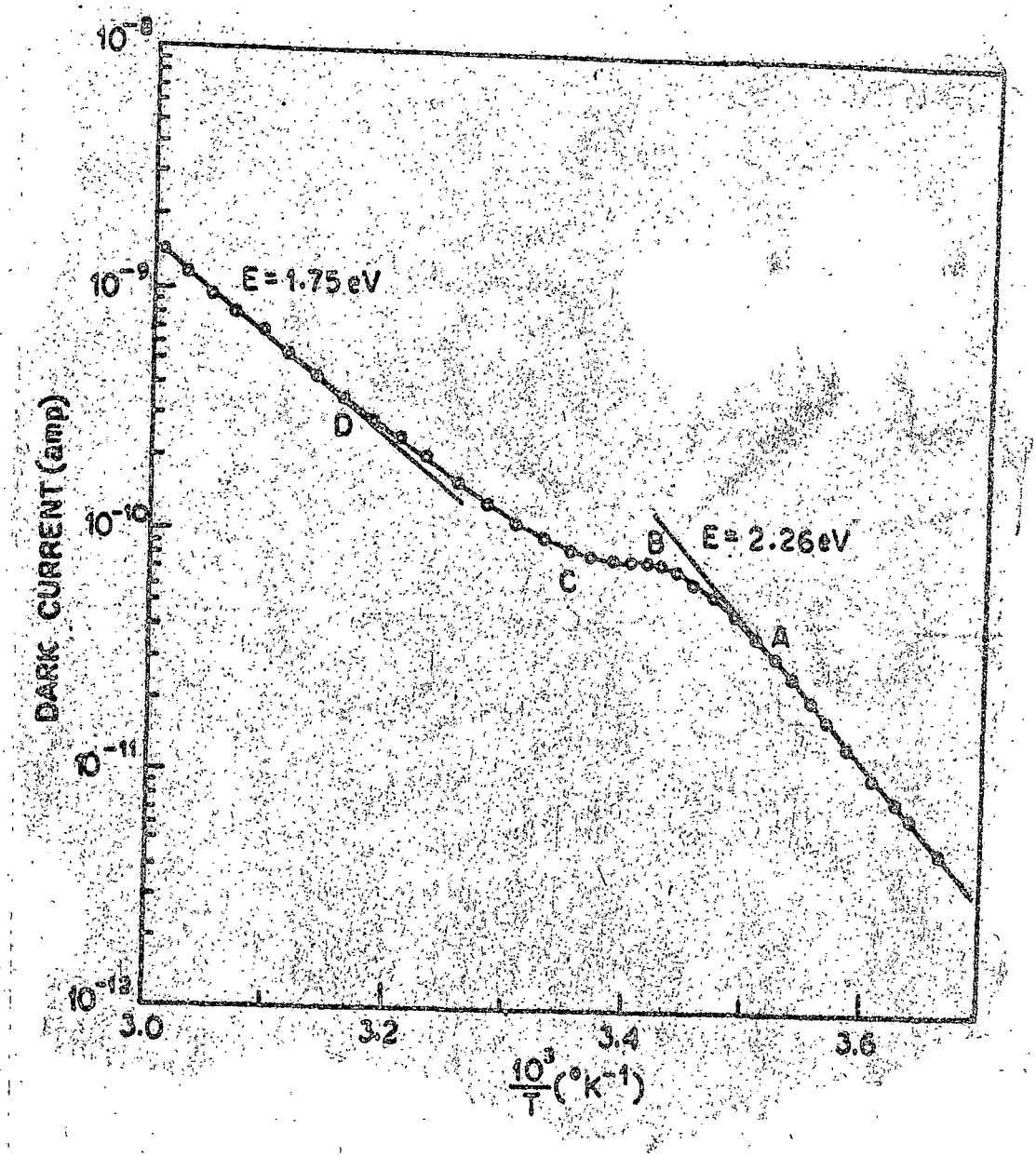

Semiconductivity in a methanol adsorbed 1,3,5-trinitrobenzene powder cell as a function of temperature. (Ambient vapour pressure 60 mm; adsorbed at sample cell temperature 22°C)

FIGURE - 4.4

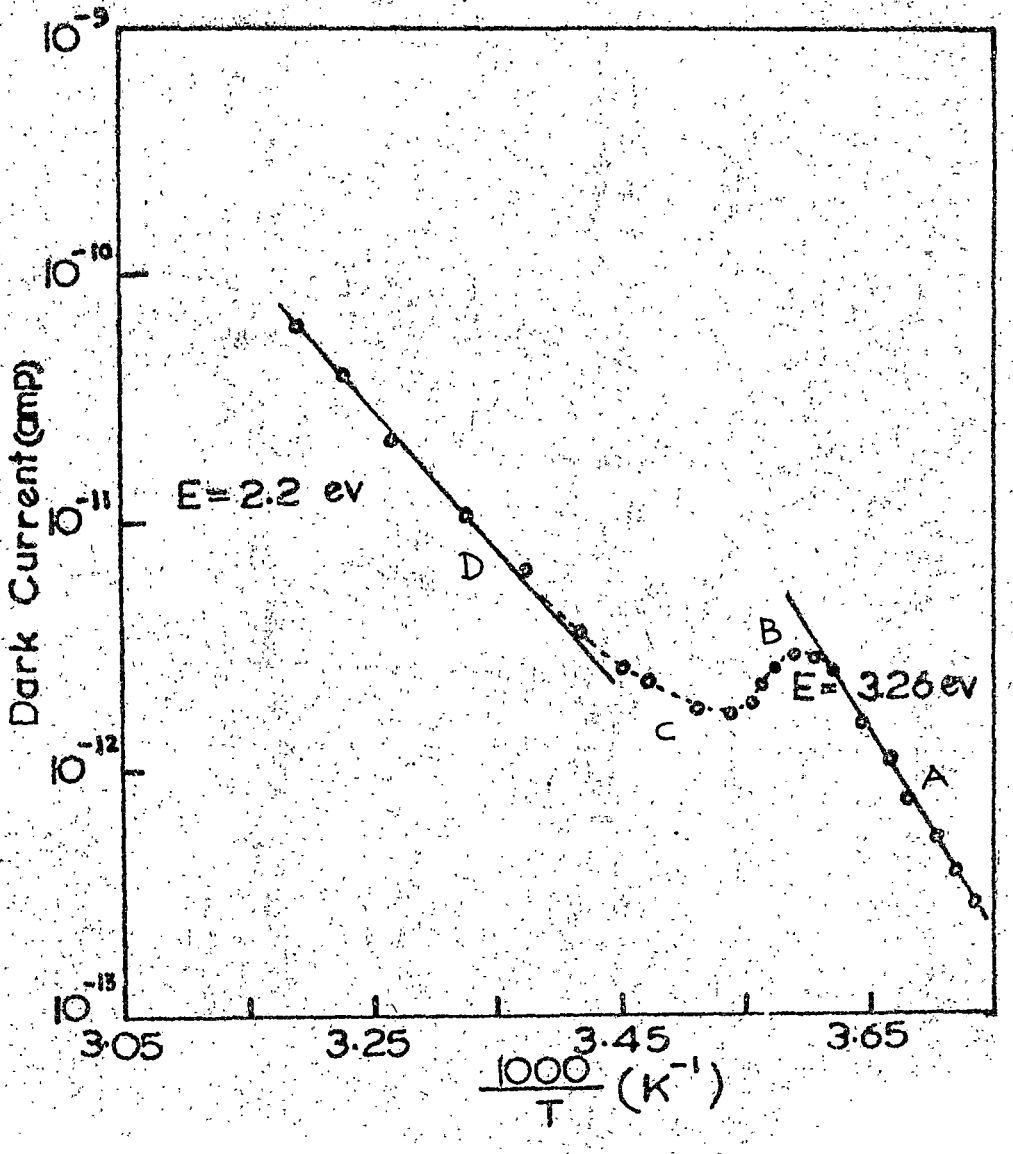

Semiconductivity in a carbontetrachloride adsorbed powder cell as a function of temperature. (Ambient vapour pressure 50 mm; adsorbed at sample cell temperature 25°C)

FIGURE - 4.6

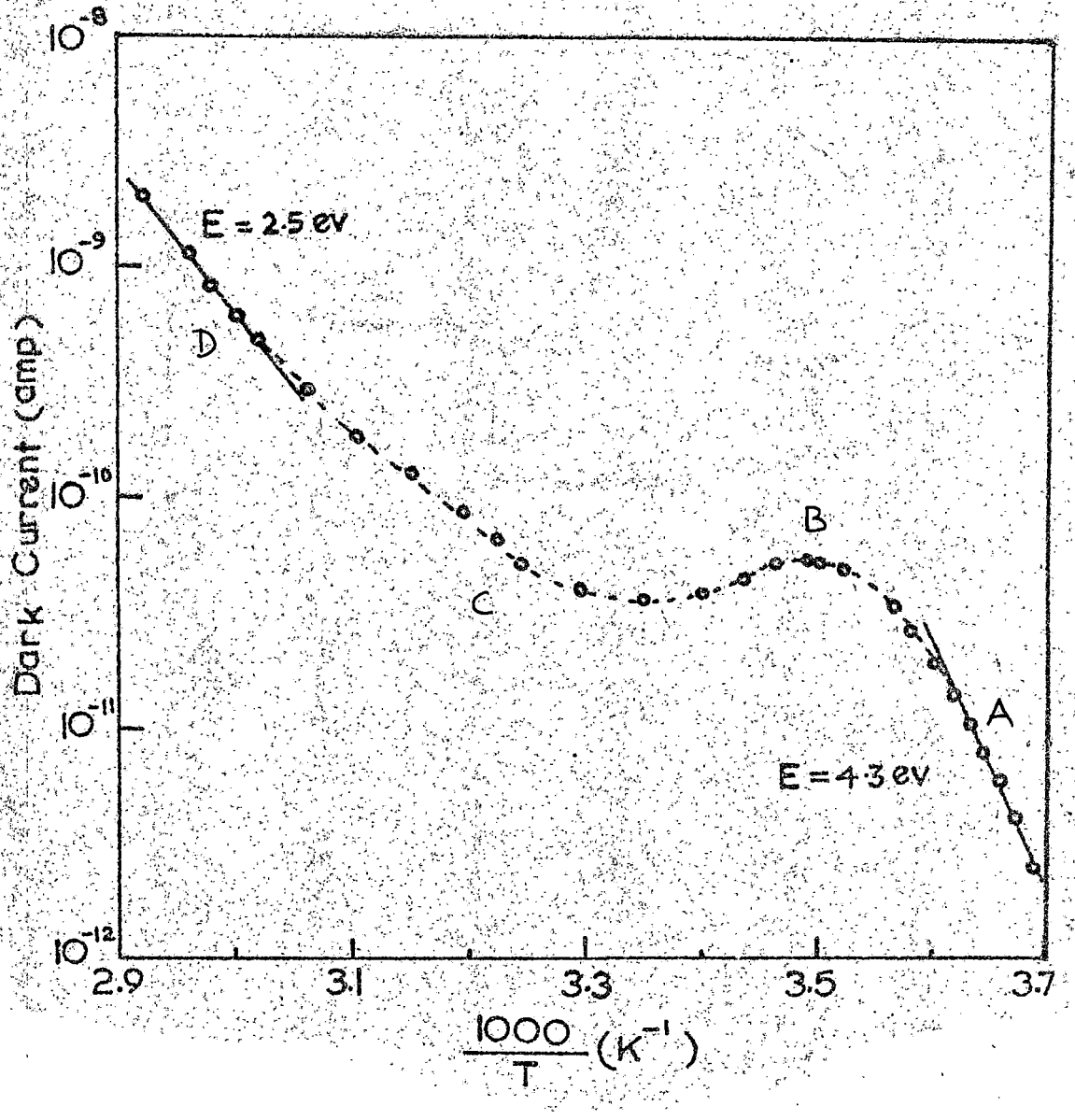

Semiconductivity in a methanol adsorbed O-nitrobenzoic acid powder cell as a function of temperature. (Ambient vapour pressure 50 mm; adsorbed at sample cell temperature 25°C)

that are found to form some sort of strong complexes (as described in the previous chapter), the current does not return to the initial value at the point C and the activation energy in the higher temperature region is not equal to the vacuum / dry nitrogen activation energy value as shown in Figs. 4.6 and 4.7 for ethyl acetate vapour adsorption on 1,4-dinitronaphthalene and 1,3,5-trinitrobenzene. For 9-nitroanthracene, 2 - nitrofluorene and 0-nitrobenzoic acid, vapours of ethanol, methanol, ethylacetate, carbon tetrachloride, benzene and n-hexane; for 1,4-dinitronaphthalene that of ethanol, methanol and cyclohexane and for 1,3,5-trinitrobenzene vapours of ethanol, methanol, cyclohexane and n-hexane were found to form weak reversible complexes and the curves are similar to that in Figs. 4.1 - 4.5.

The effect of adsorption of different vapours on the semiconduction activation energy of these nitroaromatic compounds has been made in the usual manner after adsorbing different vapours at a fixed partial vapour pressure maintaining the sample cell at a constant temperature. In Figs. 4.8 - 4.14, plots of log $\sigma(T)$ vs. 1/T for different nitroaromatic semiconductors are shown in the low temperature region for different vapour adsorption. It is observed that the activation energy values are different for different vapour adsorption. Different vapours forming weak reversible complexes change the activation energies of the nitroaromatics

FIGURE - 4.6

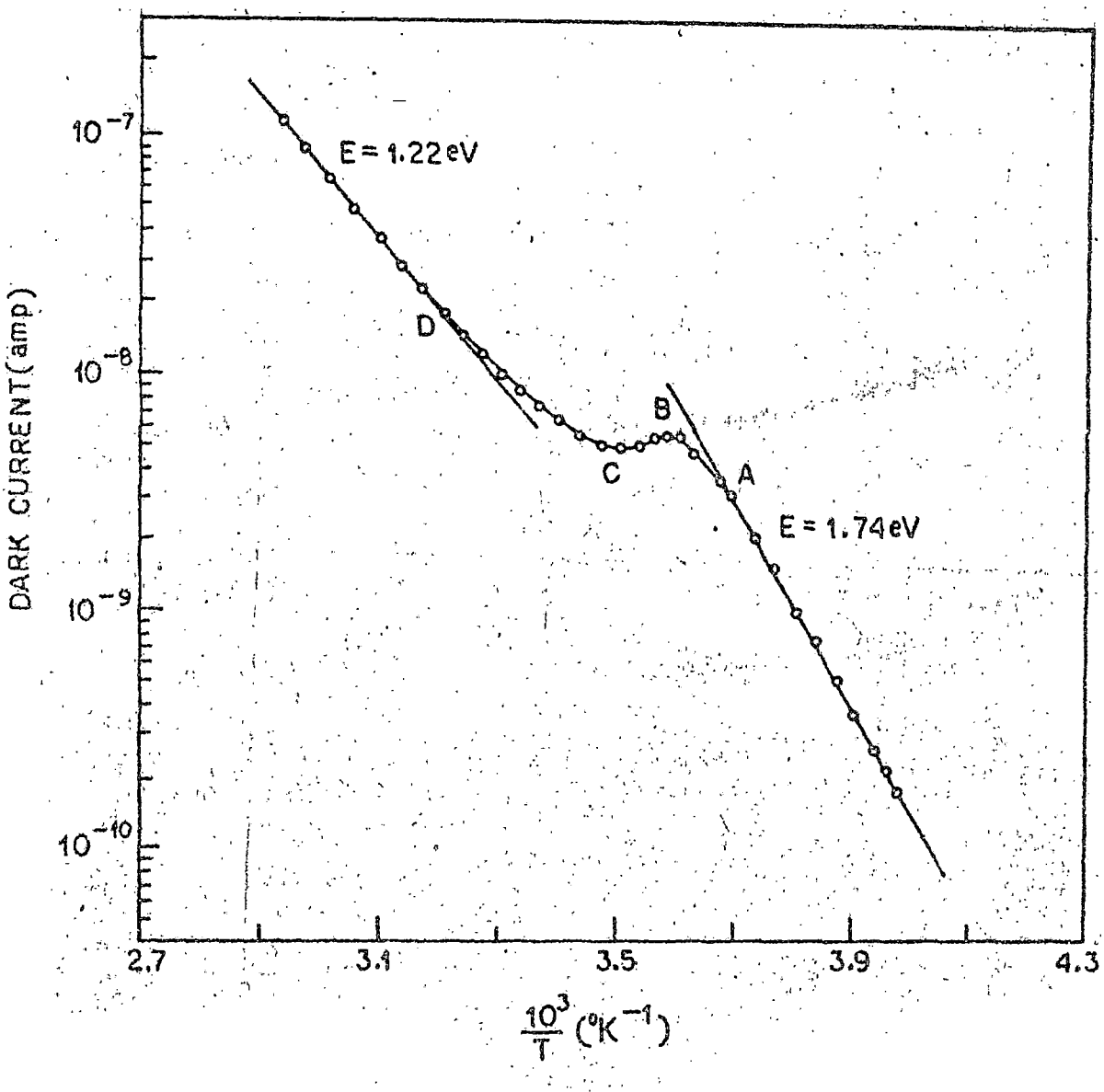

Semiconductivity in an ethyl acetate adsorbed 1,4-dinitro-naphthalene powder cell as a function of temperature. (Ambient vapour pressure 55.5 mm; adsorbed at sample cell temperature 22°C)

FIGURE - 4.7

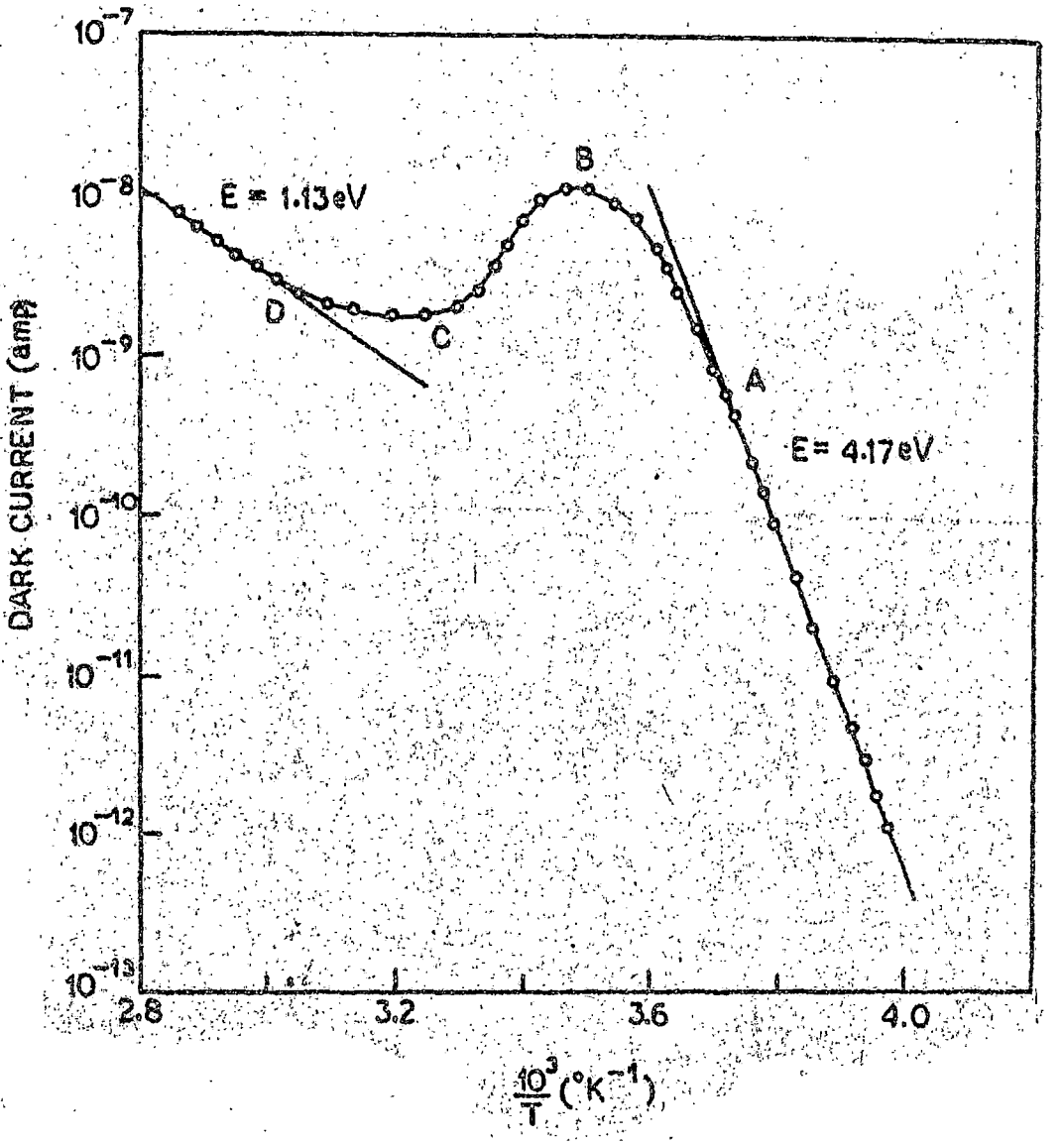

Semiconductivity in an ethyl acetate adsorbed 1,3,5-trinitrobenzene powder cell as a function of temperature. (Ambient vapour pressure 53.5 mm; adsorbed at sample cell temperature 22°C)

FIGURE - 4.8

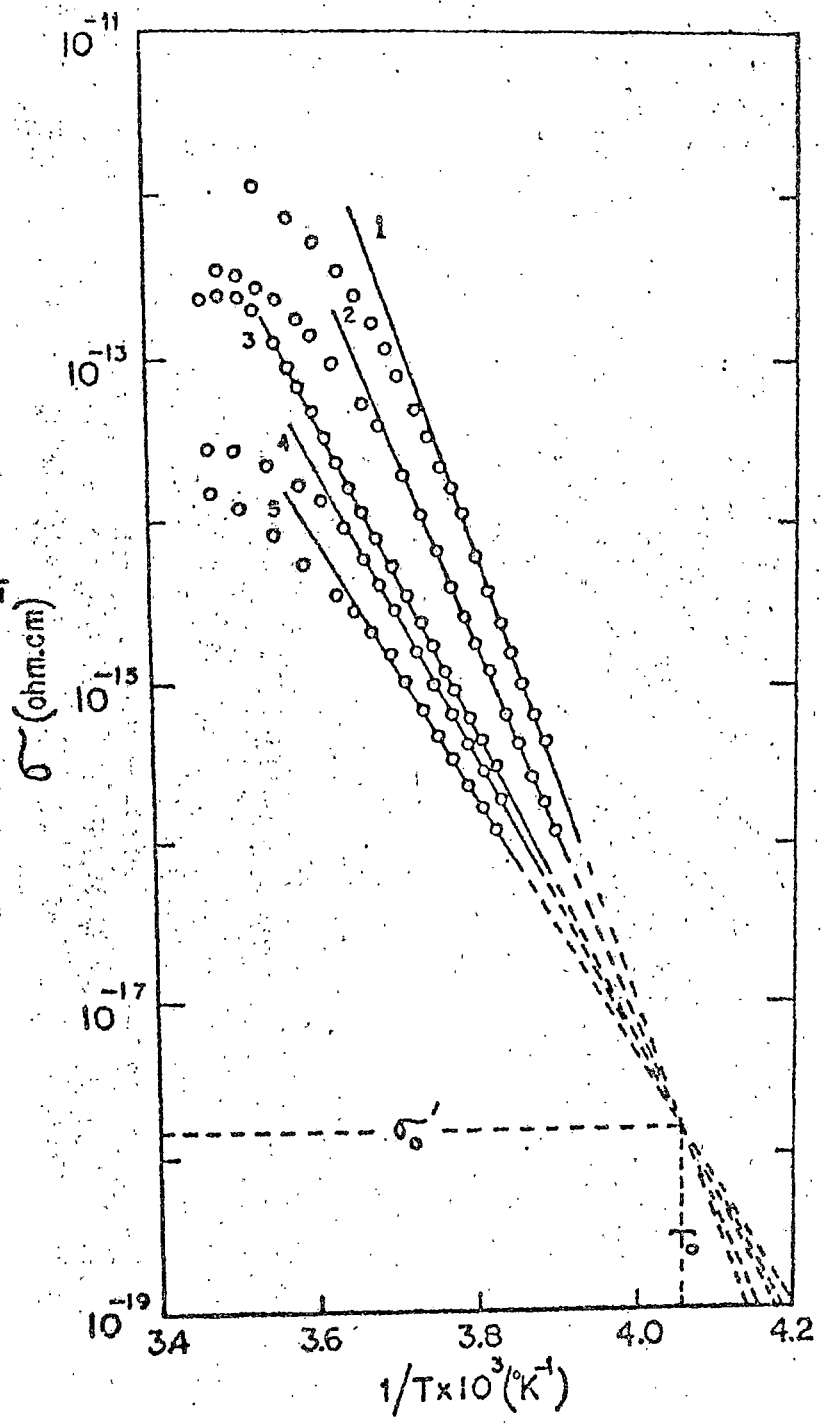

Semiconductivity in a 9-nitroanthracene powder cell (steady state condition) with the adsorption of different vapours at the same vapour pressure (50 mm) and at a sample cell temperature 22°C. Solid lines represent temperature region of measurements, broaken lines are extrapolations. Each line corresponds to a specific vapour adsorbed state : 1. ethanol, 2. ethylacetate, 3. benzene, 4. carbon-tetrachloride and 5. methanol (Refer Table 4.1, 4.3)

FIGURE - 4.9

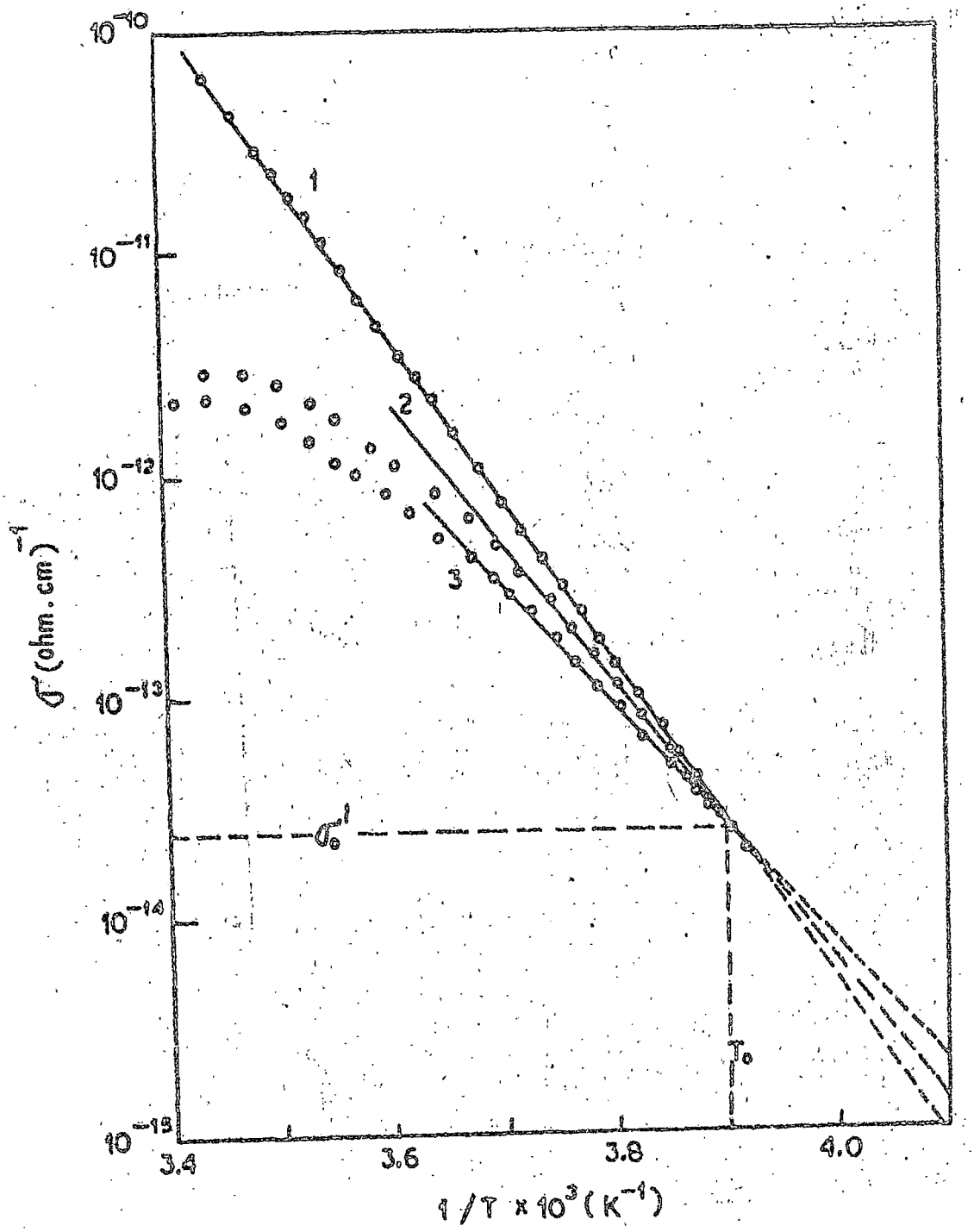

Semiconductivity in a 1,4-dinitronaphthalene powder cell (steady state condition) with the adsorption of different vapours at the same vapour pressure (50 mm) and at a sample cell temperature of 22°C. Solid lines represent temperature region of measurements, broaken lines are extrapolations. Each line corresponds to a specific vapour adsorbed state : 1. ethanol, 2. methanol and 3. cyclohexane. (Refer table 4.1, 4.4)

FIGURE - 4.10

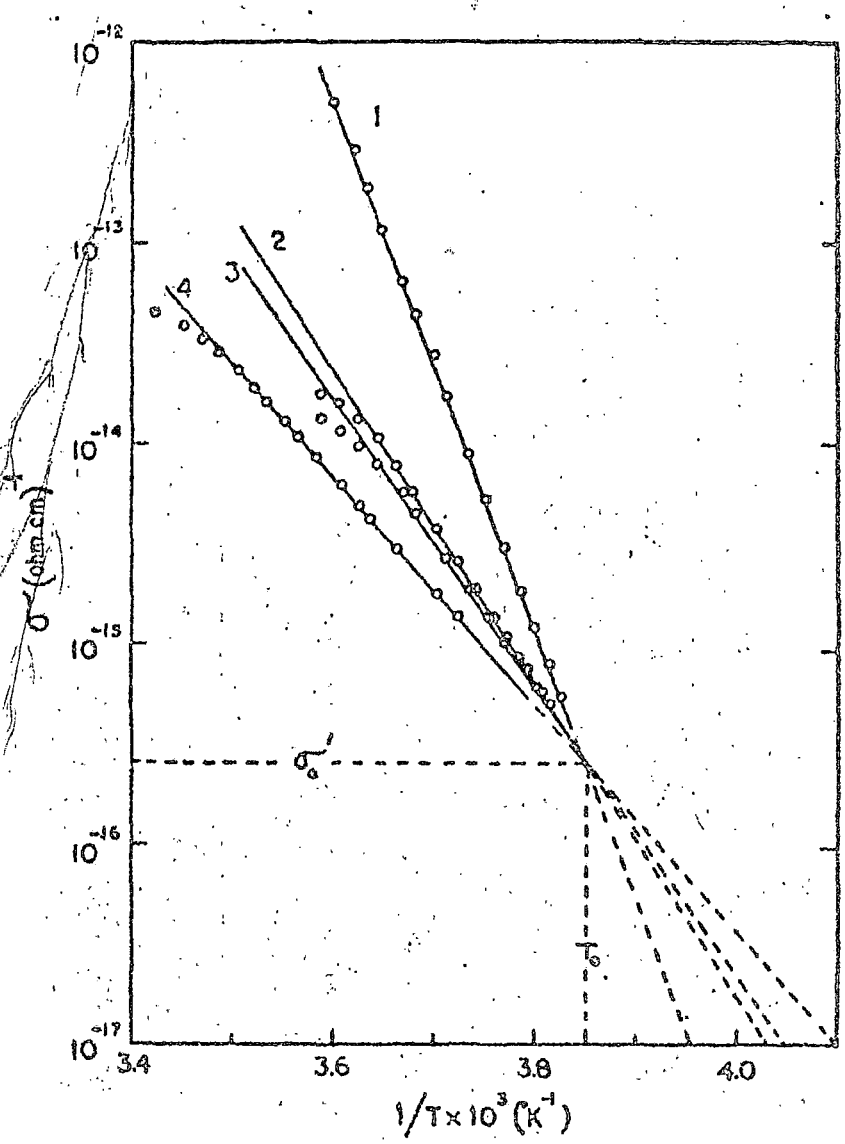

Semiconductivity in a 1,3,5-trinitrobenzene powder cell (steady state condition)with the adsorption of different vapours at the same vapour pressure (60 mm) and at a sample cell temperature of 22°C. Solid lines represent temperature region of measurements, broaken lines are extrapolations. Each line corresponds to a specific vapour adsorbed state : Vapours are 1. ethanol 2. n-hexane 3. cyclohexane and 4. methanol. (Refer Table 4.1, 4.5)

FIGURE - 4.11

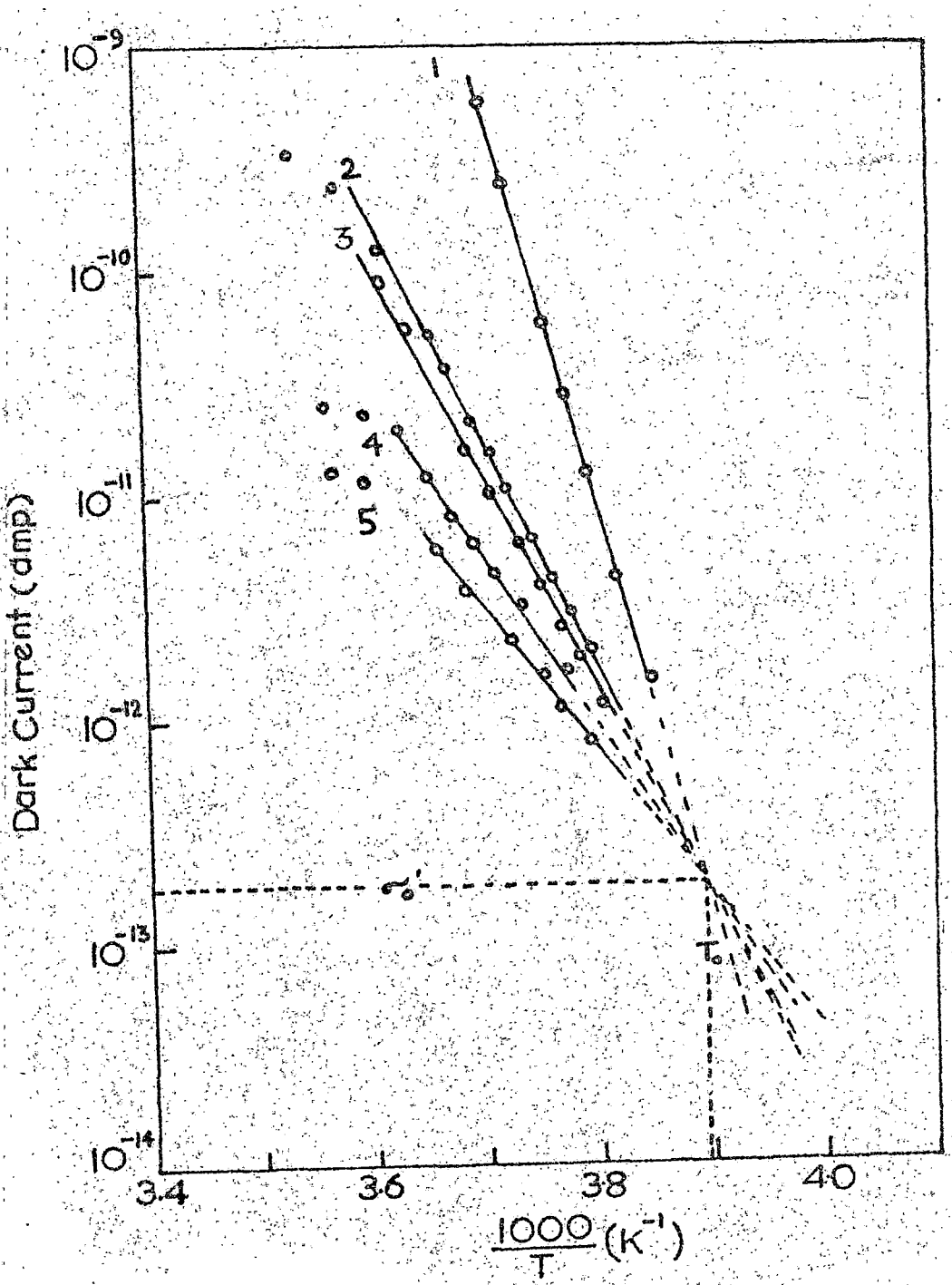

Semiconductivity in a 2-nitrofluorene powder cell (steady state condition) with the adsorption of the same amount of different vapours (solid lines represent temperature region of measurement and broken lines are extrapolations) Each line refers to a specific vapour adsorbed state : Vapours are 1. ethanol, 2. ethylacetate, 3. benzene, 4. carbontetrachloride and 5. n-hexane. (Refer Tables 4.1, 4.6)

FIGURE - 4.12

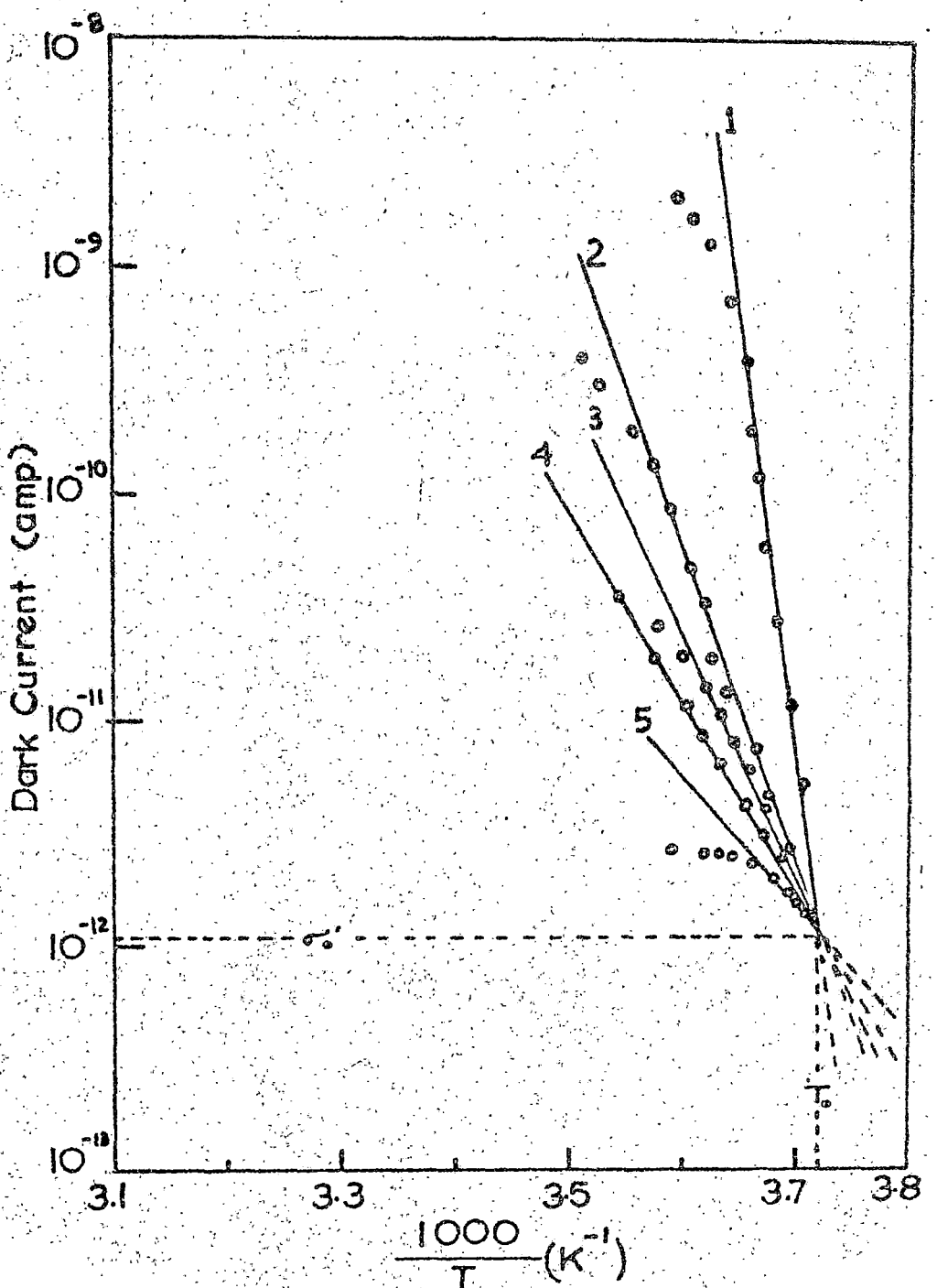

Semiconductivity in a O-nitrobenzoic acid powder cell (steady state condition) with the adsorption of the same amount of different vapours (solid lines represent temperature region of measurement and broaken lines are extra polations) Each line refers to a specific vapour adsorbed state : Vapours are 1. ethyl acetate, 2. ethanol, 3. methanol, 4. carbontetrachloride and 5. n-hexane. (Refer Tables 4.1, 4.7)

FIGURE - 4.13

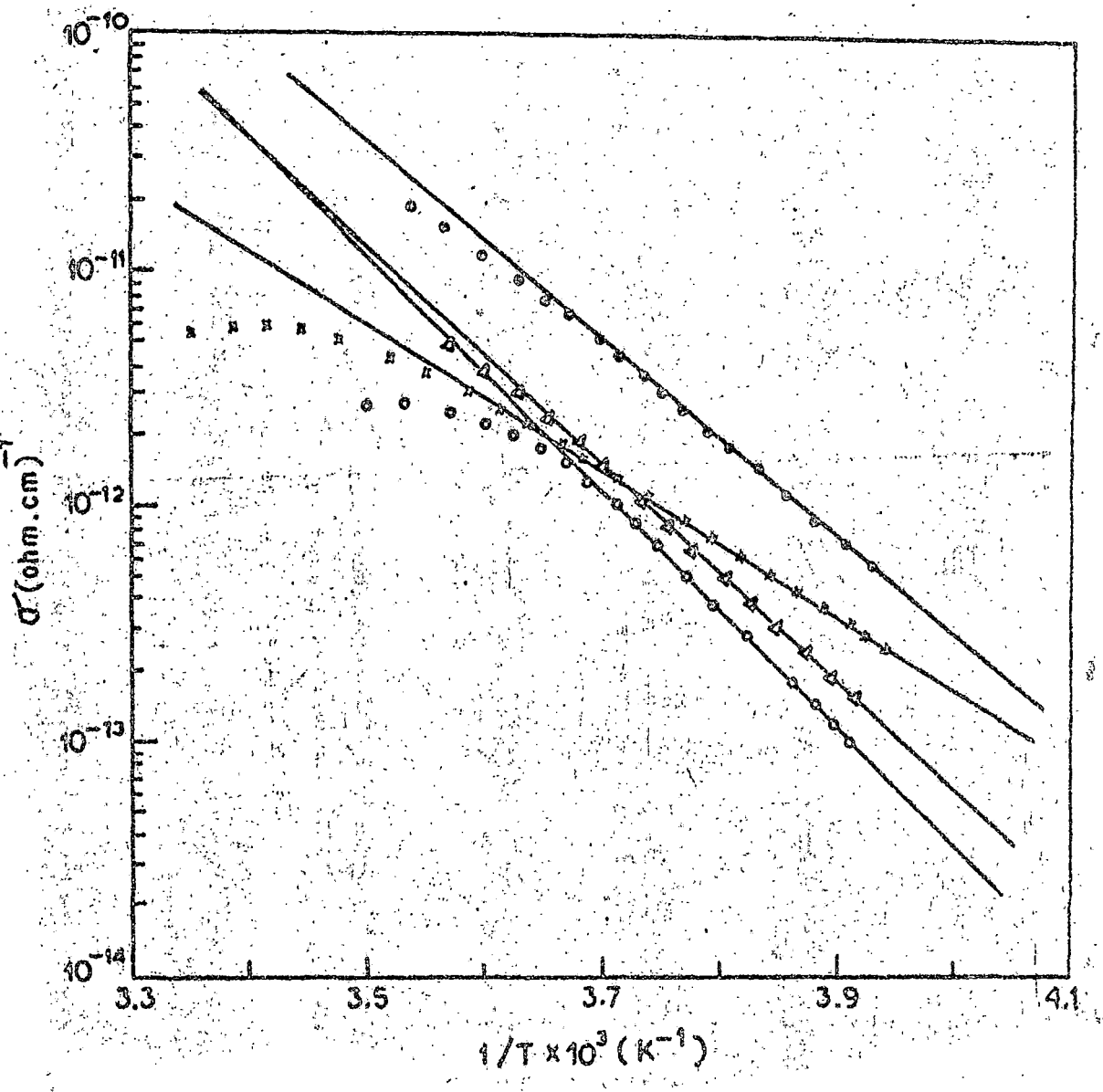

Semiconductivity in a 1,4-dinitronaphthalene powder cell (steady state condition) with the adsorption of different vapours at the same pressure (50 mm) and at sample cell temperature of 22°C. Each line refers to a specific vapour adsorbed state : Ethyl acetate (-•-, E = 1.67 ev);
Carbontetrachloride (-x-, E = 1.25 ev);
n-Hexane (-o-, E = 2.03 ev);
Benzene (-Δ-, E = 1.60 ev)

FIGURE - 4.14

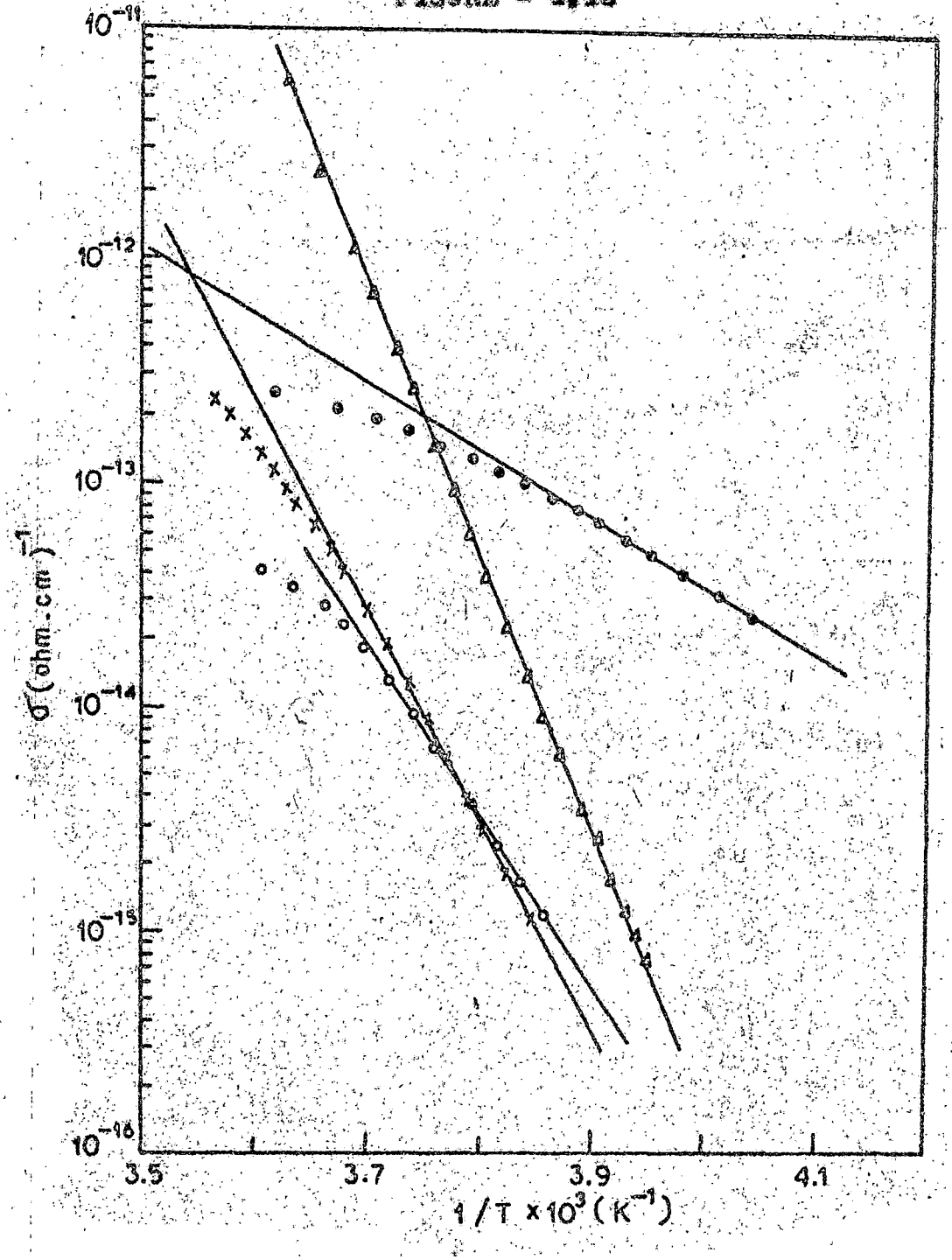

Semiconductivity in a 1,3,5-trinitrobenzene powder cell (steady state condition) with the adsorption of different vapours at the same pressure (60 mm) and at sample cell temperature of 32°C. Each line refers to a specific vapour adsorbed state :

Methylcyclohexane (-●-, E = 1.23 ev);

Ethyl acetate (-△-, E = 4.63 ev) ;

Benzene (-x-, E = 3.76 ev);

Carbontetrachloride (-○-, E = 3.06 ev)

as shown in Figs. 4.8 - 4.12 whereas those giving strong complexes produce the type of activation energy change as shown in Figs 4.13 and 4.14.

2.2 Semiconduction activation energy as a function of the amount of vapour adsorbed :

To study the dependence of the activation energy change on the amount of a particular vapour adsorbed in a sample cell, measurements were done by repeated heating, partially desorbing and cooling cycles. In Figs. 4.15 - 4-19 plots of log σ_T or log I_T vs. 1/T for adsorption of different amounts of a vapour on 9-nitroanthracene, 1,4-dinitronaphthalene, 1,3,5-trinitrobenzene, 2-nitrofluorene and O-nitrobenzoic acid are shown. The slopes of the straight lines decrease with decreasing amounts of the adsorbed vapour. Thus, the value of the activation energy decreases in a regular monotonic fashion as more vapour desorbs from the sample. Also, number of other vapours that are found to form weak complexes with these nitroaromatic semiconductors produce a similar change in activation energy value with the amount of these vapours adsorbed. A set of approximately parallel straight lines is observed in the low temperature region for log σ_T vs. 1/T plots for different amounts of ethylacetate adsorption on 1,4 dinitronaphthalene and 1,3,5-trinitrobenzene as shown in Figs. 4.20 and 4.21

FIGURE - 4.16

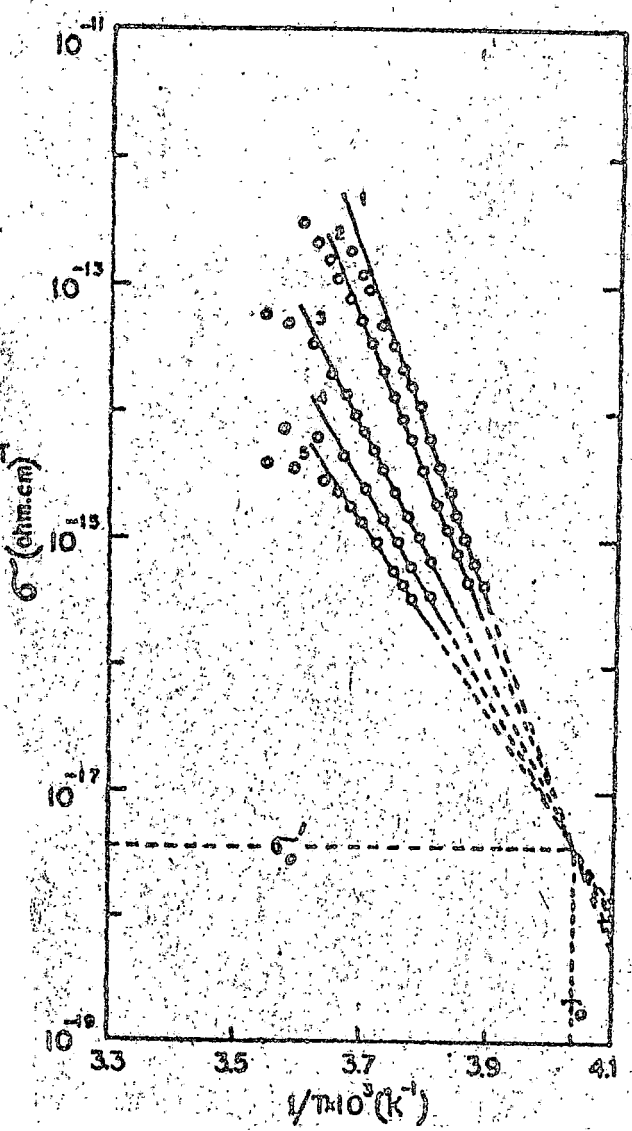

Semiconductivity data for 9-nitroanthracene powder cell (steady state condition) with the adsorption of different amounts of ethanol vapour. Solid lines represent the temperature region of measurements, broaken lines are extrapolations. The lines (1)→(5) refer to the states with the decreasing amount of adsorbed vapour. (Refer Tables 4.1, 4.8)

FIGURE - 4.10

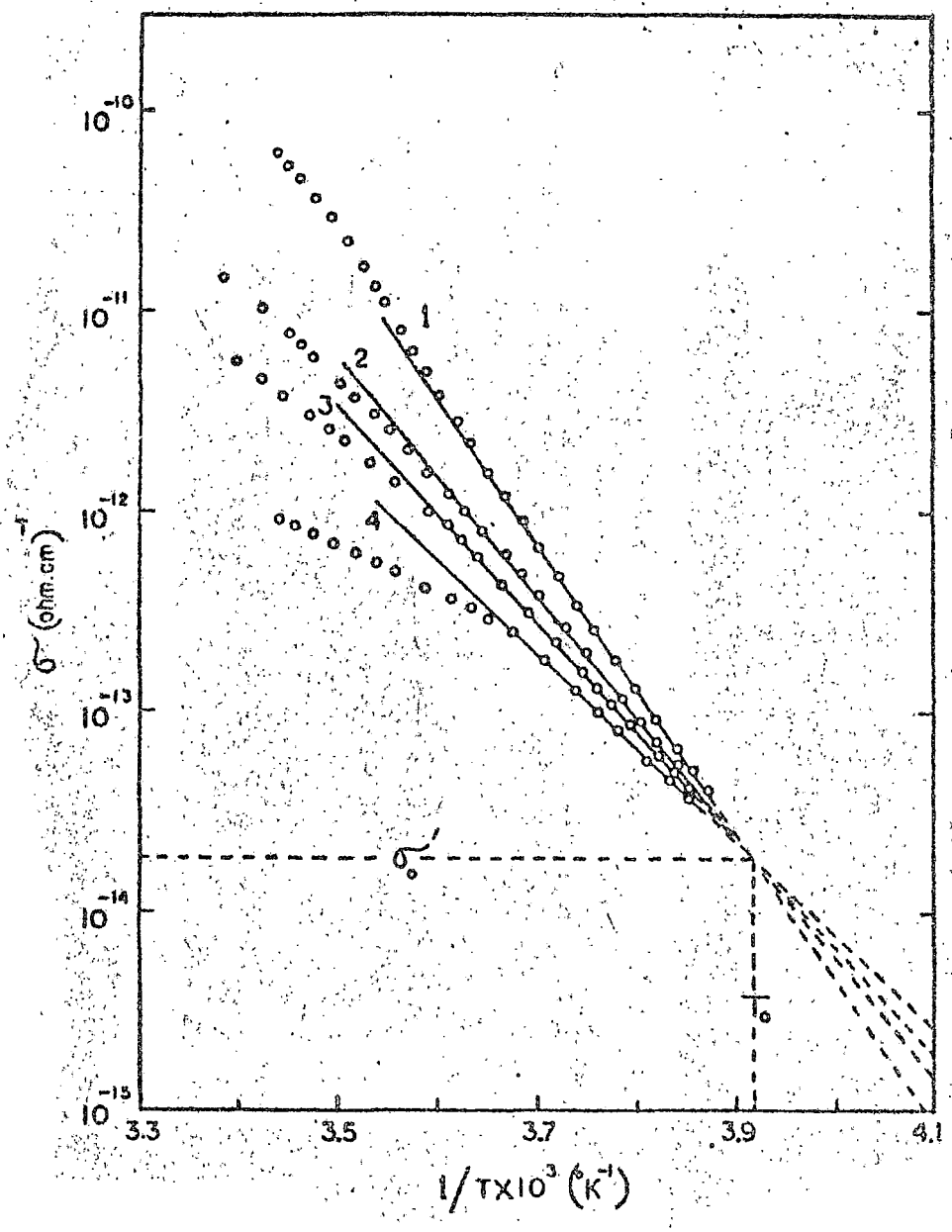

Semiconductivity data for 1,4-dinitronaphthalene powder cell (steady state condition) with the adsorption of different amounts of ethanol vapour. Solid lines represent the temperature region of measurements, broken lines are extrapolations. The lines (1) → (4) refer to the states with the decreasing amount of adsorbed vapour. (Refer Tables 4.1, 4.2)

FIGURE - 4.17

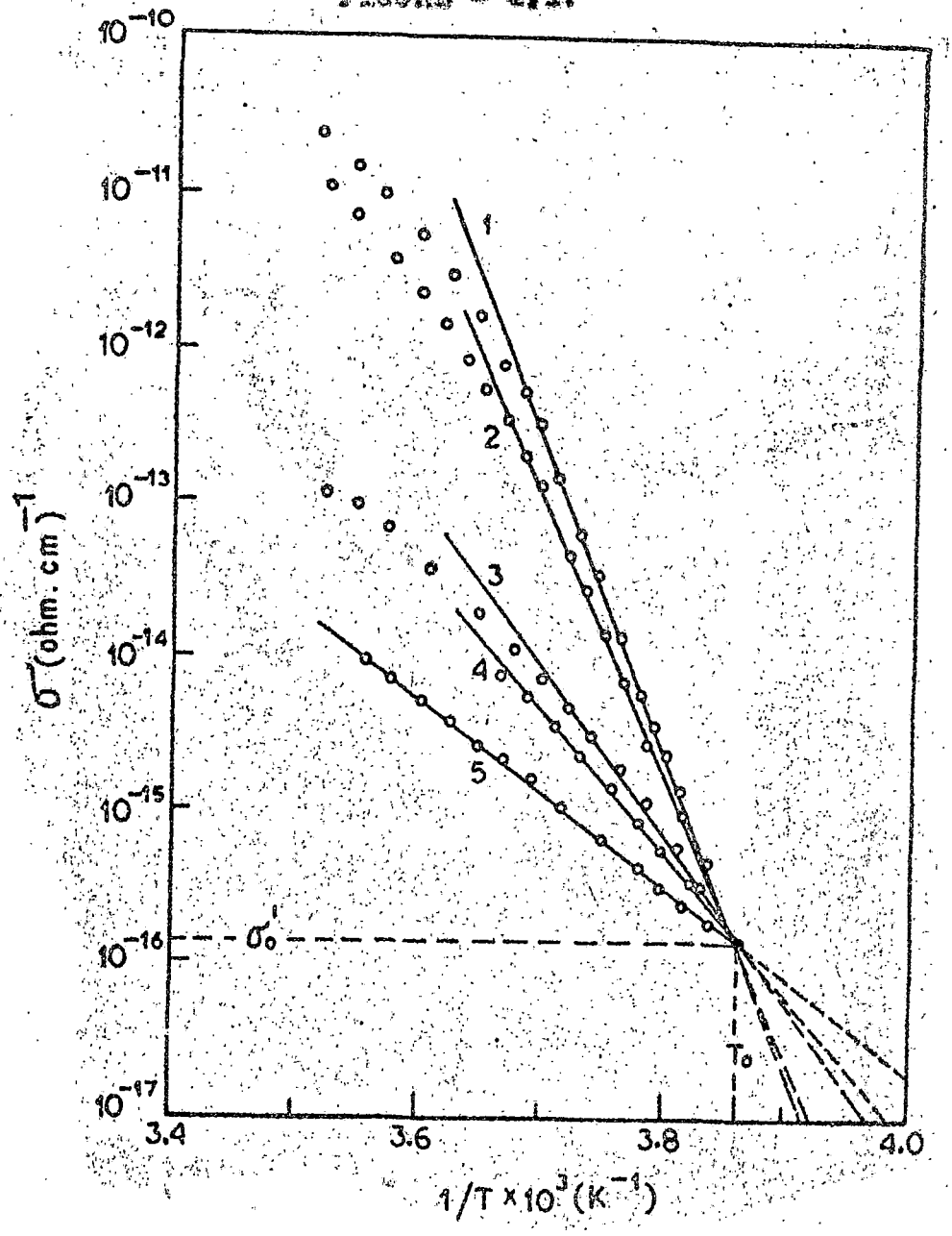

Semiconductivity data for 1,3,6-trinitrobenzene powder cell (steady state condition) with the adsorption of different amounts of ethanol vapour. Solid lines represent the temperature region of measurement, broaken lines are extrapolations. The lines (1) → (5) refer to the states with the decreasing amount of adsorbed vapour. (Refer Tables 4.1 and 4.10)

FIGURE - 4.12

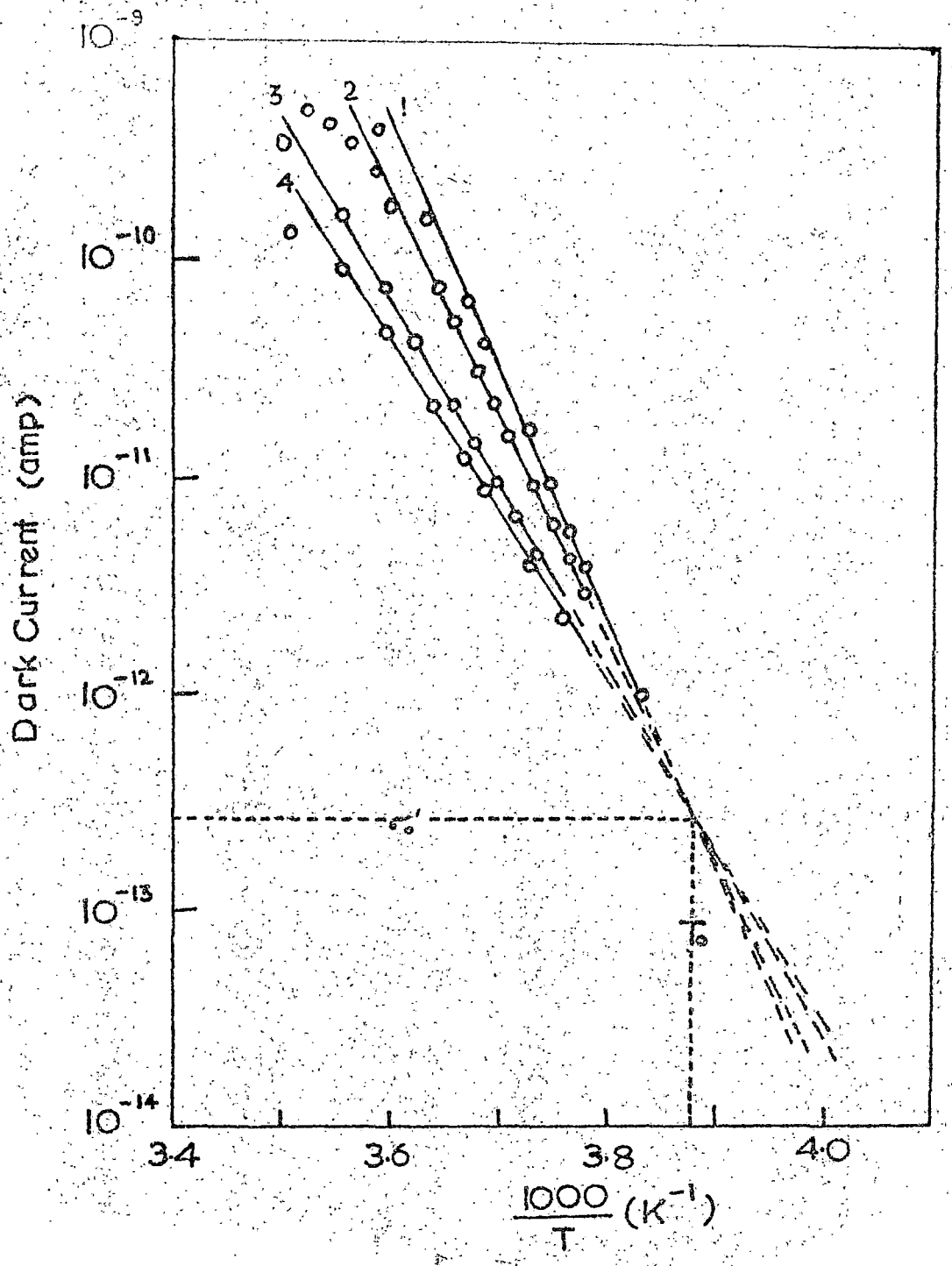

Semiconductivity data for 2-nitrofluorene powder cell (steady state condition) with adsorption of different amount of ethylacetate vapour. Solid lines represent the temperature region of measurement, broaken lines are extrapolations. The lines (1) → (4) refer to the states with decreasing amount of adsorbed vapour. (Refer Tables 4.1, 4.11)

FIGURE - 4.19

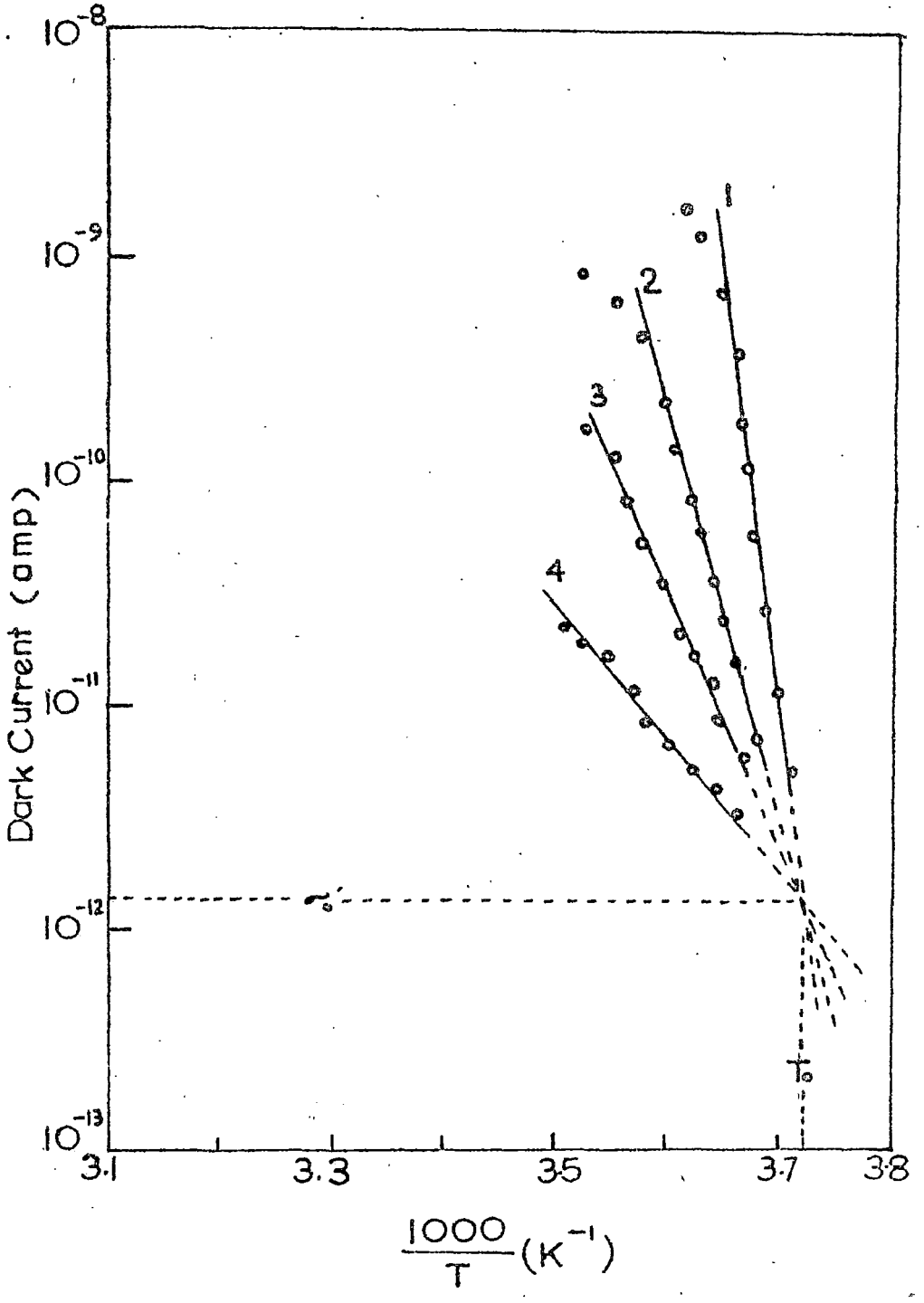

Semiconductivity data for O-nitrobenzoic acid powder cell (steady state condition) with adsorption of different amount of ethylacetate vapour. Solid lines represent the temperature region of measurement, broaken lines are extrapolations. The lines (1)→(4) refer to the states with decreasing amount of adsorbed vapour. (Refer Tables 4.1 and 4.12)

FIGURE - 4.20

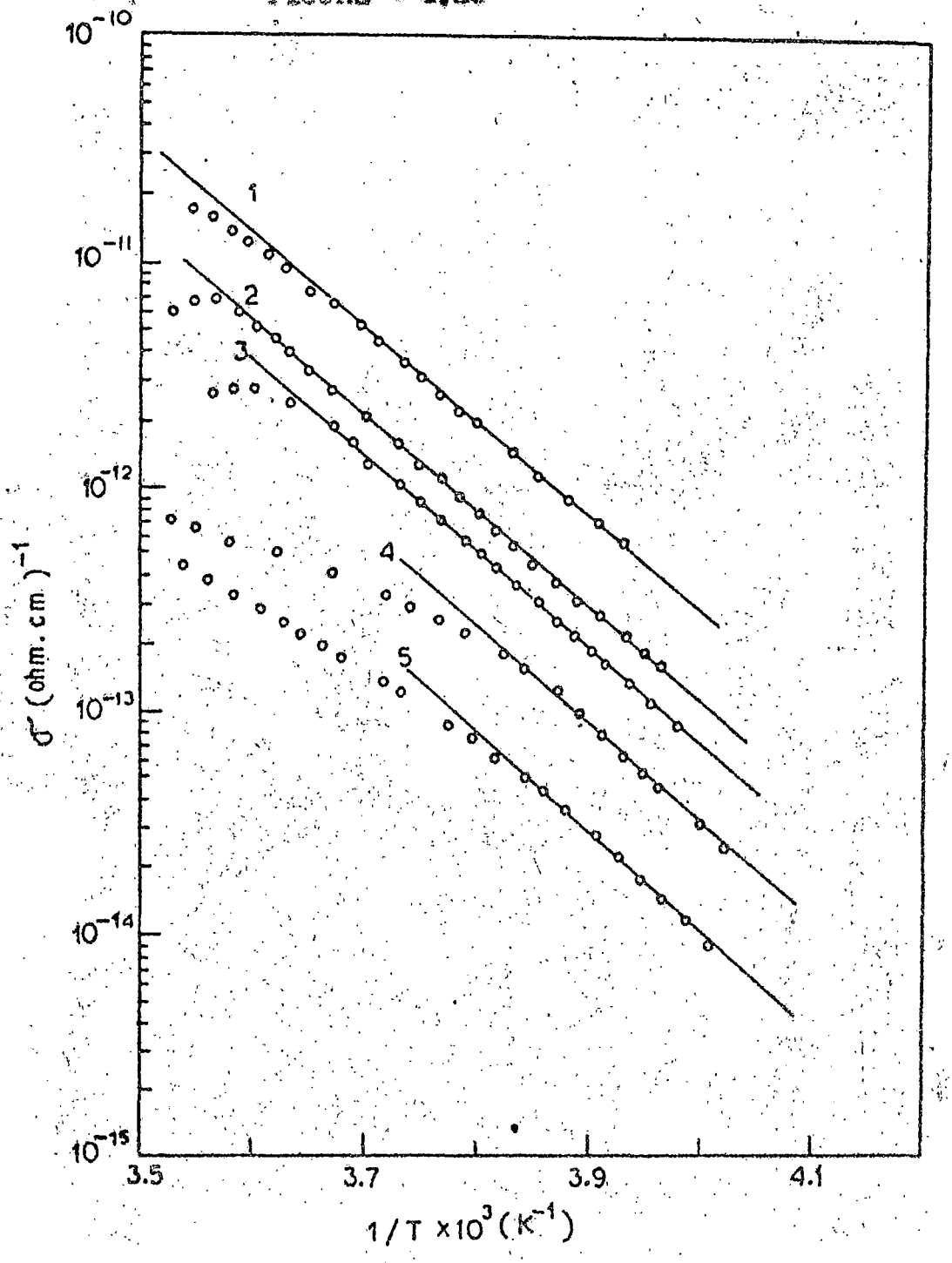

Semiconductivity data for 1,4-dinitronaphthalene powder cell (steady state condition) with the adsorption of different amounts of ethyl acetate vapour. The lines (1)→(5) refer to the states with the decreasing amount of adsorbed vapour. The E - values are (1) 1.67 ev; (2) 1.63 ev; (3) 1.67 ev; (4) 1.70 ev; (5) 1.76 ev.

FIGURE - 4.21

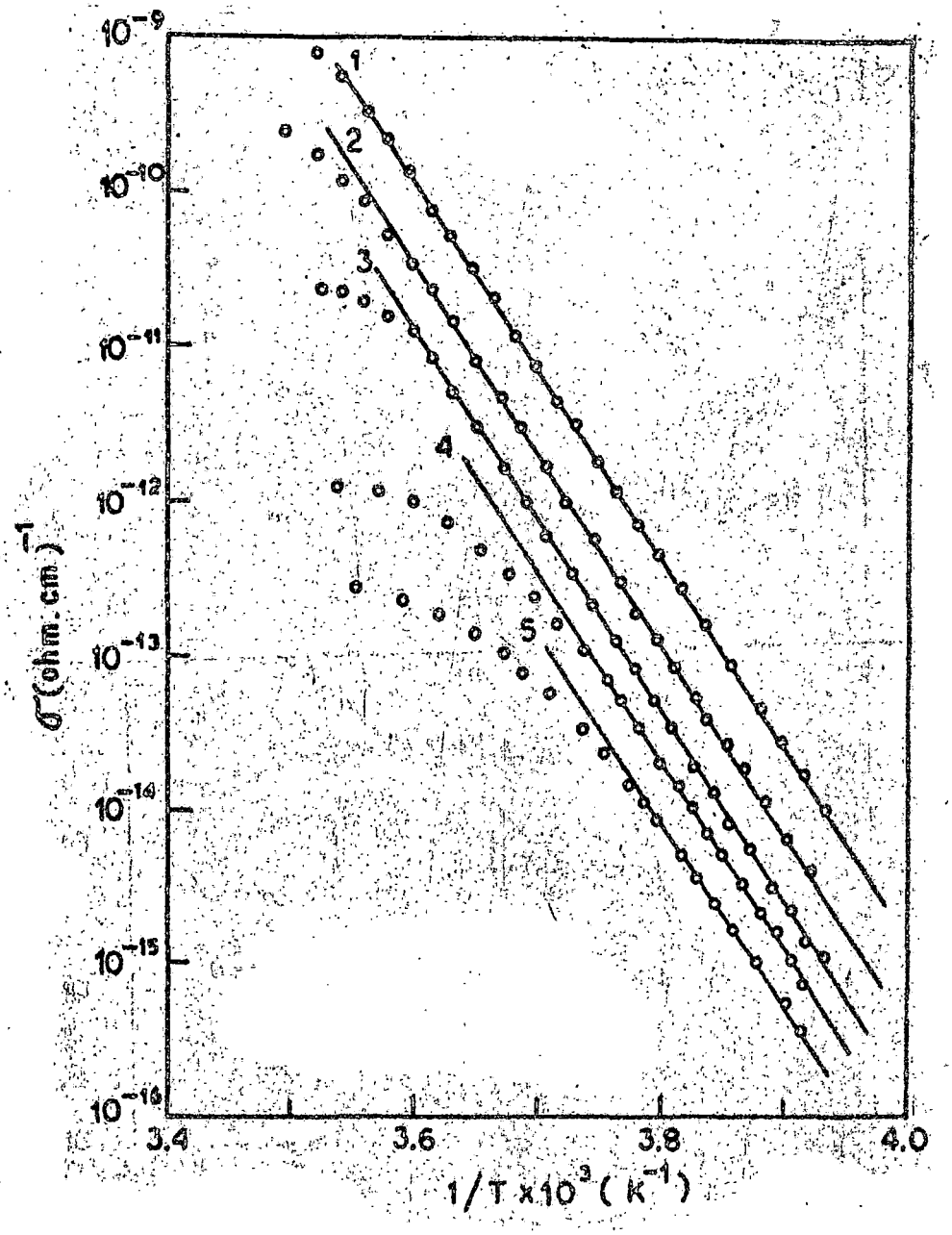

Semiconductivity data for 1,3,5-trinitrobenzene powder cell (steady state condition) with the adsorption of different amounts of ethyl acetate vapour. The lines (1) → (5) refer to the states with the decreasing amount of adsorbed vapour. The E - values are (1) 4.83 ev; (2) 4.85 ev; (3) 4.89 ev; (4) 4.98 ev; (5) 4.79 ev.

respectively. So, in this case of strong complexes approximately the same value of activation energy is obtained with decreasing amount of adsorbed vapour. The other vapours e.g. carbon-tetrachloride, benzene, toluene, methylcyclohexane, n-hexane and n-heptane on 1,4-dinitronaphthalene and carbon-tetrachloride, benzene, toluene, methylcyclohexane and n-heptane on 1,3,5-trinitrobenzene produce the same type of results. The shifting of straight lines in the log σ_T vs. $1/T$ plots i.e. the decrease in the observed conductivity values with less amount of adsorbed vapour may be due to variation in the equivalent thickness of the strongly bound vapour - semiconductor complex.

2.3 Compensation temperature for the nitroaromatic semiconductors

As shown in Figs. 4.8 - 4.12 and 4.15 - 4.19, the extrapolated lines in log σ_T vs. $1/T$ plots of 9-nitroanthracene, 1,4 dinitronaphthalene, 1,3,5-trinitrobenzene, 2-nitrofluorene and O-nitrobenzoic acid intercept the ordinate at a wide varieties of positions and they all pass through a single point of intersection at a temperature 'T_0' as expected from equation (1.1) which can also be written as

$$\log \sigma (T) = \log \sigma_0' + \left[1/T_0 - 1/T\right] E/2.3R \quad (2.31)$$

At this compensation temperature T_0, the value of $\sigma(T_0)$ gives

value. The values of T_0's and σ_0''s obtained from different log σ vs. 1/T plots for the semiconductors studied are shown in Table 4.1. It is observed that the two sets of T_0's and σ_0''s are in good agreement. But in case of Figs. 4.13, 4.14, 4.20 and 4.21, the extrapolated lines in log σ vs. 1/T plots do not intersect at a single point and thus compensation temperature T_0 is not obtained in case of ethylacetate, benzene, carbontetrachloride, n-hexane, toluene and methylcyclohexane vapour adsorption on 1,4-dinitronaphthalene and ethylacetate, benzene, carbontetrachloride, toluene and methylcyclohexane vapour adsorption on 1,3,5-trinitrobenzene.

From functional definition of semiconductor :

$$\sigma(T) = \sigma_0 \exp(-E/2kT) \qquad (2.32)$$

and equation (2.31), it is expected that the plots of log σ_0 vs. E should be linear. In Figs. 4.22 - 4.24, such plots for 9-nitroanthracene, 1,4-dinitronaphthalene, 1,3,5-trinitrobenzene, 2-nitrofluorene and 6-nitrobenzoic acid are shown. The values of T_0's and σ_0''s obtained from the slopes and intercepts respectively of these plots for different nitroaromatics are presented in Table 4.2 for comparison with the values obtained from different log σ vs. 1/T plots. T_0 and σ_0' values obtained from various plots show excellent agreement[143]. Using the values of T_0's and σ_0''s

Table 4.1

The values of T_0's and σ_0''s obtained from different log σ vs. 1/T plots of some nitroaromatic semiconductors.

Semiconductor	Value of T_0 (°K) obtained from the log σ vs 1/T plots for		Value of σ_0' (Ω-cm)$^{-1}$ obtained from the log σ vs. 1/T plots for	
	adsorption of different vapours	adsorption of different amounts of a particular vapour	adsorption of different vapours	adsorption of different amounts of a particular vapour
9-nitro-anthracene[1]	246.4	247.6	1.43×10^{-13}	3.59×10^{-13}
1,4-dinitro-naphthalene[2]	256.4	255.1	2.46×10^{-14}	1.77×10^{-14}
1,3,5-tri-nitrobenzene[3]	259.7	259.1	2.64×10^{-16}	1.51×10^{-16}
2-nitro-fluorene[4]	257.0	257.86	1.20×10^{-16}	2.16×10^{-16}
O-nitro-benzoic-acid[5]	270.27	258.8	8.6×10^{-16}	9.37×10^{-16}

1. From Figures 4.8 and 4.15 2. From Figures 4.9 and 4.16
3. From Figures 4.10 and 4.17 4. From Figures 4.11 and 4.18
5. From Figures 4.12 and 4.19.

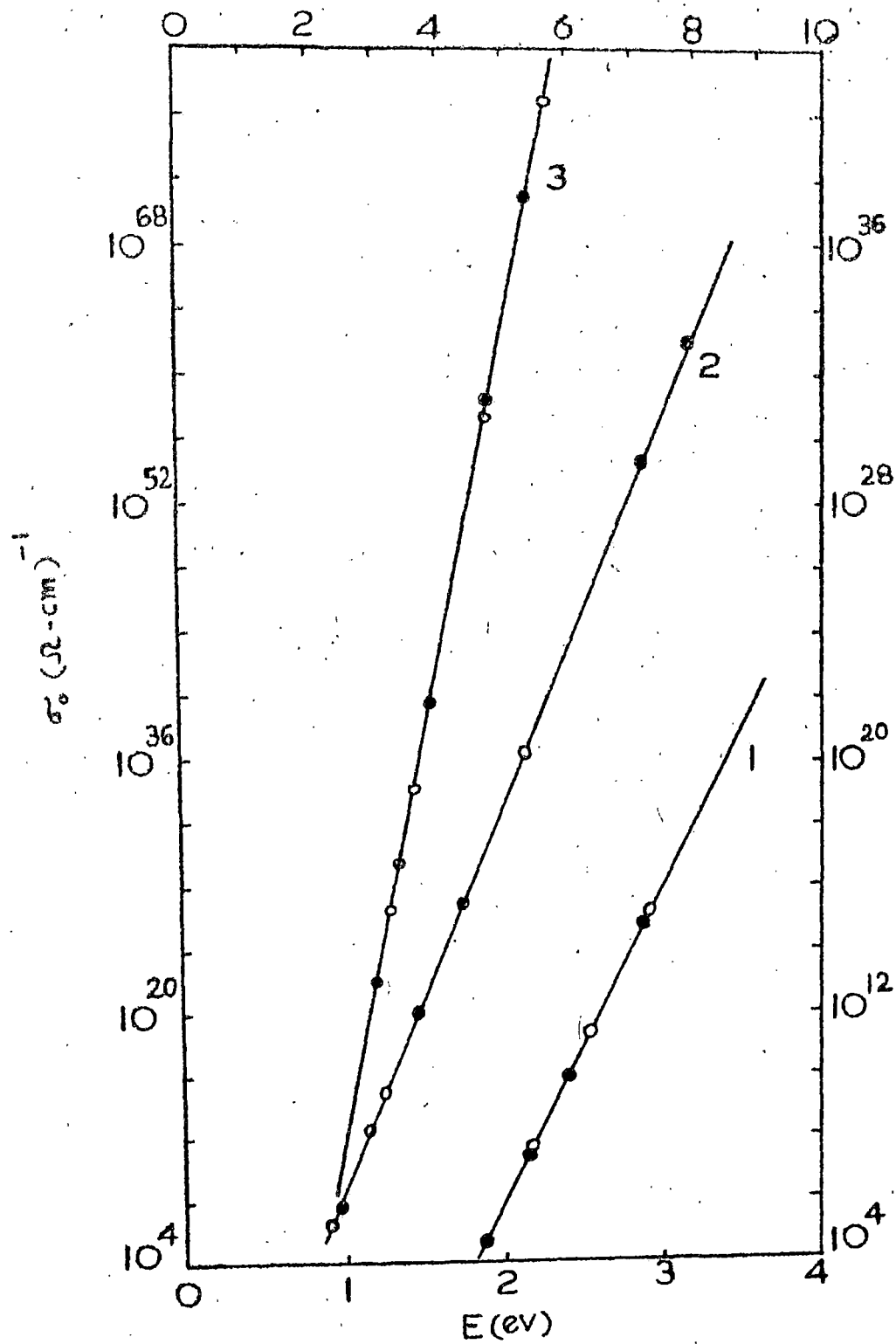

FIGURE - 4.22 : The plots of the log σ_0 at a constant temperature vs. the E - values for (1) 1,4-dinitronaphthalene (right and lower scale), (2) 1,3,5-trinitrobenzene (left and upper scale) and (3) 9-nitroanthracene (right and upper scale). The open circles refer to different vapours and the dark circles to different amounts of a particular vapour (e.g. ethanol). (Refer Table 4.2)

FIGURE - 4.23

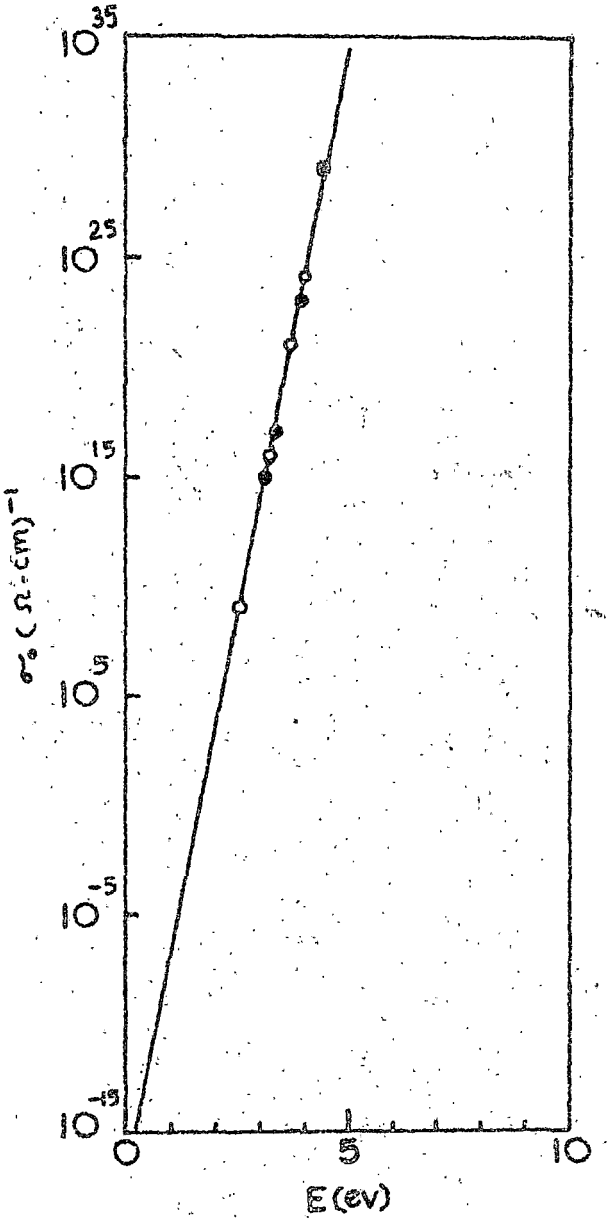

The plot of the log σ_o at a constant temperature vs. the E - values for 2-nitrofluorene. The open circles refer to different vapours and the solid circles to different amount of the same vapour (ethyl acetate) (Refer Table 4.2)

FIGURE - 4.24

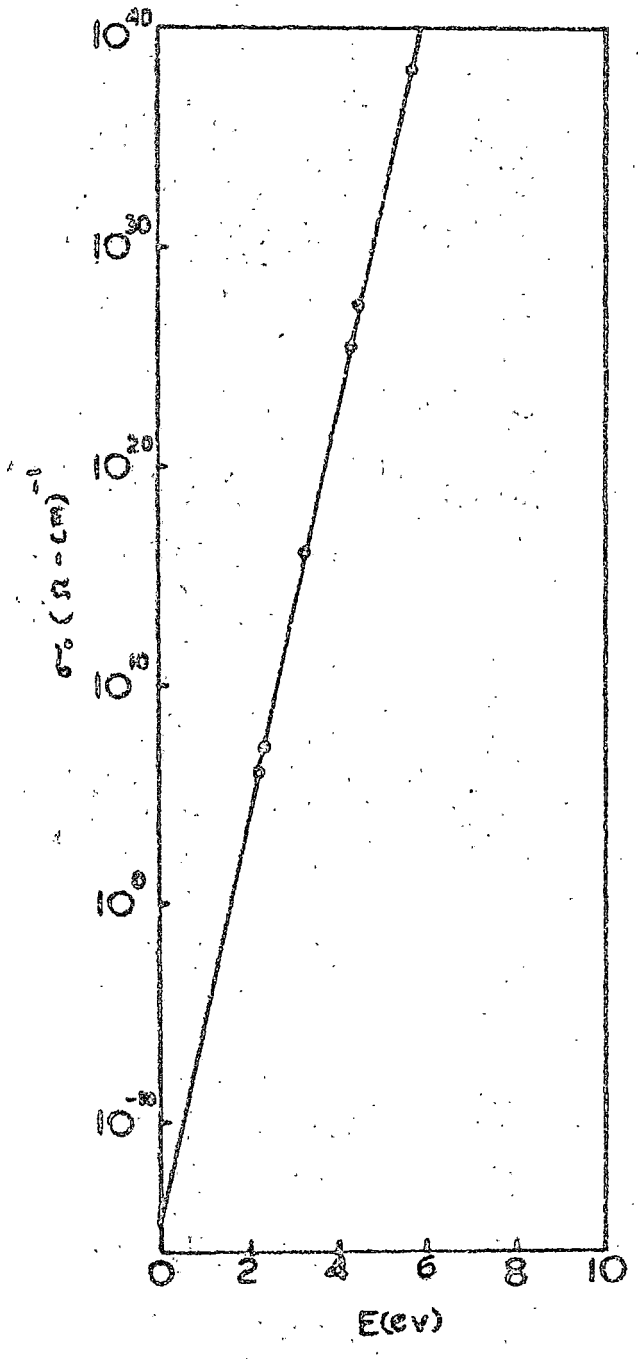

The plot of log σ_o values vs. E at a constant temperature for O-nitrobenzoic acid. The open circles refer to different vapours and the solid circles to different amount of the same vapour (ethyl acetate) (Refer Table 4.2)

Table 4.2

Values of T_0 and σ_0' obtained from various log σ_0 vs. E plots of some nitroaromatic semiconductors.

Semiconductor	Value of T_0 (°K)	Value of σ_0' $(\Omega \cdot cm)^{-1}$
9-nitroanthracene*	249.3	1.41×10^{-18}
1,4-dinitronaphthalene*	256.1	1.51×10^{-14}
1,3,5-trinitrobenzene*	261.8	2.51×10^{-16}
2-nitrofluorene**	257.5	7×10^{-17}
O-nitrobenzoic acid***	269.2	1.2×10^{-15}

* From Figure 4.22

** From Figure 4.23

*** From Figure 4.24

so obtained, we have calculated the expected σ_0 values and compared these values with experimentally measured values. These are shown in the Tables 4.3 - 4.12 for various nitroaromatic semiconductors. These results show that 'true' compensation effect is certainly observed in these semiconductors when E is changed by certain vapour adsorption.

'True' compensation effect is thought to arise from the existence of a linear relationship between the activation energy and the activation entropy of the system. It has been pointed out by Johnston and Lyons[100] that if a true linear free energy relation (LFER) does hold for dark conduction indicating a physical relationship between σ_0 and E, log σ (T_1) vs. E must also be linear, where T_1 is a specific temperature. In Figs. 4.25 - 4.27, such plots for various nitroaromatic semiconductors are shown. The observed slope of the line for each semiconductor is shown in Table 4.13 for comparision with the slope expected from equation (2.31), i.e. with $[1/T_0 - 1/T]\ 1/2K$. The values of σ_0' as obtained from the intercept of each log σ (3) vs. E plot is also shown in this table for comparision with the values obtained from the log σ vs. 1/T and log σ_0 vs. E plots. All these values show excellent consistency. These results show that the σ_0 and E are indeed physically related and thus confirm the validity of the compensation rule in case of adsorption of

Table 4.3

Semiconduction parameters for 9-nitroanthracene on adsorption of various vapours according to equation (2.31)

Vapour adsorbed	9 - nitroanthracene $(2kT_0)^{-1} = 23.43\ ev^{-1}$ $\sigma_0' = 1.41 \times 10^{-18}\ (\Omega\ cm)^{-1}$		
	E (ev)	Calculated $\sigma_0 = \sigma_0' \exp(E/2kT_0)$	measured* σ_0 $(\Omega\text{-}cm)^{-1}$
Ethanol	5.66	5.53×10^{39}	2.05×10^{40}
Ethylacetate	4.72	1.51×10^{30}	5.37×10^{30}
Benzene	3.55	2.11×10^{21}	6.41×10^{21}
Carbontetra-chloride	3.59	4.78×10^{18}	1.39×10^{19}
Methanol	3.22	8.21×10^{14}	2.03×10^{15}

* From Figure 4.8

Table 4.4

Semiconduction parameters for 1,4-dinitronaphthalene on adsorption of various vapours according to equation (2.31)

Vapour adsorbed	1,4-dinitronaphthalene $(2kT_0)^{-1}$ = 22.80 ev^{-1}, σ_0' = 1.51 x 10^{-14} (ohm- cm)$^{-1}$		
	E (ev)	calculated $\sigma_0 = \sigma_0' \exp(E/2kT_0)$ (ohm-cm)$^{-1}$	measured* σ_0 (ohm- cm)$^{-1}$
Ethanol	2.92	1.24 x 10^{15}	1.98 x 10^{15}
Methanol	2.69	1.70 x 10^{11}	2.66 x 10^{11}
Cyclohexane	2.18	3.69 x 10^{7}	5.84 x 10^{7}

* From Figure 4.9

Table 4.6

Semiconduction parameters for 1,3,5-trinitrobenzene on adsorption of various vapours according to equation (2.31)

Vapours adsorbed	1,3,5-trinitrobenzene $(2kT_0)^{-1}$ = 22.30 ev^{-1} σ_0' = 2.61 x 10^{-16} (ohm-cm)$^{-1}$		
	E (ev)	calculated $\sigma_0 = \sigma_0' \exp(E/2kT_0)$ (ohm-cm)$^{-1}$	measured* σ_0 (ohm-cm)$^{-1}$
Ethanol	5.32	8.37 x 10^{35}	2.02 x 10^{36}
n-Hexane	3.12	4.13 x 10^{14}	7.17 x 10^{14}
Cyclohexane	2.88	1.96 x 10^{12}	8.36 x 10^{12}
Methanol	2.26	1.94 x 10^{6}	2.86 x 10^{6}

* From Figure 4.10

Table 4.6

Semiconduction parameters for 2-nitrofluorene on adsorption of various vapours according to equation (2.31)

Vapours adsorbed		2-nitrofluorene $(2kT_o)^{-1}$ = 22.677 ev^{-1} σ_o' = 2 x 10^{-16} (ohm-cm)$^{-1}$	
	E (ev)	calculated $\sigma_o = \sigma_o' \exp(E/2kT_o)$ (ohm-cm)$^{-1}$	measured* σ_o (ohm-cm)$^{-1}$
Ethanol	7.20	1.62 x 10^{65}	2.38 x 10^{65}
Ethylacetate	4.04	5.0 x 10^{23}	1.12 x 10^{24}
Benzene	3.72	8.60 x 10^{20}	8.09 x 10^{20}
Carbontetra-chloride	3.26	2.5 x 10^{16}	1.83 x 10^{16}
n-Hexane	2.84	2.07 x 10^{9}	1.83 x 10^{9}

* From Figure 4.11

Table 4.7

Semiconduction parameters for O-nitrobenzoic acid on adsorption of various vapours according to equation (2.31)

Vapours adsorbed	O-nitrobenzoic acid $(2kT_0)^{-1}$ = 21.664 ev^{-1}, σ_0' = 9 x 10^{-16} (ohm-cm)$^{-1}$		
	E (ev)	calculated $\sigma_0 = \sigma_0' \exp(E/2kT_0)$ (ohm-cm)$^{-1}$	measured* σ_0 (ohm-cm)$^{-1}$
Ethanol	5.66	2.63 x 10^{38}	1.43 x 10^{38}
Methanol	4.31	4.00 x 10^{25}	3.19 x 10^{25}
Carbontetra-chloride	3.3	1.16 x 10^{16}	1.00 x 10^{16}
n-Hexane	2.24	1.138 x 10^{6}	1.06 x 10^{6}

* From Figure 4.12

Table 4.8

Semiconduction parameters for 9-nitroanthracene on adsorption of ethanol vapour of different amounts according to equation 2.31

Curve No. of figure 4.15	9-nitroanthracene $(2kT_0)^{-1}$ = 23.43 ev^{-1} σ_0' = 1.41 x 10^{-18} (ohm-cm)$^{-1}$		
	B (ev)	calculated $\sigma_0 = \sigma_0' \exp(B/2kT_0)$ (ohm-cm)$^{-1}$	measured* σ_0 (ohm-cm)$^{-1}$
1	5.36	4.00 x 10^{36}	2.04 x 10^{37}
2	4.75	3.04 x 10^{30}	1.67 x 10^{31}
3	3.83	1.32 x 10^{21}	5.03 x 10^{21}
4	3.35	1.73 x 10^{16}	6.65 x 10^{16}
5	2.93	2.07 x 10^{12}	1.03 x 10^{13}

Curve No. 1 → 5 corresponds to the decreasing amount of adsorbed ethanol vapour.

* From Figure 4.15

Table 4.9

Semiconduction parameters for 1,4-dinitronaphthalene on adsorption of ethanol vapour of different amounts according to equation (2.31)

Curve No. of Figure 4.16	1,4-dinitronaphthalene $(2kT_0)^{-1}$ = 22.80 ev^{-1} σ_0' = 1.51×10^{-14} (ohm-cm)$^{-1}$		
	E (ev)	calculated $\sigma_0 = \sigma_0' (\exp(E/2kT_0))$ (ohm-cm)$^{-1}$	measured* σ_0 (ohm-cm)$^{-1}$
1	2.87	3.96×10^{14}	6.83×10^{14}
2	2.38	6.57×10^{9}	8.06×10^{9}
3	2.13	1.86×10^{7}	2.67×10^{7}
4	1.86	3.95×10^{4}	6.36×10^{4}

Curve No. 1 $\longrightarrow$ 4 corresponds to the decreasing amount of adsorbed ethanol vapour.

* From Figure 4.16

Table 4.10

Semiconduction parameters for 1,3,5-trinitrobenzene on adsorption of ethanol vapour of different amounts according to equation (2.31)

Curve No. of figure 4.17	1,3,5-trinitrobenzene $(2kT_0)^{-1}$ = 22.90 ev^{-1} σ_0' = 2.61 x 10^{-16} (ohm-cm)$^{-1}$	
	E (ev)	calculated $\sigma_0 = \sigma_0' \exp(E/2kT_0)$ (ohm-cm)$^{-1}$	measured* σ_0 (ohm-cm)$^{-1}$
1	7.93	1.56 x 10^{61}	5.78 x 10^{61}
2	7.18	8.64 x 10^{53}	2.29 x 10^{54}
3	4.36	4.22 x 10^{26}	6.60 x 10^{26}
4	3.65	5.61 x 10^{19}	7.90 x 10^{19}
5	2.41	5.50 x 10^{7}	5.65 x 10^{7}

Curve No. 1 - 5 corresponds to the decreasing amount of adsorbed ethanol vapour.

* From Figure 4.17

Table 4.11

Semiconduction parameters for 2-nitrofluorene on adsorption of ethyl acetate vapour of different amounts according to equation (2.31)

Curve No. of figure 4.18	2-nitrofluorene $(2kT_o)^{-1}$ = 22.677 ev^{-1}, σ_o' = 2×10^{-16} (ohm-cm)$^{-1}$		
	E (ev)	calculated $\sigma_o = \sigma_o' \exp(E/2kT_o)$ (ohm-cm)$^{-1}$	measured* σ_o (ohm-cm)$^{-1}$
1	4.45	1.3×10^{28}	1.44×10^{29}
2	3.96	2.0×10^{23}	2.23×10^{23}
3	3.36	2.46×10^{17}	2.43×10^{17}
4	3.12	1.07×10^{15}	1.06×10^{15}

Curve No. 1 - 4 corresponds to the decreasing amount of adsorbed ethylacetate vapour.

* Figure 4.18

Table 4.12

Semiconduction parameters for O-nitrobenzoic acid on adsorption of ethyl acetate vapour of different amounts according to equation (2.31)

Curve No. of Figure 4.19	O-nitrobenzoic acid $(2kT_0)^{-1} = 21.664\ ev^{-1}$ $\sigma_0' = 8 \times 10^{-16}$ (ohm-cm)$^{-1}$		
	E (ev)	calculated $\sigma_0 = \sigma_0' \exp(E/2kT_0)$ (ohm-cm)$^{-1}$	measured* σ_0 (ohm-cm)$^{-1}$
1	14.7 ev	1.83×10^{123}	3.00×10^{125}
2	8.1	1.46×10^{61}	1.56×10^{61}
3	4.5	1.96×10^{27}	2.74×10^{27}
4	2.33	2.22×10^{7}	2.73×10^{7}

Curve No. 1 $\longrightarrow$ 4 corresponds to the decreasing amount of adsorbed ethylacetate vapour.

* From Figure No. 4.19

FIGURE - 4.25

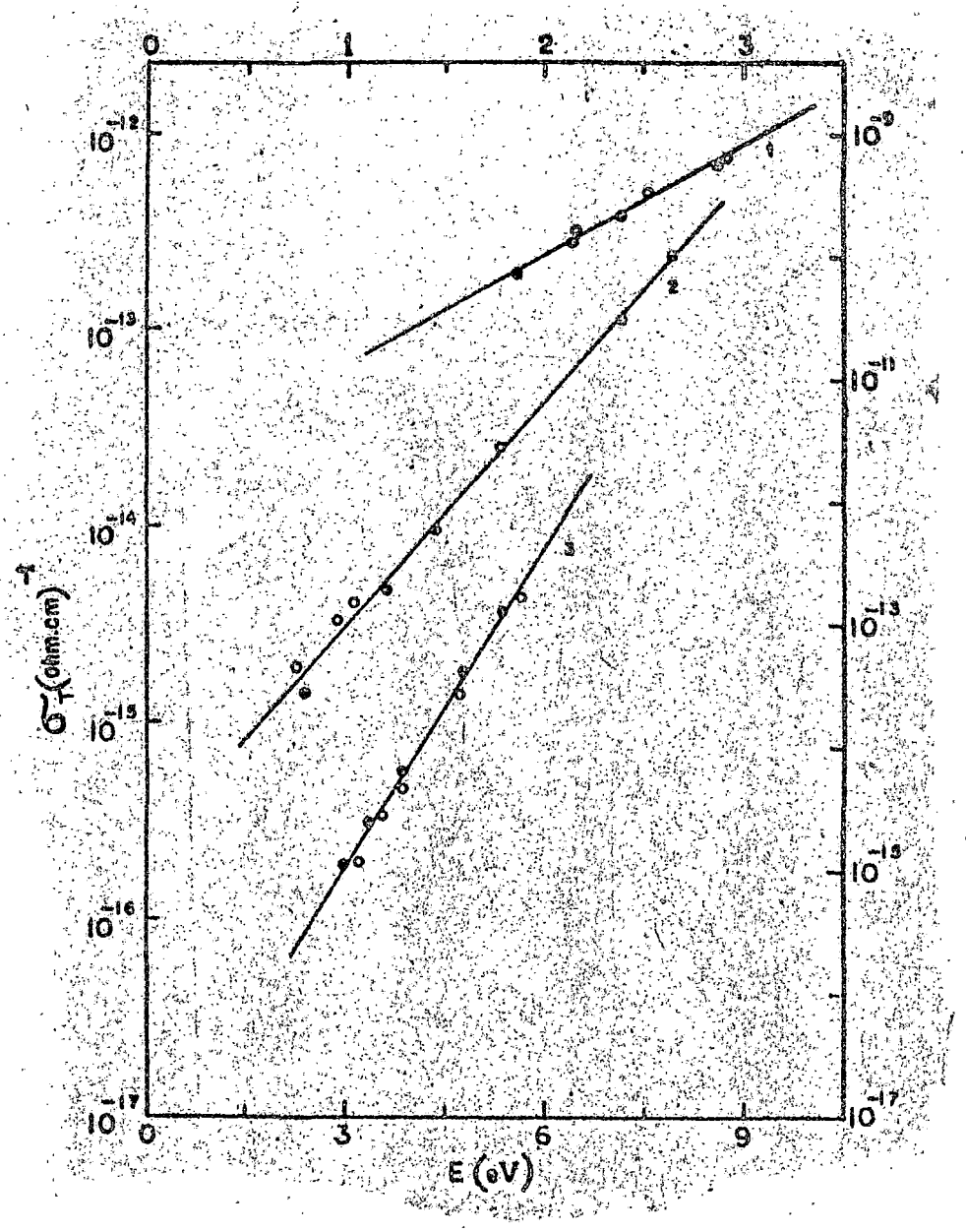

The plots of the log σ_T values at a constant temperature ($1/T_1 = 3.70 \times 10^{-3}\ ^{\circ}K^{-1}$) vs. the E - values for (1) 1,4-dinitronaphthalene (left and upper scale) (2) 1,3,5-trinitrobenzene (left and lower scale) and (3) 9-nitroanthracene (right and lower scale). (Refer Table 4.13)

FIGURE - 4.23

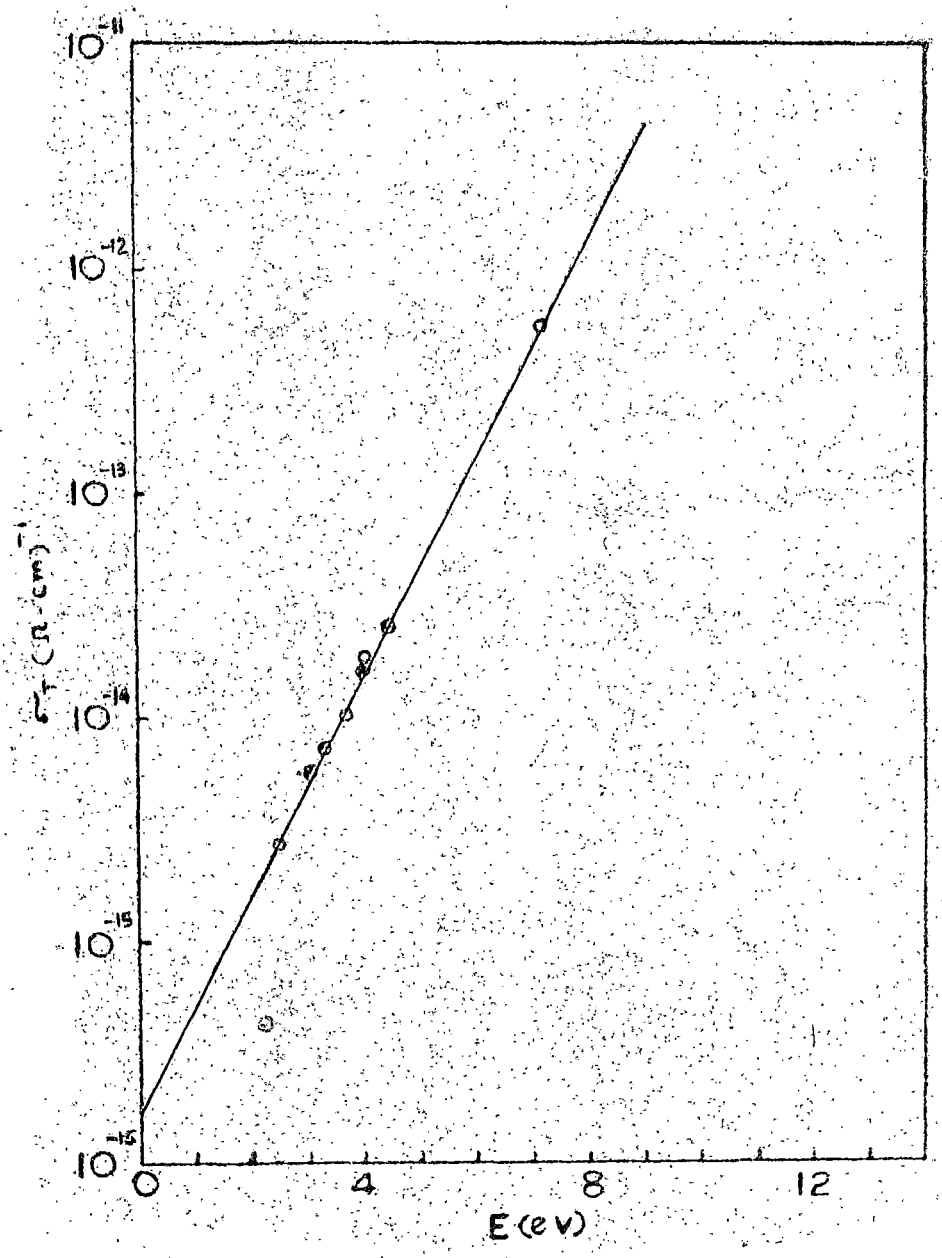

The plot of log σ_m values vs. E for 2-nitrofluorene at a constant temperature (270.25°K). The open circles refer to different vapours and the solid circles to different amount of the same vapour (ethyl acetate) (Refer Table 4.13)

FIGURE - 4.27

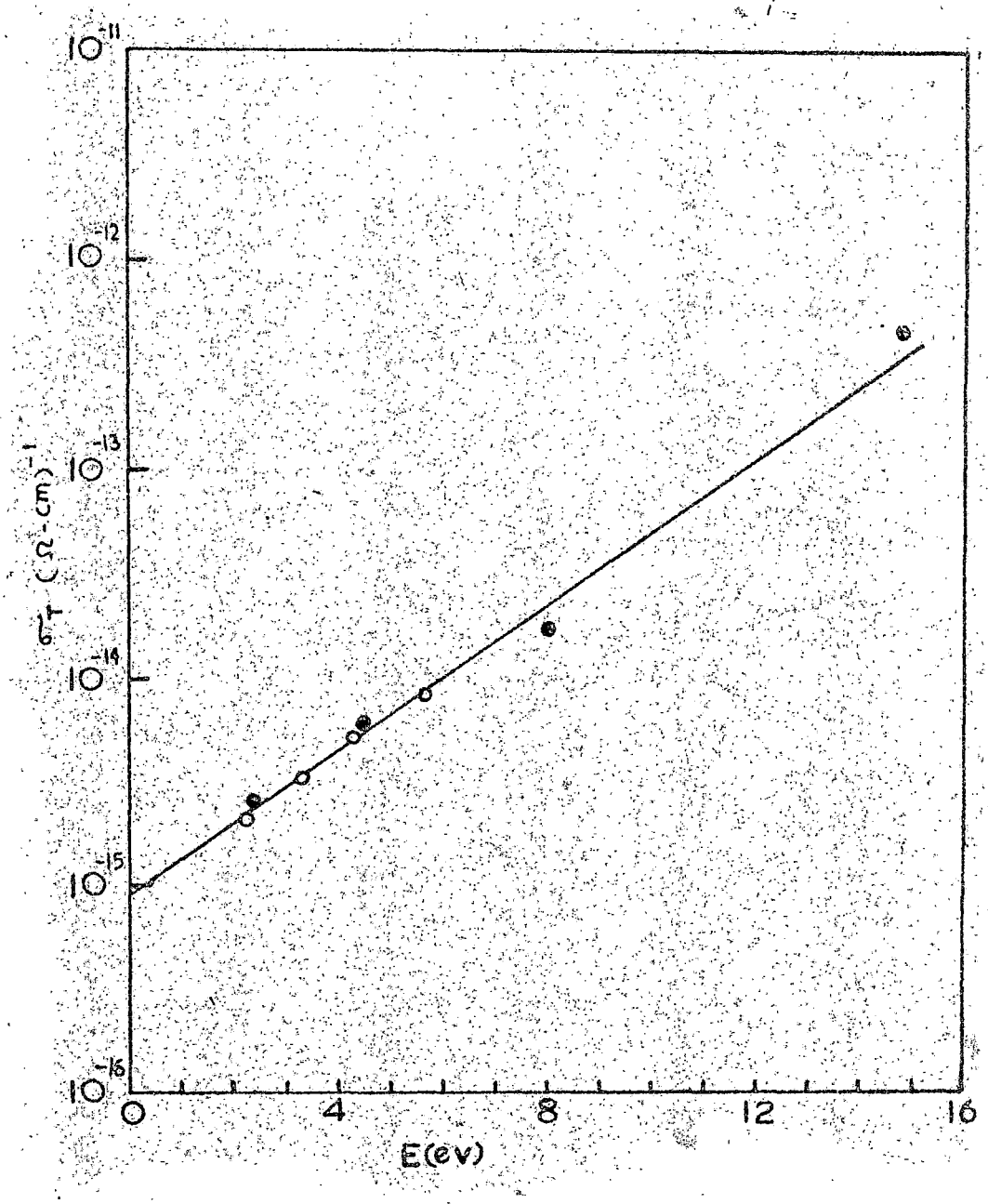

The plot of log σ_F values vs. E for O-nitrobenzoic acid at a constant temperature ($1/T_1 = 3.65\ ^{\circ}K^{-1}$). The open circles refer to different vapours and the solid circles to different amount of the same vapour (ethyl acetate) (Refer Table 4.13)

Table 4.13

Expected (equation 2.31) and observed slopes and observed σ_o' from the log σ vs. E plots for the nitroaromatic semiconductors

Semiconductors	Expected slope $(ev)^{-1}$	Observed slope $(ev)^{-1}$	Observed σ_o' $(ohm\text{-}cm)^{-1}$
9-nitro-anthracene*	0.85	0.83	3.62×10^{-13}
1,4-dinitro-naphthalene*	0.53	0.56	1.76×10^{-14}
1,3,5-trinitro-benzene*	0.36	0.38	2.10×10^{-16}
2-nitro-fluorene**	0.46	0.49	1.65×10^{-16}
O-nitrobenzoic-acid***	0.15	0.178	9.2×10^{-16}

* From Figure 4.25

** From Figure 4.26

*** From Figure 4.27

certain vapours on the nitroaromatic semiconductors.

3. Discussions

There are number of thesis about the mechanism of conduction in organic semiconductors leading to compensation effect. The carrier injection model of Green[105] produces the type of activation energy dependence of the pre-exponential factor as observed experimentally but it does not provide any physical basis for the interpretation of T_o.

Kenony and Rosenberg[41] observed compensation law in tunneling of small polaron through molecular barrier from thermally activated energy levels of molecules. Their model predicts that $T_o = \theta/2$ (where θ is the Debye temperature) and that at $T > T_o$, small polaron tunneling is not possible and compensation effect is not expected to be observed. In the present investigation, the semiconductive behaviour has been studied at $T > T_o$. The experimental results show that the compensation rule is valid in those cases also. Further, Debye - Temperature for these semiconductors are not known precisely. It has been reported[145] that the calculated values of the Debye - temperature for a series of crystals of aromatic compounds lie mainly in the range of 100 - 130°K. Thus, it seems that T_o values measured are far too high to justify the small polaron tunneling model.

Because of the widespread occurrence[103] of the compensation effect (besides semiconduction process, it is observed in chemical reactions, catalytic processes, thermal denaturation of macromolecules, thermal killing of unicellular organisms etc.), Kemony and Mohanti[45] have proposed a theory of electronic charge transport as involved in kinetic processes (also applicable to equilibrium processes) from the absolute rate theory equation[115,116] within two special models. The first one (quadratic polarons) involves the coupling of electrons with a set of oscillators, whereas the second one (magnetic polarons) involves the coupling of electrons with a set of spins. Both the models show that the activation entropy is proportional to the activation energy thus providing a compensation effect. The use of N number of oscillators or of spins to bring about the compensation effect seems to appear reasonable in view of the fact that the variable amount of adsorbed dielectric (vapour) screen off the interaction of a charge with more distant parent molecules; N depending on the number of such molecules with which the charge effectively interacts. But in quadratic polaron model, the characteristic temperature T_0 is always negative in contradiction to the experimental observation. The spin polaron model gives a positive T_0 but predicts no activation energy at very high temperatures. At a temperature around T_0, the process is activated and the activation

energy becomes a function of temperature i.e.

$$E(T) = E(0)\left[1 + \alpha T/T_0\right] \qquad (3.1)$$

Here E (0) is the activation energy at low temperature and α is a function of temperature :

$$\alpha = \left[1/\log 2\right] \log\left[1 + \exp\left\{(-2\log 2)\, T_0/T\right\}\right] \qquad (3.2)$$

Though the experiments were done in a limited temperature range, the excellent linear plots do not suggest such a temperature dependence.

Other theoretical attempts[42,44] to derive the compensation rule were restricted to the temperature dependence of the number of activated carriers in a model consisting of two electronic levels associated with each molecular site, the electronic states being coupled to a set of N oscillators associated with each molecular site. A change in the electronic state (due to vapour adsorption) gives rise to an activation entropy because of a change in vibrational frequencies. If one assumes the semiconduction equation as :

$$\sigma(T) = \sigma_0' \exp(S/K) \exp(-E/2KT) \qquad (3.3)$$

then the variation in both the electronic energy gap (E) and the activation entropy (S) can account for compensation effect if the

changes in these parameters are given by :

$$E = E_0 + nE_1 \quad \text{and} \quad S = S_0 + nS_1 \qquad (3.4)$$

where n is a definite number for each system and E_0, E_1, S_0 and S_1 are same for all the systems. In this case the characteristic temperature is given by $T_0 = [E_1 / 2S_1]$.

Unfortunately due to the fact that the nature of the activated complex (due to vapour adsorption) is not precisely known, the activation entropy S (hence S_1) is a relatively obscure quantity and any quantitative estimate of T_0 is not possible.

The experimental results presented here show that the enhancement in conductivity is associated with a change in activation energy of the semiconductors on vapour adsorption. This change in activation energy depends on the chemical nature and also on the amount of the vapour adsorbed. In all the cases studied the activation energy increases with the increase in conductivity. This behaviour, however, is quite understandable from the conductivity expression (2.31). If $T_0 < T$, where T is any temperature in the working range, then ($1/T_0 - 1/T$) becomes positive and the increase in σ at a temperature T is associated with an increase in activation energy. Thus, a semiconductor having T_0 at a lower side than the working temperature should show an enhancement

in its conductivity with the increase in its activation energy. Such behaviour has been observed in case of nitroaromatic semiconductors. Now, it is clear from the experiments that the characteristic temperature (T_o) of a semiconductor plays an important role in the dark conduction process.

The results of the nitroaromatic semiconductors studied show that when compensation relation is satisfied, the ' T_o' has a low value similar to the polyenes[146] with a conjugated carbonyl group. It is interesting as in these nitroaromatics, the nitrogroup, like that in carbonly group, is also having a nonbonding electron. Thus it seems that the presence of a nonbonding electron, in the molecule of a semiconducting material, is somehow responsible for the low compensation temperature.

4. Conclusion

The validity of the compensation rule in electrical conduction process has been examined in case of some nitroaromatic semiconductors by varying the activation energy by vapour adsorption. The validity or lack of it have been shown to be vapour-semiconductor pair dependent. The vapours for which very weak reversible complexes are formed, true compensation effect is observed. The other vapours which form strong complexes have been found not to satisfy the compensation relationship. Observed T_o value is distinctly

different for different nitroaromatics which supports the view about the dependence of T_0 on the molecular property of the semiconducting material. Our present observation of low value of T_0 is interesting and it seems that the presence of nonbonding electrons play an important role.

REFERENCES (PART - A)

(Semiconductive Investigations)

1. C. G. B. Garrett, "Semiconductors" edited by R. A. Hannay (Reinhold, NY, 1959)

2. H. Inokuchi and H. Akamatu, "Solid State Physics" edited by F. Seitz and D. Turnbull (AP, NY, 1961) p. 93.

3. L. E. Lyons, "Physics and Chemistry of the Organic Solid State" edited by D. Fox, M.M. Labes and A. Weissberger (Interscience NY, 1963) Vol. 1, p. 745.

4. D. R. Kearns, Adv. Chem. Phys., 7, 282 (1964)

5. Y. Okamoto and W. Brenner, "Organic Semiconductors" (Reinhold, NY, 1964)

6. J. Kommandeur, "Physics and Chemistry of the Organic Solid State" edited by D. Fox, M.M. Labes and A. Weissberger (Interscience, NY, 1965) Vol.II p. 1.

7. F. Gutmann and L.E. Lyons, "Organic Semiconductors" (John Wiley & Sons, Inc., NY, 1967)

8. O. H. Le Blanc, "Physics and Chemistry of the Organic Solid State" edited by D. Fox, M.M. Labes and A. Weissberger (Interscience, NY, 1967) Vol.III, p. 175.

9. J. H. Sharp and M. Smith, "Physical Chemistry : An Advance Treatise" edited by W. Jost (A.P., NY, 1970) Vol. X, p. 435.

10. D. H. Hanson,
Crit. Rev. Solid State Sci., 3, 243 (1973)

11. H. Karl,
Adv. Solid State Phys., Festkorperprobleme, 14, 261 (1974)

12. E. P. Goodings,
Chem. Soc. Rev., 5, 95 (1976)

13. H. Inokuchi and Y. Maruyama, "Photoconductivity and Related Phenomenon" edited by J. Mort and D. M. Pai (Elsevier, Amsterdam, 1976) p. 155.

14. J. O. Williams, "Advances in Physical Organic Chemistry" edited by V. Gold and D. Bothell (AP, NY, 1978)p.159.

15. C. B. Duke and L. B. Schein,
Physics Today, 33 (2), 42 (1980)

16. M. Wilk,
Z. Electro Chem., 64, 634 (1960)

17. A. Szent-Gyorgyi, "Introduction to Submolecular Biology" (AP, NY, 1960)

18. R. Mason,
Nature (London), 181, 820 (1958)

19. F. Gutmann and A. Metschey,
J. Chem. Phys., 36, 2356 (1962)

20. B. Rosenberg, R. A. Orlando and J. W. Orlando,
Arch. Biochem. Biophys., 93, 305 (1961)

21. B. W. Abrahamson, J. Marquisee, P. Cavicsi and J. Roubie,
B. Elektrochem., 64, 177 (1960).

22. B. Rosenberg,
J. Chem. Phys., 31, 239 (1959)

23. W. A. Wagins and W. H. Jennige,
Discussions Faraday Soc., No. 27, 190 (1959)

24. G. Wald,
Exptl. Cell Research, Suppl., 5, 338 (1958)

25. H. Fernandez - Moran,
Rev. Mod. Phys., 31, 319 (1959)

26. P. O. Ojostrand,
Rev. Mod. Phys., 31, 301 (1959)

27. B. Rosenberg, "Symposium on Electrical Conductivity in
Organic Solids" edited by H. Kallmann and M. Silver
(Interscience, NY, 1961) p. 291.

28. B. Rosenberg,
J. Chem. Phys., 36, 816 (1962)

29. R. S. Smart,
Trans. Faraday Soc., 58, 754 (1963)

30. D. D. Eley, "Horizons in Biochemistry" edited by M.Kasha
and B. Pullman (AP, NY, 1962)

31. B. Rosenberg,
Faraday disc., Chem. Soc., No. 51, 180 (1971)

32. B. Rosenberg,
Photochem. Photobiol., 1, 117 (1962)

33. B. Rosenberg,
J. Chem. Phys., 31, 238 (1959)

34. B. Rosenberg,
J. Chem. Phys., 34, 63 (1961)

35. B. Rosenberg,
Adv. Radiation Biol., 2, 193 (1966)

36. B. Rosenberg, T. N. Misra and R. Switzer,
Nature, 217, 423 (1968)

37. E. Postow, Ph. D. Thesis, Michigan State University,
See Diss. Abstr. Int. B 30, 77 (1968)

38. B. Rosenberg and E. Postow,
Ann. New York Acad. Sci, 158, 161 (1969)

39. H. T. Tien,
Techniques of Surface and Colloid Chemistry and
Physics, 1, 109 (1972)

40. B. Rosenberg, B. B. Bhowmik, H. C. Harder and E. Postow,
J. Chem. Phys. 49, 4108 (1968)

41. G. Kenney and B. Rosenberg,
J. Chem. Phys. 53, 3649 (1970)

42. G. Kemeny, I. M. Goklany,
J. Theor. Bio., 42, 107 (1973)

43. G. Kemeny and B. Rosenberg,
J. Chem. Phys., 52, 4151 (1970)

44. T. A. Kaplan and S. D. Mahanti,
J. Chem. Phys., 62, 100 (1975)

45. G. Kemeny and S. D. Mahanti,
Proc. Nat. Acad. Sci., U.S.A., 72, 909 (1975)

46. D. D. Eley, A. S. Fawcett and M. R. Willis,
Trans. Faraday Soc., 64, 1613 (1968)

47. E. Ulbert,
Aust. J. Chem., 23, 1347 (1970)

48. G. Sawa, K. Kitagawa and N. Ieda, Jpn. J. Appl. Phys.,
11, 416 (1972)

49. G. Sawa, N. Ieda and K. Kitagawa,
Electronics Letters, 10, 60 (1974)

50. M. Nagai, H. Nagasaka and K. Yahagi,
Jpn. J. Appl. Phys., 16, 177 (1977)

51. J. L. Hats, S. A. Rice, S. I. Choi and J. Jortner,
J. Chem. Phys., 39, 1683 (1963)

52. R. Silbey, J. Jortner, S. A. Rice and M. T. Vala, Jr,
J. Chem. Phys., 42, 733 (1965)

53. R. Silbey, J. Jortner, S. A. Rice and M. T. Vala, Jr.,
J. Chem. Phys., 43, 2925 (1965)

54. R. G. Kepler, "Organic Semiconductors" edited by J. J. Brophy and J. W. Buttrey (Macmillan, NY, 1962) p. 1.

55. F. Seitz, "Modern Theory of Solids" (McGraw Hill Book Company, Inc., NY, 1940)

56. C. Kittel, "Introduction to Solid State Physics" (Wiley Eastern Pvt. Ltd., New Delhi, 1971)

57. W. A. Harrison, "Solid State Theory" (Tata McGraw Hill Publishing Co. Ltd., Bombay and New Delhi, 1970)

58. A. J. Dekker, "Solid State Physics" (Macmillan and Co. Ltd., London, 1970)

59. F. Gutmann and L. E. Lyons, "Organic Semiconductors" (John Wiley and Sons., Inc., NY, 1967) p. 826.

60. O. H. Le Blanc, Jr., J. Chem. Phys., 35, 1275 (1961)

61. D. D. Eley and M. R. Willis, "Symposium on Electrical Conductivity of Organic Solids" edited by H. Kallmann and M. Silver (Interscience Publishers, NY, 1961) p. 257.

62. H. A. Pohl, "Modern Aspects of the Vitreous State" edited by J. D. Mackenzie (Butterworth, London, 1962) p. 105.

63. H. A. Pohl and D. A. Opp, J. Phys. Chem., 66, 2121 (1962)

64. H. Frohlich and G. L. Sewell,
Proc. Phys. Soc. (London) 74, 643 (1959)

65. W. Siebrand, Doctorate Thesis (University of Amsterdam, 1963); Abstracts : Organic Crystal Symposium (N.R.C., Ottawa, 1962) p. 56.

66. E. C. McRae and W. Siebrand J. Chem. Phys. 41, 905 (1964)

67. W. Siebrand,
J. Chem. Phys. 41, 3574 (1964)

68. O. H. LeBlanc, Jr,
J. Chem. Phys. 37, 916 (1962)

69. S. Brunauer, "The adsorption of gases and vapours" (Oxford University Press, London, 1945) Vol. I.

70. D. M. Young and A. D. Crowell, "Physical Adsorption of Gases" (Butterworths, London, 1962)

71. G. C. Bond, "Catalysis by Metals" (AP, NY, 1962)

72. J. H. de Boer,
Adv. Catal. Relat. Subj., 8, 67 (1954)

73. A. D. Crowell, "The Solid-Gas Interface" edited by E. A. Flood (Marcel Dekker, NY, 1967) Vol. I.

74. T. Engel and R. Gomer,
J. Chem. Phys. 52, 5572 (1970)

75. J. Bardeen,
Phys. Rev., 58, 727 (1940)

76. J. E. Lennard-Jones,
Trans. Faraday Soc., 28, 333 (1932)

77. H. Margenau and W. G. Pollard,
Phys. Rev., 60, 128 (1941)

78. E. G. R. Frosen and R. G. Sachs,
Phys. Rev., 61, 65 (1942)

79. I. E. Dzyaloshinskii, E. M. Lifshitz and L. P. Pitaevskii,
Adv. Phys., 10, 165 (1961)

80. C. Mavroyannis,
Mol. Phys., 6, 593 (1963)

81. A. D. Mclachlan,
Mol. Phys., 7, 381 (1964)

82. E. M. Lifshitz,
Zh. Eksp. Theor. Fis., 29, 94 (1955) [Sov. Phys. - J E T P 2, 73 (1956)]

83. W. G. Pollard,
Phys. Rev., 60, 578 (1941)

84. K. F. Wojciechowski,
Acta Phys. Pol., 29, 119 (1966); 33, 363 (1968)

85. G. G. Kleiman and U. Landman,
Phys. Rev. Lett., 31, 707 (1973)

86. G. G. Kleiman and U. Landman,
Phys. Rev. B, 8, 5484 (1973)

87. D. E. Sullivan,
Phys. Rev. B, 20, 3991 (1979)

88. P. C. Hemmer and J. L. Lebowitz, "Phase Transitions and critical Phenomena" edited by C. Domb and M. S. Green (AP, NY, 1976) Vol V B.

89. N. G. Van Kampen, Phys. Rev., 135, A362 (1964)

90. J. K. Percus, Trans. N.Y. Acad. Sci., 26, 1062 (1964)

91. J. L. Lebowitz and J. K. Percus, J. Math. Phys., 4, 116 (1963)

92. C. C. Gimmons and C. Garrod, J. Math. Phys., 14, 1075 (1973)

93. D. Henderson, F. F. Abraham and J. A. Barker, Mol. Phys., 31, 1291 (1976)

94. E. Waisman, D. Henderson and J. L. Lebowitz, Mol. Phys., 32, 1373 (1976)

95. D. E. Sullivan and G. Stell, J. Chem. Phys., 62, Appendix (1975)

96. A. Many, S. Harnik and D. Gerlich, J. Chem. Phys., 23, 1733 (1955)

97. F. Gutmann and L. E. Lyons, "Organic Semiconductors" (John Wiley and Sons., Inc., NY, 1967) p. 423-435

98. N. N. Cardew and D. D. Eley, Discussions Faraday Soc., 27, 115 (1959)

98. D. D. Eley,
J. Polymer Sci, Pt. C, 17, 73 (1967)

100. G. R. Johnston and L. E. Lyons,
Aust. J. Chem., 23, 2137 (1970)

101. G. R. Johnston and L. E. Lyons,
Phys. Status Solidi, 37, K 43 (1973)

102. O. Exner,
Collh. Czech. Chem. Commun., 29, 1094 (1964)

103. G. Kemeny and B. Rosenberg,
Nature, 243, 400 (1973)

104. B. E. C. Banks, V. Damjanovic and C. A. Vernor,
Nature, 240, 147 (1972)

105. M. E. Green,
J. Chem. Phys., 51, 3279 (1969)

106. G. C. Robert,
J. Phys. C, 4, 3167 (1971)

107. M. E. Green,
J. Phys. Chem., 69, 3510 (1965)

108. J. Bardeen,
Phys. Rev., 71, 717 (1947)

109. N.F. Mott and I.N. Sneldon, "Wave Mechanics and its Applications" (Dover Publications, Inc., NY, 1963)

110. S. Yomosa, "Quantum Aspects of Polypeptides and Polynucleotides" edited by M. Weissbluth (Interscience, NY, 1964)

111. M. G. Evans and J. Gergely,
Biochim. Biophys. Acta, 3, 188 (1949)

112. T. Holstein,
Ann. Phys. (NY), 8, 343 (1959)

113. T. Holstein,
Ann. Phys. (NY) 8, 325 (1959)

114. M. V. Volkenstein,
J. Theor. Biol., 24, 193 (1972)

115. S. Glasstone, K. J. Laidler and H. Eyring, " The Theory of Rate Processes" (McGraw-Hill, NY, 1941)

116. E. E. Weston, JR. and H. A. Schwartz, "Chemical Kinetics" (Prentice-Hall, Englewood Cliffs, N.J., 1972)

117. T. N. Misra, B. Rosenberg and R. Switzer,
J. Chem. Phys. 48, 2036 (1968)

118. B. Rosenberg and H. C. Harder,
Photochemistry and Photobiology, 6, 629 (1967)

119. K. M. Jain, A. Ghosh, B. Mallik and T. N. Misra,
Indian J. Phys. 52A, 643 (1978)

120. B. Rosenberg,
J. Chem. Phys. 34, 812 (1961)

121. B. Rosenberg,
J. Chem. Phys. 36, 816 (1962)

122. P. J. Rencroft, O. N. Rudyj and M.N. Labes,
Mol. Cryst., 1, 429 (1966)

123. M. M. Labes and C. N. Rudyj,
J. Am. Chem. Soc., 28, 2055 (1963)

124. P. J. Roucroft, C. N. Rudyj and M. M. Labes,
J. Am. Chem. Soc. 25, 2069 (1963)

125. B. Rosenberg and J. F. Comiscoli,
J. Chem. Phys. 25, 982 (1961)

126. A. G. Chynoweth,
J. Chem. Phys., 22, 1029 (1954)

127. O. Fritsch,
Ann. Physik, 22, 975 (1935)

128. W. Hartmann,
Z. Physik, 102, 709 (1936)

129. H. Mayer and H. Neidel,
Physik. Z. 38, 1014 (1937)

130. T. J. Gray and P. W. Darby,
J. Chem. Phys. 60, 201 (1956)

131. A. D. Martin and K. J. Nolcan,
J. Appl. Phys. 42, 2950 (1977)

132. W. G. Schneider and T. C. Waddington,
J. Chem. Phys., 25, 358 (1956)

133. A. Ghosh, K. N. Jain and T. N. Misra,
Proc. Indian Acad. Sci. (Chem. Sci.)
(in press) 1981

134. B. Mallik, A. Ghosh and T. N. Misra,
Proc. Indian Acad. Sci. (Chem. Sci.)
86A, 25 (1979)

135. A. Ghosh, B. Mallik and T. N. Misra,
Proc. Indian Acad. Sci.(Chem. Sci.)
92, 209 (1980).

136. Ya. Zeldovich,
Acta Physicochim. USSR, 1, 449 (1934)

137(a) S. Roginsky and Ya. Zeldovich,
Acta Physicochim. USSR, 1, 554, 595 (1934)

137(b) S. Elovich and S. Roginsky,
Acta Physicochim. USSR, 7, 235 (1937)

137(c) S. Elovich and O. N. Zhabrova,
Zhur. Fiz. Khim. 13, 1761, 1775 (1939)

138. D. D. Eley and R. B. Leslie, "Advances in Chemical Physics"
(Inter Science Publishers, NY, 1964) Vol 7
p. 238.

139(a) T. L. Hill, Advan. Catalysis 4, 211 (1952)

139(b) T. L. Hill, J. Chem. Phys. 17, 520 (1949); 18, 246 (1950)

139. S. Glasstone, "Text Book of Physical Chemistry" (Macmillan
and Co. Ltd., London, 1951) p. 1200.

140. F. S. Stone, "Chemistry of the Solid State" edited by
W. E. Garner (Butterworths, London, 1955)p. 367.

141. B. Rosenberg,
Nature, 193, 364 (1962)

142. B. Rosenberg, "Physical Processes in Radiation Biology" edited by L. Augenstein, R. Mason and B. Rosenberg (AP, NY, 1964) p. 120.

143. A. Ghosh, K. M. Jain, B. Mallik and T. N. Misra,
Jpn. J. Appl. Physics (in press, 1981)

144. K. M. Jain, A. Ghosh and T. N. Misra,
Proc. Indian Acad. Sci.(Chem. Sci.) (in press, 1981)

145. E. I. Mukhtarov, A. A. Pichurin, A. I. Kitaigorodskii,
Sov. Phys. Solid State (USA), 17, 1371 (1975)

146. B. Mallik, A. Ghosh and T. N. Misra,
Phys. Stat. Sol. (a) 62 (1980)

147. K. M. Jain, A. Ghosh and T. N. Misra,
Jpn. J. Appl. Phys. 19, 1847 (1980)